

VAPOR PHASE ACETYLATION OF ACETIC ACID TO VINYL ACETATE

- I. CHARACTERIZATION OF $Zn(OAc)_2$ — C SYSTEM**
- II. KINETICS AND MECHANISM**
- III. THERMODYNAMIC PROPERTIES**

A Thesis Submitted
In Partial Fulfilment of the Requirements
for the Degree of

DOCTOR OF PHILOSOPHY

by

HARI BHAGWAN GOYAL

to the

**DEPARTMENT OF CHEMICAL ENGINEERING
INDIAN INSTITUTE OF TECHNOLOGY, KANPUR**

MAY, 1976

I.I.T. KANPUR

CENTRAL LIBRARY

Acc. No. A 51195

23 SEP 1977

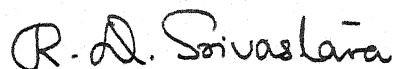
CHE-1976-D-GOV-NAP

TO

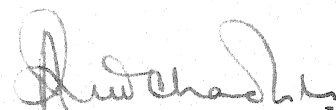
MY PARENTS

CERTIFICATE

This is to certify that the work 'VAPOR PHASE ACETYLATION OF ACETIC ACID TO VINYL ACETATE, I. CHARACTERIZATION OF $Zn(OAc)_2$ -C SYSTEM, II. KINETICS AND MECHANISM, III. IDEAL GAS THERMODYNAMIC PROPERTIES' has been carried out under our supervision and that this has not been submitted elsewhere for a degree.



R.D. Srivastava
Assistant Professor of
Chemical Engineering
Indian Institute of Technology
Kanpur-208016, India



A.P. Kudchadker
Professor of Chemical
Engineering
Indian Institute of Technology
Kanpur-208016, India

Date: May , 1976

ACKNOWLEDGEMENTS

The author wishes to express his appreciation to Professor A.P. Kudchadker and Professor R.D. Srivastava for their inspiring guidance and advice, and for their close supervision and constant encouragement at all stages of this investigation.

To Dr.(Mrs) S.A.Kudchadker for her inspiring guidance in carrying out the thermodynamic studies.

To Professor V. Srinivasan, Indian Institute of Technology, Madras for providing BET facilities.

To Dr. L.M. Pandey and Mr. Raman of Defence Research Laboratories (Materials), Kanpur for their help in carrying out TG analysis.

To Professor D.N. Saraf for his graciousness for providing constant inspiration during the work.

To Mr. A.K. Agarwal, M.O. Garg, Rajeev Goel and other friends for their helpful cooperation from time to time.

To the helpful cooperation offered by the staff of the Department of Chemical Engineering at Indian Institute of Technology, Kanpur particularly Mr. S.S. Chauhan and Ram Ashish Rai.

To Mr. B.S. Pandey for his unfailing patience in typing the manuscript and Mr. D.S. Panesar for tracing the figures.

To his wife for her patience and encouragement throughout the course of this investigation.

To his son for providing a welcome and refreshing change at home after a hard day's work in the laboratory.

Author

CONTENTS

	Page
List of Figures	viii
List of Tables	x
Nomenclature	xiii
Synopsis	xvi
INTRODUCTION	1
SECTION I CHARACTERIZATION OF $\text{Zn}(\text{OAc})_2\text{-C}$ SYSTEM	
1.1 Introduction	4
1.2 Experimental Methods	5
1.2.1 Preparation of Catalysts	5
(a) Preparation of Activated Carbon	5
(b) Preparation of Catalysts	7
1.2.2 Physicochemical Characterization	8
(a) X-ray Powder Analysis	8
(b) Infrared Spectroscopy	9
(c) TG and DT Analysis	10
(d) Surface Area, Pore Volume and Pore Size Distribution	10
1.3 Results and Discussion	11
1.3.1 X-ray Powder Spectra	11
1.3.2 Infrared Spectra	13
1.3.3 DT and TG Analysis	15
1.3.4 Surface Area and Pore Distribution	18

	Page
SECTION II: KINETICS AND MECHANISM	
2.1 Introduction	24
2.2 Experimental	27
2.2.1 Overall Description	27
2.2.2 Reactor	29
2.2.3 Acetic Acid Vaporizer	32
2.2.4 Flow Meters	34
2.2.5 Condensers	34
2.2.6 Purifier and Driers	34
2.2.7 Experimental Procedure	35
2.2.8 Analysis	36
2.3 Results and Discussion	38
2.3.1 Catalytic Activity of Various Catalysts	39
2.3.2 Effect of Zinc Acetate Concentration	39
2.3.3 Comparison of Rate with Surface Area	41
2.3.4 Effect of Acetylene-Acetic Acid Ratio in Feed	43
2.3.5 Effect of W/F Ratios	43
2.3.6 Effects of Diffusion	47
2.3.7 Kinetic Models	51
SECTION III: THERMODYNAMIC PROPERTIES	
3.1 Introduction	64
3.2 The Departure Functions for Vinyl Acetate	66
3.3 Ideal Gas Thermodynamic Properties of Vinyl Acetate	66
3.3.1 Molecular Structure	66
3.3.2 Vibrational Assignments	67
3.3.3 Thermodynamic Functions	72

	Page
3.4 Ideal Gas Thermodynamic Properties of Crotonaldehyde	74
3.4.1 Molecular Structure	74
3.4.2 Vibrational Assignments	75
3.4.3 Thermodynamic Functions	77
3.5 Acetone, Acetic Acid and Acetaldehyde	80
3.6 Acetylene, Carbon Dioxide and Water	80
3.7 Thermodynamic Properties of Mixtures	81
3.8 Enthalpy, Gibbs Energy and Equilibrium Constants of Reactions	82
3.8.1 Reaction Number 1	82
3.8.2 Reaction Number 2	83
3.8.3 Reaction Number 3	83
3.8.4 Reaction Number 4	83
CONCLUSION: AND RECOMMENDATIONS	
Conclusion	84
Recommendations	86
REFERENCES	
APPENDIX A: CHARACTERIZATION OF $Zn(OAc)_2-C$ SYSTEM	94
APPENDIX B: KINETICS AND MECHANISM	100
APPENDIX C: THERMODYNAMIC PROPERTIES	114
COMPUTER PROGRAM C1	131
COMPUTER PROGRAM C2	134

+ + + + +

+ + +

LIST OF FIGURES

Figure		Page
1	Differential Thermal Analysis Thermograms	16
2	TG Analysis: Percentage Weight Loss of $Zn(OAc)_2-C$ System as Function of Temperature	17
3	Surface Areas as Function of $Zn(OAc)_2$ Composition	20
4	Relative Volume of Capillaries as Function of Capillary Radius	22
5	Schematic Diagram of the Experimental Set-up	28
6	Reactor Details	30
7	Performance of Various Catalysts at $180^{\circ}C$ and 25 per cent Metal Acetate by Weight on Activated Carbon	40
8	Percentage Yield of Vinyl Acetate as Function of Zinc Acetate Concentration at $180^{\circ}C$; (W/F) = 30; and (R)=3.0	42
9	Effect of Reactant Mole Ratio, Acetylene to Acetic Acid, on Percentage Conversion of Acetic Acid at Various Temperatures, (W/F)=30	44
10	Effect of Reactant Mole Ratio, Acetylene to Acetic Acid on Percentage Selectivity for Vinyl Acetate at Various Temperatures, (W/F)=30	45
11	Effect of Reciprocal Space Velocity on Percentage Conversion of Acetic Acid and Yield of Vinyl Acetate at $180^{\circ}C$ and (R)=3.0	46
12	Effect of Feed Velocity on Percentage Conversion of Acetic Acid at $180^{\circ}C$; (R)=3.0 and (W/F)=30	50

Figure		Page
13	Acetylene Adsorption Model on Carbon	56
14	Comparison of Observed and Calculated Rates at 155°C and (W/F) = 30	59
15	Comparison of Observed and Calculated Rates at 180°C and (W/F) = 30	60
16	Comparison of Observed and Calculated Rates at 192°C and (W/F) = 30	61
17	Molecular Structure of Vinyl Acetate	68
18	Molecular Structure of Crotonaldehyde S-Trans Form	76
APPENDIX		
A1	Pore Size Distribution of Zn^{2+} -000	94
A2	Pore Size Distribution of Zn^{2+} -005	95
A3	Pore Size Distribution of Zn^{2+} -010	96
A4	Pore Size Distribution of Zn^{2+} -015	97
A5	Pore Size Distribution of Zn^{2+} -020	98
A6	Pore Size Distribution of Zn^{2+} -025	99

+ + + + +

+ + +

LIST OF TABLES

TABLE		Page
1	'd' Values for Zinc Acetate	12
2	Infrared Frequencies (cm^{-1}) of $\text{Zn(OAc)}_2\text{-C}$ Catalysts ...	14
3	Surface Area, Pore Volume and Average Pore Radius of Various Catalysts	19
4	Boiling Points of Organic Substances	33
5	Retention Time and Area Mole Factors of Various Components ...	37
6	Role of Internal Diffusion	48
7	Role of External Diffusion	49
8	Rate Equations Derived Using Hougen-Watson Method ...	52
9	Comparison of Some In-plane Frequencies	70
10	Adopted Fundamental Frequencies of Vinyl Acetate (cm^{-1}) ...	71
11	Molecular Parameters of Vinyl Acetate	73
12	Adopted Fundamental Frequencies of Crotonaldehyde ...	78
13	Molecular Parameters of Crotonaldehyde	79

APPENDIX B

B1	Performance of $\text{Zn}^{2+}\text{-025}$ Catalyst	100
B2	Performance of $\text{Cd}^{2+}\text{-025}$ Catalyst	101
B3	Performance of $\text{Ni}^{2+}\text{-025}$ Catalyst	102
B4	Effect of Zinc Acetate Concentrations on Per Cent Yield of Vinyl Acetate	103
B5	Effect of \bar{R} on Per cent Conversion of Acetic Acid and Per Cent Selectivity for Vinyl Acetate at 155°C	104

Table

		Page
B6	Effect of R on Per Cent Conversion of Acetic Acid and Per Cent Selectivity for Vinyl Acetate at 165°C ...	105
B7	Effect of Reactant Mole Ratio on per cent Conversion of Acetic Acid and Per Cent Selectivity for vinyl Acetate at 180°C	106
B8	Effect of Reactant Mole Ratio on Per Cent Conversion of Acetic Acid and Per Cent Selectivity for Vinyl Acetate at 192°C	107
B9	Effect of Reactant Mole Ratio on Per Cent Conversion of Acetic Acid and Per Cent Selectivity of Vinyl Acetate at 199°C	108
B10	Effect of Reciprocal of Space Velocity on Per Cent Conversion of Acetic Acid and Per Cent Yield of Vinyl Acetate at 180°C	109
B11	Heat and Mass Transfer Effects	110
B12	Comparison of Observed and Predicted Rates at 155°C ...	111
B13	Comparison of Observed and Predicted Rates at 180°C ...	112
B14	Comparison of Observed and Predicted Rates at 192°C ...	113

APPENDIX C

C1	Vapor Pressure Boiling Point of Vinyl Acetate ...	114
C2	Physical Properties of Vinyl Acetate	115
C3	Martin-Hou Constants and the Departure Functions for Vinyl Acetate	117
C4	Ideal Gas Thermodynamic Properties of Vinyl Acetate ...	119
C5	Ideal Gas Thermodynamic Properties of Crotonaldehyde ...	120

Table		Page
C6	Ideal Gas Thermodynamic Properties of Acetone	121
C7	Ideal Gas Thermodynamic Properties of Acetic Acid	122
C8	Ideal Gas Thermodynamic Properties of Acetaldehyde	123
C9	Ideal Gas Thermodynamic Properties of Acetylene	124
C10	Ideal Gas Thermodynamic Properties of Carbon Dioxide	125
C11	Ideal Gas Thermodynamic Properties of Water	126
C12	Enthalpy, Gibbs Energy, and Equilibrium Constant at Various Temperatures, Reaction Number 1	127
C13	Enthalpy, Gibbs Energy, and Equilibrium Constant at Various Temperatures, Reaction Number 2	128
C14	Enthalpy, Gibbs Energy, And Equilibrium Constant at Various Temperatures, Reaction Number 3	129
C15	Enthalpy, Gibbs Energy, and Equilibrium Constant at Various Temperatures, Reaction Number 4	130

+ + + + +
+ + +

NOMENCLATURE

$A_1 \dots A_5$,	
$B_1 \dots B_5$,	Martin-Hou Constants
$C_1 \dots C_5$,	
and b	
C	Carbon
C_p	Heat capacity
F	Total flow rate (feed)
G	Gibbs energy
H	Enthalpy
ΔH_R	Heat of reaction
K_1, K	Equilibrium constant
P	Total pressure
R	Gas constant
R	Reactant mole ratio, acetylene to acetic acid
S	Selectivity, entropy
T	Temperature
V	Volume
W	Weight of the catalyst
X	Conversion of acetic acid
Y	Yield
d	Distance between each set of atomic planes of the crystal lattice
g	Gas
k	Rate constant

k_1, k_3	Adsorption constants
k_2	Adsorption constant, rate constant
m	Order of diffraction
p	Partial pressure
r	Rate of reaction, pore radius
\bar{r}	Mean pore radius
s	Solid
x	Mole fraction

Greek Symbols

ϕ	Function
ν	Fundamental stretching frequency
θ	Angle of diffraction
μl	Microlitres
μ	Microns
λ	Wave length of x-ray beam
δ	In-plane bend frequency
γ	Out-of-plane bend frequency
τ	Torsional frequency

Subscript

A	Acetic acid
B	Acetylene
C	Critical properties
R	Vinyl acetate
S	Surface

o Property at 0°K

a Assymmetric

s Symetric

Superscript

o Property of ideal gas at 1 atm pressure

VAPOR PHASE ACETYLATION OF ACETIC ACID TO VINYL ACETATE

- I. Characterization of $Zn(OAc)_2$ -C System,
- II. Kinetics and Mechanism,
- III. Thermodynamic Properties

A THESIS SUBMITTED
IN PARTIAL FULFILMENT OF THE REQUIREMENT
FOR THE DEGREE OF
DOCTOR OF PHILOSOPHY
by
HARI BHAGWAN GOYAL

to the
DEPARTMENT OF CHEMICAL ENGINEERING
Indian Institute of Technology, Kanpur
MAY 1976

SYNOPSIS

The thesis consists of three major sections. Section I deals with the physicochemical characterization of zinc acetate-activated carbon system. Carbon supported catalysts-containing up to 25 weight per cent metal acetate were prepared by the impregnation technique. Section II deals with the kinetics and catalytic activity of zinc acetate-activated carbon system for the vapor phase acetylation of acetic acid to vinyl acetate. Calculations of the ideal gas thermodynamic properties of vinyl acetate and crotonaldehyde are dealt in section III.

The vapor phase acetylation of acetic acid to vinyl acetate over zinc, cadmium and nickel acetates supported on

activated carbon were examined at 180°C. The catalytic activity increased as follows: $Zn^{2+} > Cd^{2+} > Ni^{2+}$

Supported zinc acetate on carbon catalysts containing up to 25 weight per cent zinc acetate have been studied by means of DTA, TGA, x-ray, IR and BET techniques in a wide temperature range (100° - 1000°C). Evidence is presented for a monolayer deposition up to about 15 per cent zinc acetate. The zinc acetate species, present in the dried catalyst did not interact with the carrier to form any stable carbon-zinc acetate complexes at the surface. The zinc acetate peaks were well defined.

The heterogeneous interaction of acetylene and acetic acid with activated carbon based catalysts containing up to 25 weight per cent zinc acetate have been investigated in an isothermal packed bed reactor at atmospheric pressure between 155° - 200°C. The effect of several variables, molar feed ratio of acetylene to acetic acid, reaction temperature and the reciprocal of space velocity on the conversion and product distribution were examined by gas chromatography.

Though 15 different mechanisms were postulated, the rate of reaction was most satisfactorily correlated by a mechanism of surface reaction between charged adsorbed acetic acid and acetylene, which assumes that the rate-controlling step was the irreversible charged adsorption of acetylene and acetic acid.

$$\text{rate} = \frac{K_A p_A}{1 + \left(\frac{K_A}{K_B}\right) \left(\frac{p_A}{p_B}\right)}$$

where K_A and K_B are adsorption equilibrium constants for acetic acid and acetylene, respectively.

Complete vibrational assignments and calculations of the ideal gas thermodynamic properties of vinyl acetate and crotonaldehyde have been made for the first time from 298.15 to 1500°K using the literature information on the fundamental frequencies and the molecular parameters. Internal rotational contributions due to CH_3 -group have been obtained for both the molecules using Pitzer and Gwinn's tables.

For vinyl acetate the departure functions, that is, the difference between the real gas and the ideal gas property, have been computed using the Martin-Hou equation of state. As the pressure-volume-temperature data are not available for this compound, the Martin-Hou constants have been predicted from the critical constants and the vapor pressure-boiling point data of vinyl acetate. These departure functions in combination with the ideal gas properties will give the values of the real gas thermodynamic properties of vinyl acetate. It is hoped that in the absence of the experimental values, these predicted values will be of use to the design engineer.

+++

INTRODUCTION

Vinyl acetate an industrially important monomer is polymerized into polyvinyl acetate which is used in latexes, emulsion paints, adhesives, and various paper and textile coatings, or further processed into polyvinyl alcohol or polyvinyl butyral. Part of vinyl acetate produced is also copolymerized with vinyl chloride, ethylene and other monomers.

There are five different processes for making vinyl acetate (1-4). These processes are differentiated primarily by their feed stock requirements.

1. Acetylene-acetic acid liquid phase process
2. Acetylene-acetic acid vapor phase process
3. Acetaldehyde-acetic anhydride process
4. Ethylene-acetic acid liquid phase process
5. Ethylene-acetic acid vapor phase process.

Until 1967, the acetylene vapor phase route accounted for most of the production of vinyl acetate. The ethylene route became operational in 1967 and because of the lower cost of ethylene as compared to acetylene offered attractive economics. However, the investment cost is stated to be about 50 per cent higher than for an acetylene-based plant. Electrical energy consumption is also higher. The picture

changed considerably in recent years. Also the countries who do not have adequate petroleum reserves but have large coal reserves need to seriously consider the acetylene route.

In the vapor phase acetylene route, purified acetylene is mixed in excess with acetic acid in the vapor state and then fed to a fixed bed or a fluidized bed reactor using zinc acetate on activated carbon as the catalyst. The operating conditions are: temperature, 180-200°C; pressure, slightly above atmospheric. It is an exothermic reaction, the enthalpy of reaction being $-23.4 \text{ kcal mol}^{-1}$. The selectivity of the zinc acetate catalyst is high and hence small amount of side products are formed, namely, acetone, acetaldehyde, crotonaldehyde, water and ethylidine diacetate. The separation of vinyl acetate from the reaction products is achieved either by fractional distillation or by liquid-liquid extraction. The yield of vinyl acetate varies from 92 to 95 per cent based on acetylene and from 97 to 99 per cent based on acetic acid (1-4).

India imports all its requirements of vinyl acetate at present. Because of the availability of the raw materials, it was felt that the vapor phase acetylene-acetic acid technology should be developed in India. The present investigation is the first step in this direction.

The objective of the present investigation was to characterize zinc acetate-activated carbon catalysts, study the kinetics and mechanism of the vapor phase acetylene - acetic acid reaction with the proposed catalyst, and to compute the required thermodynamic properties not available in the literature for the substances involved for process engineering calculations. For the separation of vinyl acetate from other reaction products some vapor liquid equilibrium studies have already been carried out in this laboratory (5). This information could then be used for modelling and scale-up which would be the second step in achieving the ultimate objective of providing the complete technical know-how for this process.

The present investigation consists of three major sections. Section I deals with the physicochemical characterization of zinc acetate -activated carbon system. Carbon supported catalysts containing up to 25 weight per cent metal acetate were prepared by the impregnation technique. Section II deals with the kinetics and catalytic activity of zinc acetate-activated carbon system for the vapor phase acetylation of acetic acid to vinyl acetate. Calculations of the real gas and the ideal gas thermodynamic properties of vinyl acetate and the ideal gas thermodynamic properties of crotonaldehyde are dealt in section III.

SECTION I

CHARACTERIZATION OF $\text{Zn}(\text{OAc})_2$ - C SYSTEM

1.1 INTRODUCTION

Catalysts based upon $Zn(OAc)_2$ -C are remarkable for the acetylation of acetic acid to vinyl acetate. Very little work has been reported in the literature concerning the physicochemical properties of these catalysts. All those reported have been carried out mainly by the Russian and Japanese workers (6-13).

Surface area and pore structure of $Zn(OAc)_2$ -C catalyst have been discussed by Yamada (9). Recently, Liverovskaya, et al (13) have presented some data on the particle size and specific surface of various types of carbon, containing varying amounts of zinc acetate.

There appears to be no prior detailed study on the solid state properties of $Zn(OAc)_2$ -C system. In order to contribute to the literature and to clear up some aspects concerning the nature of the active sites in relation to the catalytic activity, investigations have been carried out with a series of supported $Zn(OAc)_2$ -C catalysts; proper choice of the support has allowed studies of compositions up to 25 weight per cent zinc acetate.

This investigation comprised the measurements of specific surface area, capillary structure, DT and TG analysis, infrared, and x-ray analysis. The acetylation of acetic acid has been chosen as the test reaction and its kinetics were studied (Section II).

1.2 EXPERIMENTAL METHODS

1.2.1 Preparation of catalysts

For vinyl acetate manufacture from acetylene and acetic acid suitable catalysts include zinc or cadmium acetates, mercuric chloride, and others (2). These compounds may be supported on carriers such as activated carbon, wood charcoal, silica gel, activated alumina, etc. An improved technique for catalyst manufacture has been described by Bristol and Call (14). It comprised of dry mixing of zinc oxide powder and activated carbon, contacting the mixture with at least 4.5 mols of acetic acid and drying the catalyst by agitating under reduced pressure. They have claimed increased productivity and less lump formation.

The overall procedure followed for making the catalyst was divided in two steps:

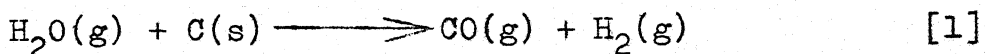
- (a) Preparation of activated carbon.
- (b) Preparation of catalyst.

(a) Preparation of activated carbon:

The catalyst support activated carbon, was prepared in the laboratory using the steam activation technique. The basic idea of activating the carbon was to remove non carbonaceous impurities from the surface and the pores, and thus providing more surface area and high adsorption power to the carbon.

Coconut shells were used as the raw material. As described by Hassler (15) it is a very suitable starting material for gas adsorbing granular carbon. The first step in activation was the 'charring' of shells. The term refers to the partial oxidation by burning the shells, which is carried out in order to obtain a material with a high carbon content (about 90 per cent carbon) which may then be subjected to activation and further oxidation (16).

During the activation with steam the reaction between water vapor and carbon, even at temperatures as high as 700°C , involves first the adsorption of H_2O on the carbon surface, followed by evolution of CO and H_2 . The CO is the most difficult energetically to remove from the surface. The overall reaction can be expressed as,



and the rate expression for reaction [1], can be given by

$$\text{Rate} = \frac{k_1 p_{\text{H}_2\text{O}}}{1 + k_2 p_{\text{H}_2} + k_3 p_{\text{H}_2\text{O}}} \quad [2]$$

According to Strickland-Constable (17) the rate determining step in the mechanism is the slow desorption of CO from the surface.

In the laboratory the activation was carried out by suspending a bulk of carbon granules, packed in a 5 cm diameter and 25 cm long 316 stainless steel tube, in a furnace

heated up to 900°C. The steam was passed at the bottom of the stainless steel tube holder. The activation of each batch was carried out for about two hours and then the furnace was cooled and activated carbon was screened and stored.

(b) Preparation of catalyst:

During the preparation of metal acetate on activated carbon catalysts, the equipments used were rotary vacuum film evaporator and water ejector. For zinc acetate catalyst, calculated amount of zinc oxide based on the percentage of zinc acetate required in the final product, was dry mixed with 100 grams of granular activated carbon in the rotary vacuum film evaporator for one hour. Glacial acetic acid, in weight ratio of two to one to zinc oxide, and water in approximate weight ratio of two and a half to one to acetic acid, were added. For example, to prepare 15 per cent $Zn(OAc)_2$ sample the following proportions were required; 7.84 grams of zinc oxide, 15.5 grams of acetic acid, 100 grams of carbon and 40 grams of water. The whole mixture was agitated for one hour for completion of the reaction between acetic acid and zinc oxide to form zinc acetate on the surface of carbon. The whole mass was dried by agitating at 60°C under vacuum. The vacuum was applied with the help of water ejector. The catalyst was further heated up to 150°C.

In the case of cadmium and nickel acetate catalysts, calculated amount of cadmium or nickel acetates based on percentage required, was dry mixed with 100 grams of activated carbon in rotary vacuum film evaporator. Calculated amount of water was added, agitated, and the whole mass was dried by agitating under vacuum at 60°C followed by heating up to 150°C .

1.2.2 Physicochemical Characterization

(a) X-ray powder analysis:

Each atom in a crystal has the power of scattering an x-ray beam incident on it. The sum of all the scattered waves in the crystal results in the x-ray beam being, in effect, diffracted from each allowed crystal plane. Every crystalline substance scatters the x-rays in its own unique diffraction pattern, producing a 'fingerprint' of its atomic and molecular structure. The intensity of each reflection forms the basic information required in crystal structure analysis. One unique feature of x-ray diffraction is that components are identified as specific compounds.

Virtually monochromatic radiation is obtained by reflection of x-rays from crystal planes. The relationship between the wave length of x-ray beam, the angle of diffraction, and the distance between each set of atomic planes of the crystal lattice d , is governed by the Bragg condition,

$$m\lambda = 2d \sin \theta$$

[3]

where m represents the order of diffraction. First order diffraction is, usually, used for structure study.

The x-ray diffraction patterns were recorded using a General Electronics Diffractometer (XRD-VI generator, SPG-4 detector and SPG-2 diffractometer) with copper (K_{α}) radiation. The diffractometer was operated with 2° diverging and receiving slits at a scan rate of 1° per minute and a continuous trace of intensity as a function of 2θ was recorded. The accuracy of Bragg's angle positions were checked using a permoquartz standard sample. Spectra of finely ground samples were run in the 2θ range $10 - 80^{\circ}$.

(b) Infrared spectroscopy:

The range in electromagnetic spectrum extending from 0.8 to 200μ is referred to as the infrared. Most organic and inorganic materials show absorption and, in all but a few cases, this absorption includes several characteristic wavelengths. In fact, the infrared spectrum is one of the most characteristic properties of a compound. It provides a fingerprint for identification and a powerful tool for the study of molecular structure.

Transmittance spectra for powder samples (400 mesh) were recorded on a Perkin-Elmer - 137 Grating IR spectrophotometer using KBr disc.

(c) TG and DT Analysis:

Thermogravimetric analysis (TGA) involves changes in weight of a system under investigation as the temperature is increased at a predetermined rate. Differential thermal analysis (DTA) consists of measuring changes in heat content, as a function of the difference in temperature between the sample under investigation and a thermally inert reference compound, as the two materials are heated to elevated temperatures (or cooled to subnormal temperatures) at predetermined rate. In this manner enthalpic changes, such as melting, vaporization, crystallographic phase transition, or chemical changes, are detected from the endo-and exothermal bands and peaks that appear on the thermograms. The corresponding weight changes are detected by TGA.

DTA measurements were carried out on a Dupont 900 apparatus equipped with high temperature cell using calibrated Platinum/Platinum-13 per cent Rhodium thermocouples. TGA was performed on Cahn Thermo-Gravimetric apparatus, with programmed temperature increase, under atmospheric conditions.

(d) Surface area, pore volume and pore size distribution:

Surface area (SA) and pore structure (V_p and PSD) of catalysts are of major importance to catalysis since catalytic rates depend primarily on available active surface. Pore structure affects surface access, surface stability, and

resistance to poisoning, and selectivity as well as heat transfer. To correlate adsorption data and to determine the surface area, the multimolecular adsorption equation of Brunauer, Emmett and Teller (BET) is often applied.

Surface area of powdered catalysts were calculated from N_2 adsorption isotherms using BET apparatus. Pore volume and pore size distribution were measured by a mercury porosimeter, Carlo-Erba Model-70 for the 2000 atmosphere range.

1.3 RESULTS AND DISCUSSION

Reference to the various samples will be made by giving their composition as weight per cent Zn^{2+} : hence $Zn^{2+}-025$ means a sample of zinc acetate supported on activated carbon having 25 per cent of the active element as $Zn(OAc)_2$.

1.3.1 X-ray powder spectra:

The prepared samples of zinc acetate were examined under x-ray to determine the purity. The 'd' values for zinc acetate are given in Table 1, calculated from x-ray powder diffraction patterns. The 'd' values are in excellent agreement with 'd' values reported for zinc acetate (ASTM 1-0089). The x-ray diffraction pattern showed that the prepared samples have pure zinc acetate and there was no impurity within the detection limit of the x-ray.

The x-ray powder spectrum of the $Zn^{2+}-015$, $Zn^{2+}-020$ and $Zn^{2+}-025$ samples showed the presence of crystalline zinc

TABLE 1: 'd' VALUES FOR ZINC ACETATE

ASTM 1-0089 'd' Values (\AA)	Calculated 'd' Values (\AA)
7.50	7.496
4.55	4.529
4.02	3.926
3.68	3.693
3.46	3.477
3.28	3.267
3.12	3.143
2.90	2.949
2.80	2.735
2.72	2.622
2.50	2.495
2.29	2.165

acetate. The intensity of diffraction peaks were increased with the increase in the concentration of zinc acetate in the samples. In the 5-10 wt per cent samples the diffraction peaks of zinc acetate fell below the detection level. Powder spectra of all catalyst samples showed the absence of the characteristic diffraction bands of zinc oxide and hydrated molecules of zinc acetate.

1.3.2 Infrared spectra

Intensities of the various frequencies recorded by the transmittance techniques are given in Table 2. Slight differences are apparent in the case of pure compound, at variance with supported catalysts, which show distinct surface and bulk structures.

The stretching vibrational frequencies of the C-O and C-C bonds and the deformation vibration of the CO_2 are listed in Table 2, which includes the corresponding frequencies of the hydrated species. The spectrum of the prepared catalysts is very close to that of anhydrous zinc acetate (18-20). X-ray spectrum agrees with this structure.

In the highest zinc acetate concentration (25 weight per cent Zn(OAc)_2) the transmittance spectra showed distinct absorptions at 1540, 1440, 950 and 694 cm^{-1} , which are attributable to free zinc acetate present in the bulk. The decrease in the zinc acetate concentration leads to the

TABLE 2: INFRARED FREQUENCIES (Cm⁻¹) OF Zn(OAc)₂-C CATALYSTS^a

Compound	Assignment (4-Atom System) and Description				
	C - O Stretching		C - CH ₃	COO	Bending
	Antisym, γ_8	Sym, γ_3			
Zn(OAc) ₂ (Model Compound)	1545		1446	954	694 (18-20)
Zn(OAc) ₂ · 2H ₂ O (Model Compound)	1550		1456	955	695 (18)
Zn(OAc) ₂ (Prepared)	1540 (vs)		1440 (s)	950 (m)	694 (s)
Zn ²⁺ - 025	1540 (s)		1440 (m)	950 (m)	694 (w)
Zn ²⁺ - 020			()	950 (m)	694 (w)
Zn ²⁺ - 015			1600-1400 (s, b)	950 (w)	694 (w)
Zn ²⁺ - 010			1600-1400 (s, b)	950 (w)	694 (w)
Zn ²⁺ - 005			no absorption		

^avs, very strong; s, strong; m, medium; w, weak; b, broad

absorptions which concentrate in a broad band in the 1600 - 400 cm^{-1} region. The supported catalyst of 5 weight per cent zinc acetate did not show any diagnostic vibrational frequency.

1.3.3 DT and TG analysis

A programmed heating at a rate of 15 $^{\circ}\text{C}$ per minute between 25 $^{\circ}$ and 1000 $^{\circ}\text{C}$ was used. The DTA thermograms for the catalysts are shown in Figure 1. The thermograms revealed three regions of thermal activity: (i) a weak endotherm peaking near 100 $^{\circ}\text{C}$ very similar in appearance to the 100 $^{\circ}\text{C}$ endotherm observed for the bare carbon, (ii) a strong and broad exotherm between 400 $^{\circ}$ and 800 $^{\circ}\text{C}$ peaking near 508 $^{\circ}\text{C}$, and (iii) a medium and broad endotherm (depending upon the composition of the catalyst) between 220 $^{\circ}$ and 360 $^{\circ}\text{C}$ peaking near 280 $^{\circ}\text{C}$. The thermogram for pure zinc acetate exhibited a sharp endotherm of medium strength between 220 $^{\circ}$ and 340 $^{\circ}\text{C}$ peaking at 280 $^{\circ}\text{C}$ and 320 $^{\circ}\text{C}$. The peaks at 280 $^{\circ}$ and 310 $^{\circ}\text{C}$ are due to the decomposition of zinc acetate to ZnO and Ac_2O , and to ZnO and acetone, respectively. The results of the catalysts also agree with this; however, the intensity of the endotherms depend upon the composition of the catalyst. The peak in the 500 $^{\circ}\text{C}$ region represents burning of the carbon.

TG analysis was performed with programmed temperature increase at a rate of 10 $^{\circ}\text{C}$ per minute. The per cent weight changes as a function of temperature are illustrated in Figure 2.

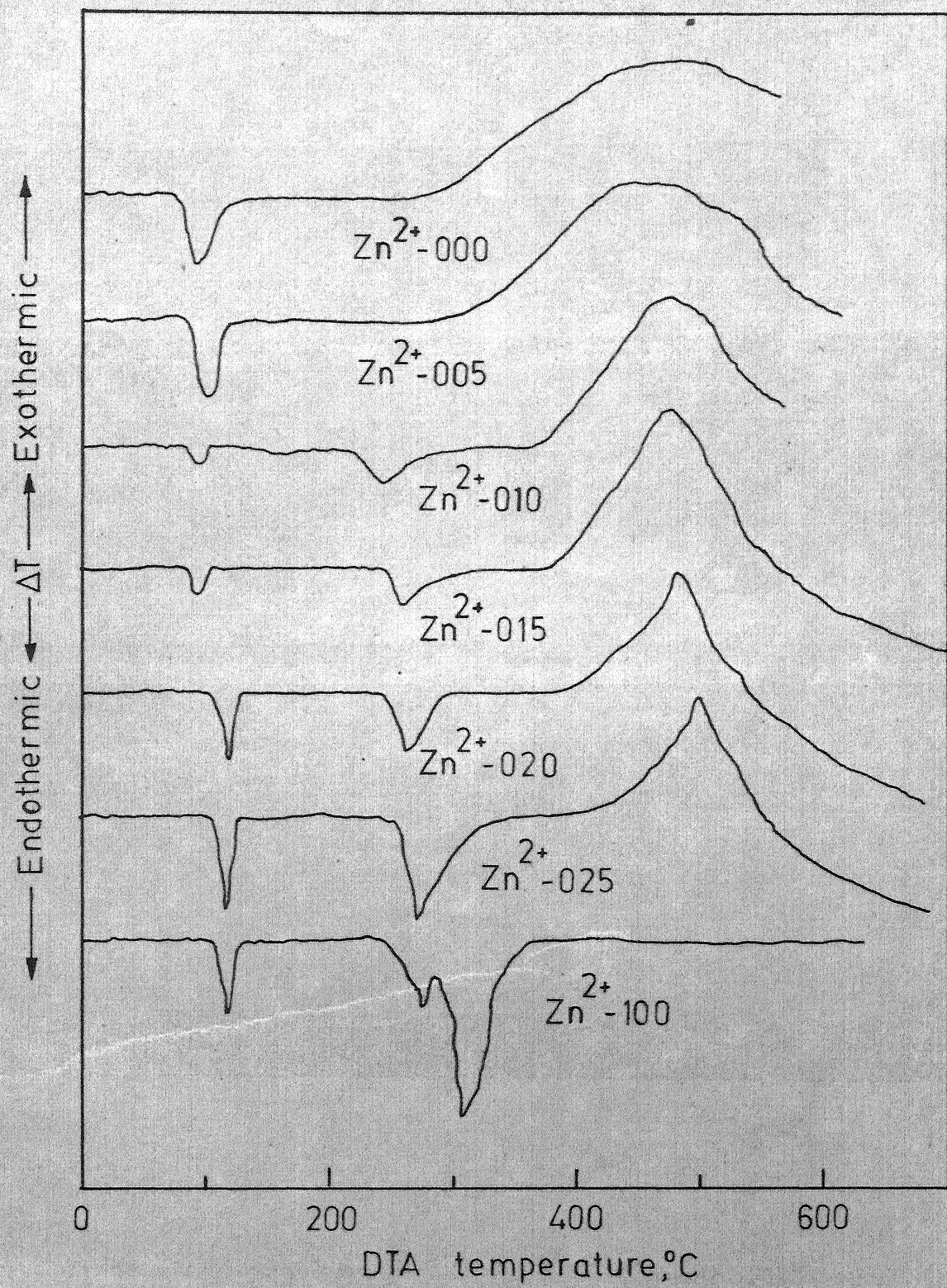


Fig. 1 - Differential thermal analysis thermograms.

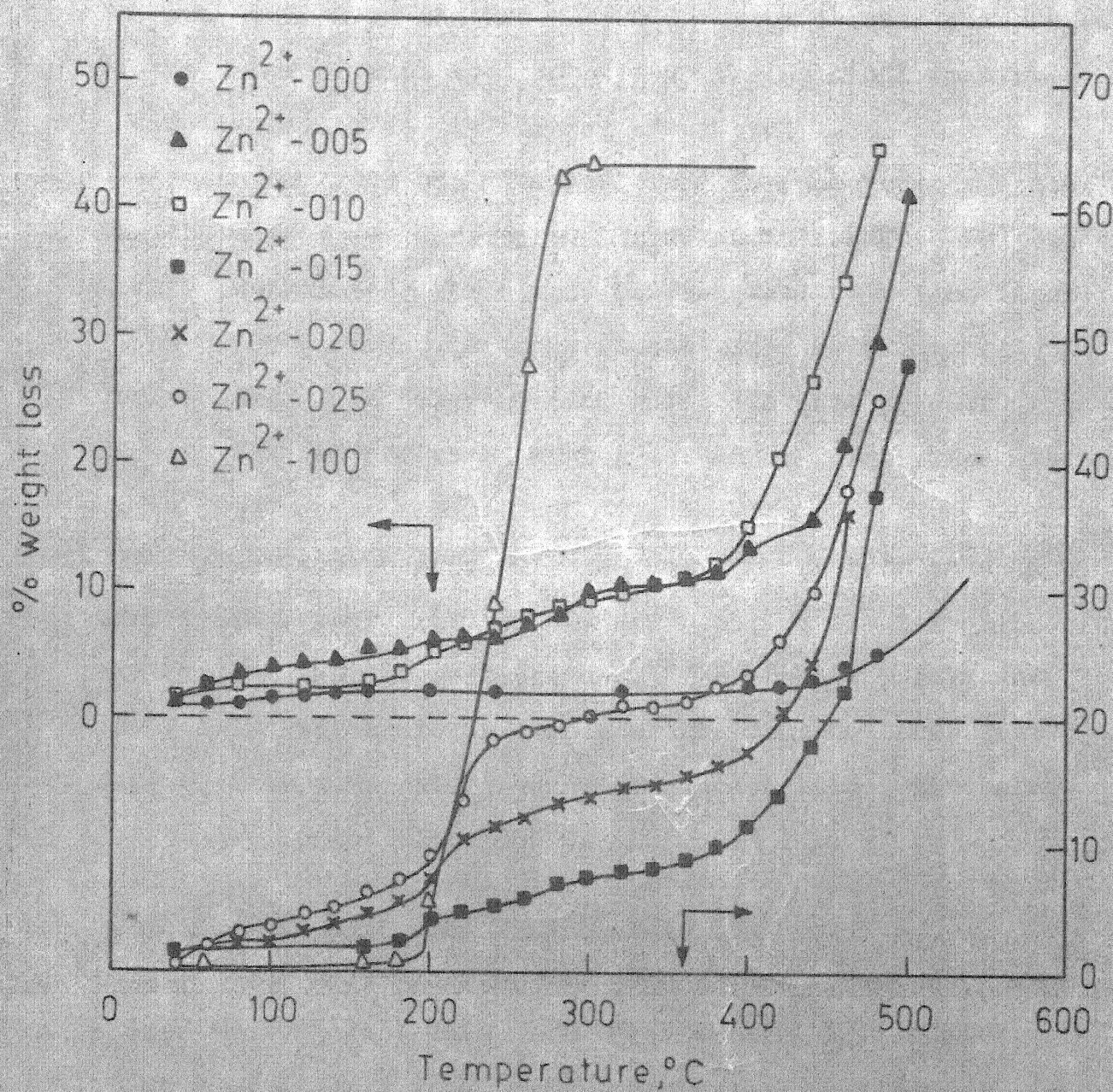


Fig. 2 - Thermogravimetric analysis - percentage weight loss of $\text{Zn(OAc)}_2\text{-C}$ system as function of temperature.

The weight loss in the 200° - 320°C region is mainly because of the decomposition to zinc oxide. The weight loss above 400°C is mainly due to burning of carbon.

An analysis was also performed for pure zinc acetate. The thermogram was flat up to 180°C . Between 200° and 300°C a sharp weight loss was observed. The observed weight loss of about 60 per cent is in agreement with the calculated weight loss of 56 per cent (ZnO being the sole product). The results for the activated carbon showed no weight loss except above 400°C .

The decomposition of zinc acetate has been studied by Edward and Hayward (19) by TGA and reported the formation of ZnO at 350°C as the sole product. The present results of DTA and TGA which are in complete agreement by themselves confirm this temperature range of decomposition, ZnO being completely formed below 350°C .

1.3.4 Surface area and pore distribution

Results obtained by BET and mercury porosimetry are presented in this section. Surface areas (SA) and pore volumes (V_p) for all the catalyst samples are given in Table 3 together with the calculated values of the mean pore radii ($\bar{r} = 2V_p/\text{SA}$). Values of SA for the samples are plotted in Figure 3 against values calculated on the basis of the contribution of activated carbon only. Figure 3 shows

TABLE 3: SURFACE AREA, PORE VOLUME AND AVERAGE PORE RADIUS OF
VARIOUS CATALYSTS

Compounds	Specific Surface Area, $\text{m}^2 \text{ gm}^{-1}$	Pore Volume ^a , $\text{cm}^3 \text{ gm}^{-1}$	Average Pore Radius, Å
$\text{Zn}^{2+} - 000$	594.1	0.300	10
$\text{Zn}^{2+} - 005$	397.0	0.300	15
$\text{Zn}^{2+} - 010$	170.0	0.232	27
$\text{Zn}^{2+} - 015$	482.0	0.250	10
$\text{Zn}^{2+} - 020$	104.0	0.201	39
$\text{Zn}^{2+} - 025$	55.0	0.200	73

^aReferred to 1500 atm.

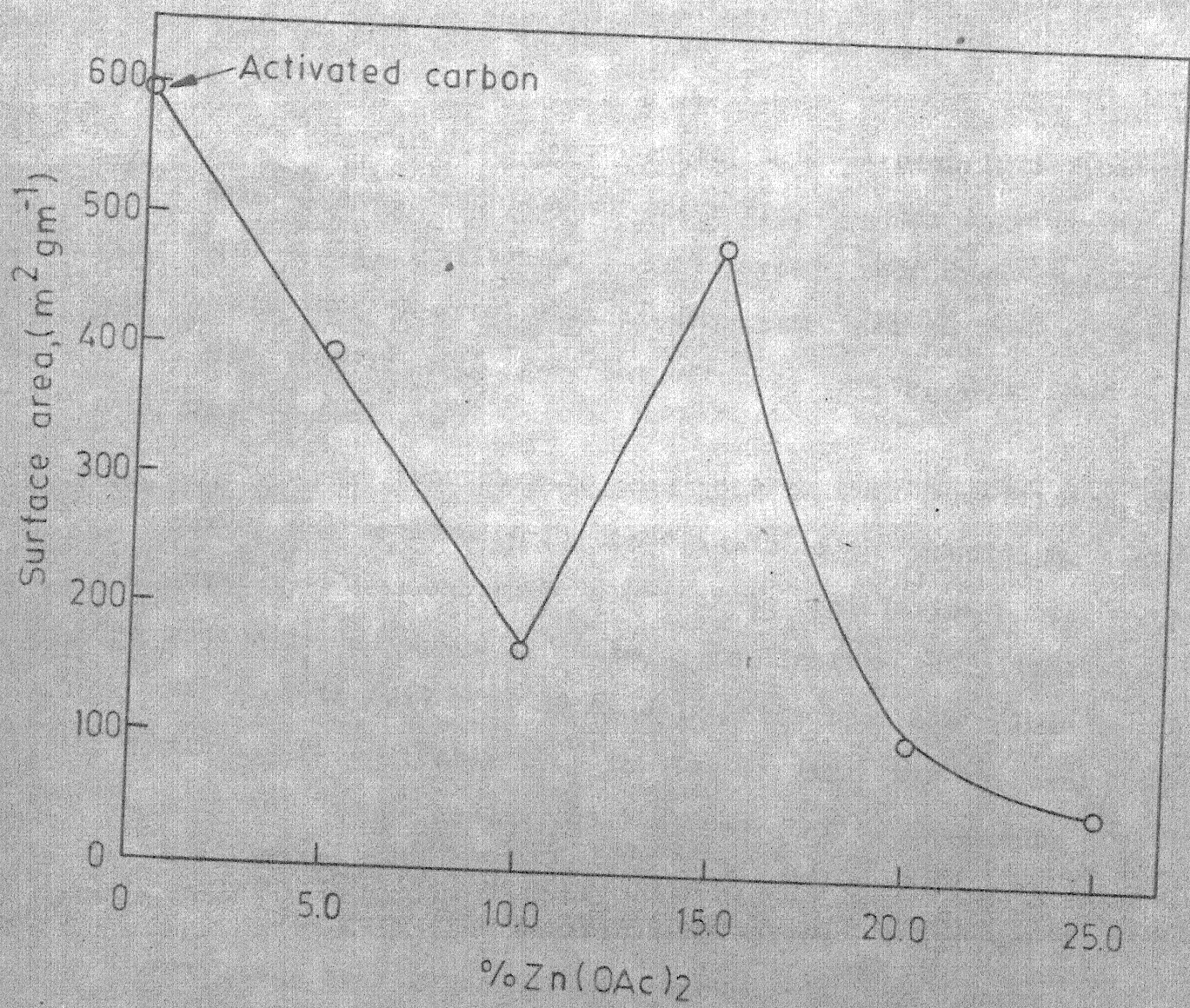


Fig. 3 - Surface area as function of Zn(OAc)_2 composition.

variation of surface area with a reproducible discontinuity at 15 per cent and an almost linear decrease in the range of 0 - 10 per cent.

The curves represented in Figure 4 clearly indicate that $Zn(OAc)_2$ deposited on the surface of carbon plugs at first small capillaries. As its amount increases, capillaries of greater and greater radii are closed and in the catalyst containing 15 to 20 per cent of zinc acetate, large capillaries dominate.

It is necessary to point out that differentiation of curves represented in Figure 4 leads to the conclusion that greater values should be ascribed to capillaries whose radius is below 100 \AA^0 . This is in disagreement with the value of the order of 10 \AA^0 , calculated from the volume to surface ratio (Table 3). The latter value was however computed on the assumption that capillaries have tube like shape.

The pore size distribution curves for all the catalysts are given in Figures A1 - A6, Appendix A.

An important point of discussion is whether zinc acetate is present on the surface of carbon as a monolayer, as a distinct phase in the form of clusters, or as interaction products with the carriers. Surface areas and pore volumes of the samples up to 15 weight per cent favor undoubtedly the monolayer deposition as they fit closely values calculated

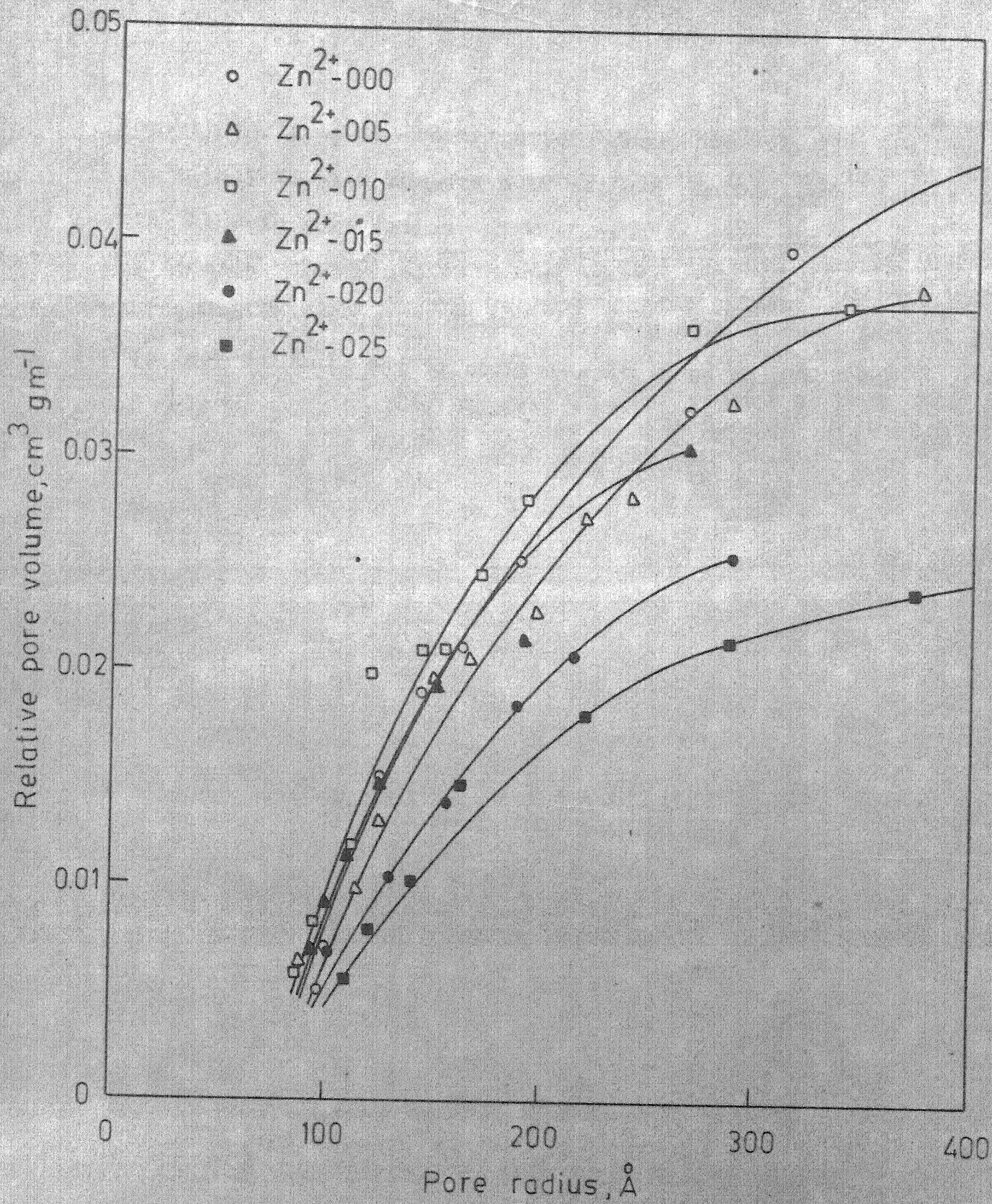


Fig. 4 - Relative volume of capillaries as function of capillary radius.

on the basis of the contribution of support only (Figure 3). In catalysts with more than 15 per cent $Zn(OAc)_2$ the increase in the mean pore radius and surface area suggests other processes. X-ray and IR failed to identify the formation of any well defined compound. It is possible that clustering as free $Zn(OAc)_2$ may be occurring at these compositions.

+ + + + +

+ + +

SECTION II

KINETICS AND MECHANISM

2.1 INTRODUCTION

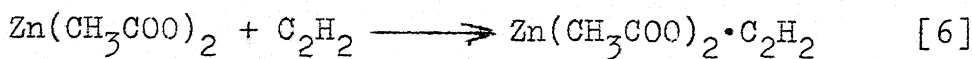
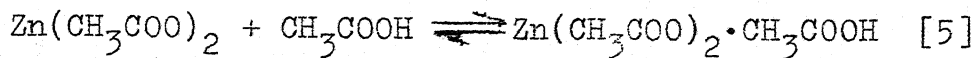
During the last 25 years, increasing attention has been given to the vapor phase catalytic acetylation of acetic acid to vinyl acetate. However, the entire source of literature on this subject is either in Russian or in Japanese. Among the various studies reported, there is wide disagreement in the reported data, and kinetics of the reaction are still not well understood (7,8,10,13,21-34).

Furukawa (21) carried out kinetic measurements at 200°C in a flow system on a zinc acetate-activated carbon catalyst. The order of the reaction with respect to acetylene was 1.65, and 0.65 with respect to acetic acid. From an investigation of the same reaction on a similar catalyst Janada and Vanko (26) obtained a second order equation. Also, from a similar study at 120 mm and 160°C it has been suggested (23, 24) that the rate proceeds according to,

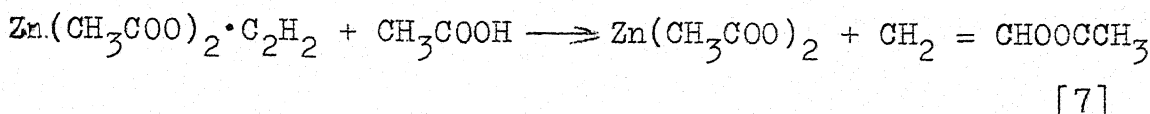
$$r = \frac{k p_{C_2H_2} p_{CH_3COOH}}{(1 + K p_{CH_3COOH})^2} \quad [4]$$

The reaction on the surface is the rate controlling step.

Based on the theory that reaction of acetylene and acetic acid takes place via intermediate formation of complexes of metal salts i.e. catalysts with acetylene and acetic acid, Vasileva et al. (34) have examined the general scheme of the reaction mechanism by analogy with the hydro-chlorination of acetylene (39).



Reaction between the complex of this salt with acetylene and acetic acid gives the following products:



They assumed that the formation of a complex with acetylene by reaction [6] is the limiting stage of the process and derived a rate law given by,

$$r = k_2 \frac{p_{\text{C}_2\text{H}_2}}{1 + K_1 \frac{p_{\text{CH}_3\text{COOH}}}{p_{\text{C}_2\text{H}_2}}} \quad [8]$$

where k_2 is the rate constant of the limiting stage, and K_1 is the equilibrium constant of reaction [5]. At temperatures above 180°C , reaction is not retarded by acetic acid and equation [8] becomes a first order equation:

$$r = k_2 p_{\text{C}_2\text{H}_2} \quad [9]$$

The chemisorption of acetylene is the rate determining step in the kinetics of the acetylene, acetic acid reaction (8, 22, 28, 30, 31).

In addition to the heterogeneous mechanisms, a homogeneous route involving free radicals is also believed to be involved (10).

It is very probable that one of the causes of the discrepancy between the reported results of kinetic measurements is inadequate isothermicity of the catalyst layer; in the given case this is an important factor, as the reaction is highly exothermic ($\Delta H_{298} = -23.4 \text{ kcal mol}^{-1}$). These discrepancies may also be due to the mass transfer limitations, component concentrations, and high conversions.

With increasing concentration of zinc acetate (30), the activity is proportional to the specific surface area and approximately to the cube of the zinc acetate concentration; but the surface area decreases exponentially with increase in zinc acetate concentration, and a decrease in activity at higher concentrations. The decrease of surface area with increase in zinc acetate is also reported by Mitsutani and Kominami (8). On the contrary Nakamura et al. (32) reported that the rate was independent of the amount of zinc acetate deposited on the catalyst.

The body of results (8,13,30,32) from all these investigations has concurred in indicating singularities in catalytic activity as a function of composition, thus justifying attempts to clear up relationship with its properties.

In this work, the reaction between acetylene and acetic acid was studied in the temperature range of $150^\circ - 200^\circ\text{C}$ using zinc acetate supported on activated carbon catalyst. The size of the support, the metal acetate content of the

catalyst, and the reactor dimensions were made small enough to eliminate mass and heat transfer effects and permit a study of the intrinsic kinetics. In addition, an attempt has been made to correlate the results of this acetylation with the studies on the properties reported in Section I.

2.2 EXPERIMENTAL

Preliminary runs were carried out in a 2.5 cm dia and 120 cm. length packed bed reactor with zinc acetate supported on carbon catalyst. The conversion per pass obtained in the series of runs at 180°C was more than 50 per cent. With the success of these experiments it was then decided to study in detail the kinetics of the reaction employing the catalyst developed in this laboratory. The laboratory reactor was fabricated without giving any consideration to high conversion and yield. An overall description of the experimental apparatus, followed by detailed description of individual pieces is given below.

2.2.1 Overall description

A general schematic diagram of the experimental equipment is shown in Figure 5.

The basic apparatus consisted of a fixed bed reactor, flowmeters, control valves, purifier, driers, vaporizer, and condensers. All equipments were made of glass and interconnected

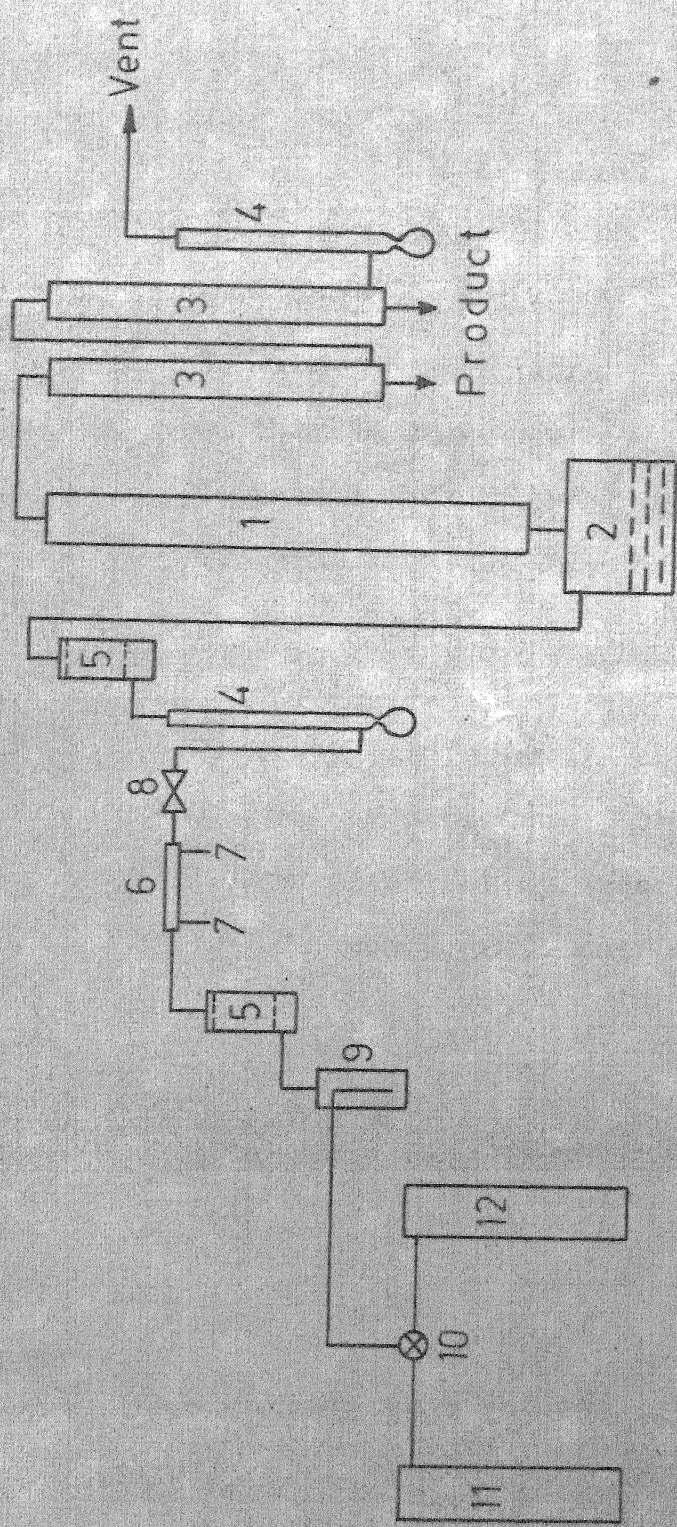


Fig. 5 - Schematic diagram of the experimental set-up.

KEY TO FIGURE 5

1. Test Reactor
2. Acetic Acid Vaporizer
3. Product Condensers
4. Soap Bubble Meters
5. Silica Gel Driers
6. Capillary Flow Meter
7. Manometer
8. Needle Valve
9. Acetylene Purifier
10. Two Way Stop Cock
11. Acetylene Gas Cylinder
12. Nitrogen Gas Cylinder

with ground glass joints, polyethylene and silicon rubber tubings. The following capabilities and characteristics are provided for:

- (i) The flow rate of acetylene can be controlled relatively accurately for flows to less than 1 per cent.
- (ii) The temperature of the reactor can be controlled to within $\pm 0.5^{\circ}\text{C}$.
- (iii) The heat evolved in the exothermic reaction did not affect the temperature of the reactor.
- (iv) The output response from the thermocouples had been measured accurately by means of a Honeywell potentiometer.
- (v) The product was completely condensed in the condensers.

2.2.2 Reactor

The jacketed reactor was 1.25 cm diameter and 60 cm long, provided with flexible preheating zone of maximum length of 16 cm. The preheating zone contained a 316 stainless steel tubing packed with stainless steel foils to provide more heat transfer area. The stainless steel screens of 100 mesh size were attached at both ends of the preheater. A diagram of the reactor is shown in Figure 6.

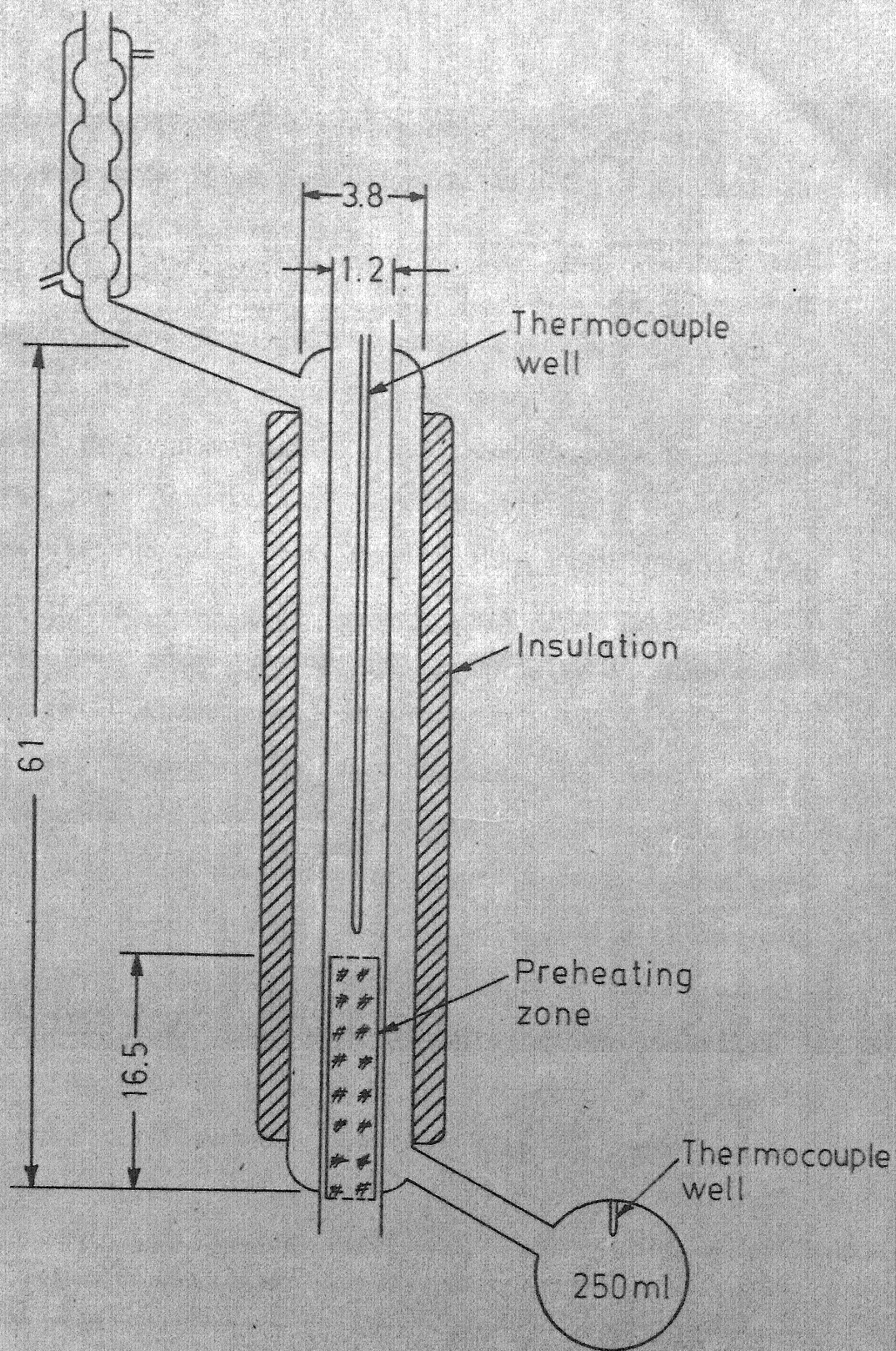


Fig. 6 - Reactor details.
(dimensions in cms)

The temperature in the reactor was maintained by condensing vapors of various organic liquids. The substances used for various temperatures are listed in Table 4.

The organic liquid was heated in a vaporizer. The vapors were passed through the jacket, condensed in the condenser at the top, and refluxed back.

Heating by condensing vapors was found satisfactory in maintaining a constant temperature within $\pm 0.5^{\circ}\text{C}$. Approximately two hours were required to reach the steady state temperature.

The reactor was insulated by wrapping with approximately 5 cms of glass wool and asbestos insulation to minimize heat losses to the surrounding.

Temperatures at various points in the reactor including the catalyst bed and the heating liquid were measured with the help of iron-constantan thermocouples. The thermocouples were calibrated against a 25 ohm Leeds and Northrup platinum resistance thermometer and a resistance bridge assembly.

The reactor was connected to the acetic acid vaporizer and the condenser (product) with the help of ground glass joints (Figure 5).

2.2.3 Acetic acid vaporizer

The vaporizer was a flask of one litre capacity and was heated by heating mantle. The desired temperature

TABLE 4: BOILING POINTS OF ORGANIC SUBSTANCES

Temperature, °C	Substance
155	n-Hexanol
165	2-Methyl cyclohexanol
180	Aniline
192	Ethylene glycol
199	γ -Butyrolactone

of acetic acid was obtained by supplying controlled voltage to the heating mantle.

2.2.4 Flow meters

The calibrated capillary flow meters (capillary size of 0.5 mm) and soap bubble meters were used to measure the flow rate of acetylene.

2.2.5 Condensers

Two double walled condensers were used in series to condense the product gases. Ice water was circulated through the condensers to ensure complete condensation of the products. This was confirmed by gas chromatographic analysis of the condenser exit gases which contained mainly acetylene.

2.2.6 Purifier and driers

Acetylene was passed through a purifier and series of driers. The purity of the gas was checked by gas chromatographic analysis.

PH_3 and NH_3 present in acetylene act as poisons to the catalyst. The purifier was used to eliminate these gases.

The purifier contained a mixture of solutions of 30 per cent CuCl_2 , 30 per cent FeCl_3 and 35 per cent HCl in a volume ratio of 3:7:1. This mixture could be reactivated by adding HCl to maintain 14 per cent HCl in the liquor. The gases from the purifier were dried with indicating blue

silica gel. The deactivated silica gel was replaced and reactivated by heating in the oven at around 100°C . The silica gel also absorbed acetone present in acetylene.

2.2.7 Experimental procedure

The reactor was filled with fresh catalyst and the acetic acid vaporizer was charged with glacial acetic acid. The purifier and driers were filled with purifying solution and silica gel respectively. Nitrogen flow was started primarily to check the leak in the system and also to keep inert atmosphere while the system was heated during the experimentation. The reactor, heated by condensing vapors, and the acetic acid vaporizer were heated up to the required steady state temperature.

Preliminary runs were taken in order to find the temperature of the acetic acid vaporizer at which it gave the required vaporization rate of acetic acid corresponding to a particular flow of acetylene. These runs indicated the temperature of the vaporizer to be maintained in a range of $100\text{-}117^{\circ}\text{C}$.

The flow rate of acetylene was controlled with the help of a brass needle valve (Figure 5). Samples were collected in sample bottles from the product condensers after every half an hour. The sampling bottles were kept in ice. In order to check whether vinyl acetate is

passing through the effluent, the uncondensed product gases were analyzed periodically.

2.2.8 Analysis

The analyses were performed by employing a Perkin Elmer 820 gas chromatograph provided with thermostated temperature control of detector, oven and injector, and temperature programming facilities. The output response of the chromatograph was recorded on a Honeywell recorder. The analysis of each sample required around 25 minutes.

A 300 cm long and 0.64 cm diameter 316 stainless steel tube, packed with 20 per cent FFAP on chromosorb P was used as the analyzing column in the chromatograph. Nitrogen was used as a carrier gas (60 ml per minute flow rate). Temperature of the detector and the injector blocks were maintained at 250°C and 220°C, respectively. Temperature of the oven was kept at 110°C for acetylene, acetone, acetaldehyde, vinyl acetate, benzene, water, and crotonaldehyde elusion. For acetic acid the temperature programming was used from 110° to 160°C at a rate of 16°C per minute. Sample size of 2 μ l was used.

The retention time and area mole factors of various components were found and are given in Table 5.

During the runs, different feed ratios (acetylene/acetic acid) were obtained by adjusting the acetylene flow

TABLE 5: RETENTION TIME AND AREA MOLE FACTORS OF
VARIOUS COMPONENTS

Component	Retention Time (Approx), secs.	Area Mole Factor
Acetaldehyde	90	1.744
Acetone	120	1.000
Vinyl Acetate	155	1.669
Benzene	200	-
Crotonaldehyde	290	0.892
Acetic Acid	8 minutes after the start of temperature programming	1.604

rate in conjunction with the temperature of the vaporizer, while the reciprocal of space velocity was varied by changing the amount of catalyst and the total feed rate.

2.3 RESULTS AND DISCUSSION

Experimental data were obtained by means of an isothermal fixed bed reactor. The steady state was not only realized from the operating conditions but also from the product analysis. There was essentially no deactivation of the catalyst within 12 hrs. X-ray diffraction patterns showed that the used catalyst retained its activity.

Among the byproducts, only acetone was in a measurable quantity. Acetaldehyde and crotonaldehyde were detectable in the gas chromatograph analysis, but the intensities of thermal conductivity were too small for accurate measurements.

The effect of various variables, acetylene to acetic acid in feed (R), reaction temperature (T), the reciprocal of space velocity, (W/F), on the conversion of acetic acid, the yield of vinyl acetate (VA), and the selectivity for vinyl acetate were investigated. The conversion (X), the yield of VA or acetone (Y), the selectivity (S), and the rate of the reaction (r) are defined as follows:

conversion (per cent)

$$= \frac{\text{moles of acetic acid reacted}}{\text{moles of acetic acid fed}} \times 100$$

yield (per cent)

$$= \frac{\text{moles of VA or acetone produced}}{\text{moles of acetic acid fed}} \times 100$$

selectivity (per cent)

$$= \frac{\text{moles of VA produced}}{\text{moles of acetic acid reacted}} \times 100$$

rate of reaction

$$r = \frac{\text{moles of acetic acid reacted}}{(\text{hr}) (\text{gm of catalyst})}$$

2.3.1 Catalytic activity of various catalysts

The catalytic activities of zinc, cadmium and nickel acetates supported on activated carbon were examined. The conditions were as follows: reaction temperature, 180°C ; concentration of metal acetate by weight, 25 per cent, catalyst weight, 15 gm. The data are summarized in Tables B1 - B3, Appendix B.

The yield of vinyl acetate against feed ratio (R), for various catalysts are shown in Figure 7. For the Zn sub-groups the catalytic activity increases as follows: $\text{Zn}^{2+} > \text{Cd}^{2+} > \text{Ni}^{2+}$. Since zinc acetate on activated carbon gives the best yield, all experiments described below were made exclusively with zinc acetate.

2.3.2 Effect of zinc acetate concentration

The experimental data for the effect of zinc acetate concentration on yield are presented in Table B4, Appendix B.

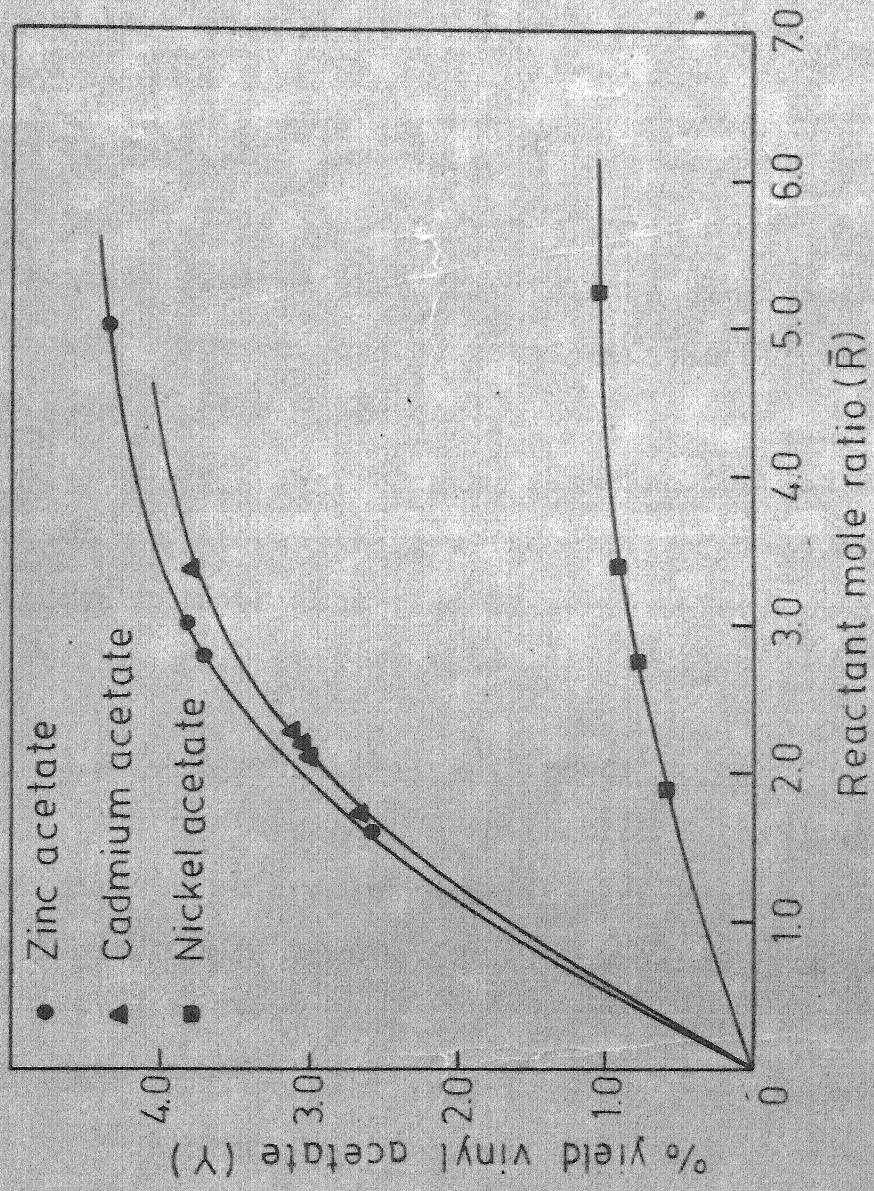


Fig. 7 - Performance of various catalysts at 180°C and 25% metal acetate by weight on activated carbon.

Figure 8 shows the per cent yield of vinyl acetate plotted as a function of the concentration of zinc acetate. The reaction conditions were as follows: reaction temperature, 180°C ; $(W/F) = 30 \text{ gm-cat.hr mol}^{-1}$; $(\bar{R}) = 30$. The yield passes through a maximum at the concentration of about 15 per cent. This is in agreement with Rostovskii and Arbuzova(7) who have reported that the yield of vinyl acetate passed through a maximum over a catalyst concentration of about 18 weight per cent Zn(OAc)_2 .

Since 15 weight per cent zinc acetate on activated carbon was proven to give the maximum yield of vinyl acetate, all experiments described below were performed exclusively with the catalyst of this composition.

2.3.3 Comparison of rate with surface area

It has been shown in Section I that the surface area decreases with the increase in zinc acetate composition up to about 10 per cent and then increases from 10 per cent to 15 per cent. This compares well with the maximum rate observed at 180°C at a composition of 15 per cent with the surface area.

Rostovskii and Ushakov (30) have obtained a limiting value of activity which is proportional to the specific surface, and beyond this value the activity decreased abruptly. The maximum activity has been assigned to the unimolecular layer.

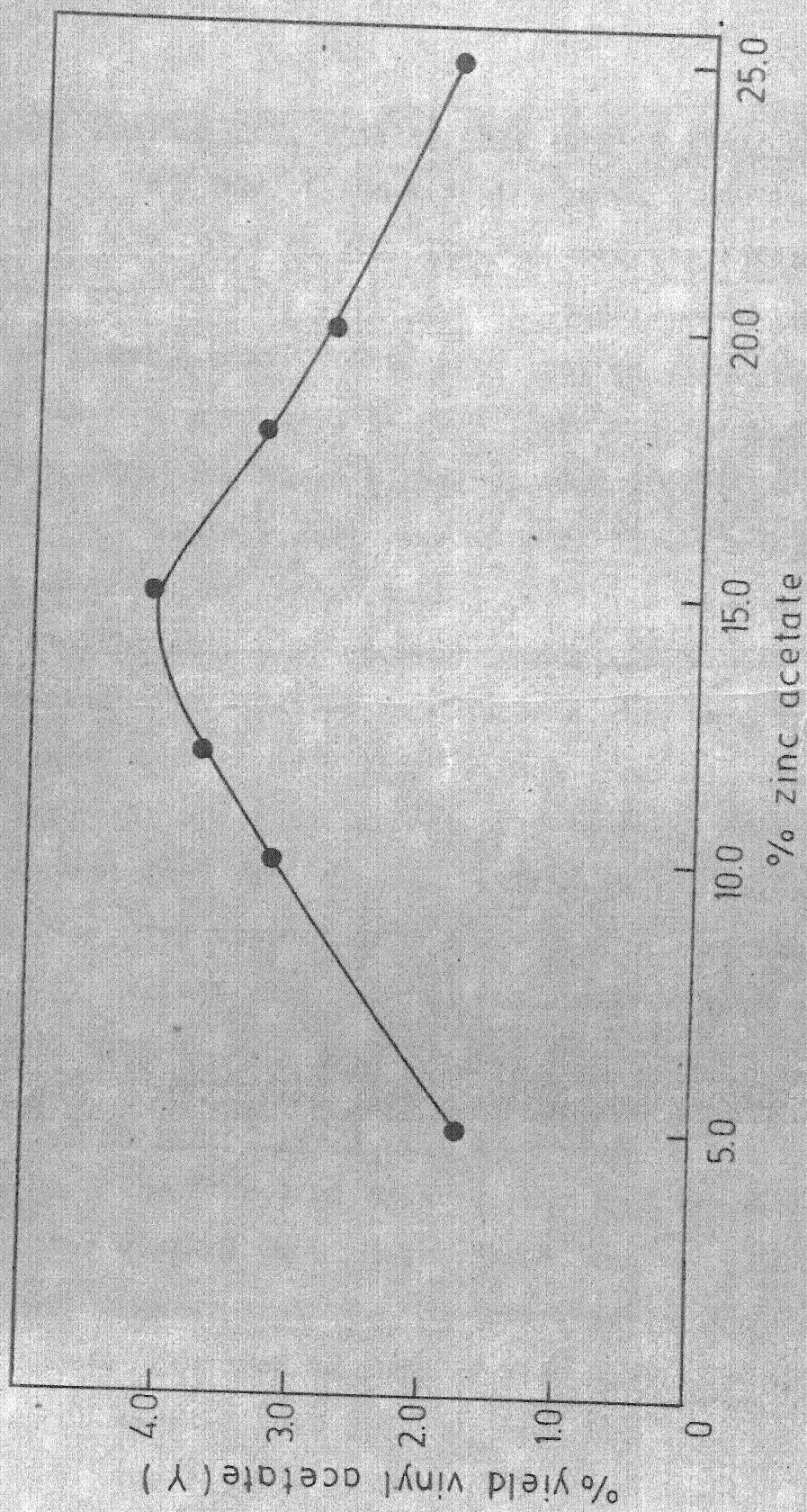


Fig. 8 - Percentage yield of vinyl acetate as function of zinc acetate concentration at 180°C, $(W/F) = 30$ and $(\bar{R}) = 3.0$.

2.3.4 Effect of acetylene acetic-acid ratio in feed

A study of the reaction rate of acetic acid versus the feed ratio should give more precise information on the role of feed ratio in the conversion and selectivity of vinyl acetate. Reaction kinetics was examined in the temperature range 155° - 200° C. The experimental data are presented in Tables B5 to B9, Appendix B.

Figure 9 shows the effect of feed ratio (\bar{R}) on the conversion of acetic acid over 15 per cent zinc acetate catalyst in the temperature range 155° - 200° C, for a (W/F) ratio of 30. The conversion of acetic acid increases with the feed ratio as well as with the reaction temperature.

Figure 10 shows the effect of feed ratio (\bar{R}) on the selectivity. It is seen that though the selectivity increased up to a temperature of 190° C at all (\bar{R}) ratios, the change in the selectivity for the temperatures between 190° - 200° C was very small.

2.3.5 Effect of (W/F) ratios

The effect of the reciprocal of space velocity (W/F) on the conversion of acetic acid, and the yield of VA and acetone were examined. The reaction conditions were as follows: reaction temperature, 180° C; (\bar{R}) = 3.0. The data are summarized in Table B10, Appendix B.

The results of Table B10 are presented in Figure 11. It is seen that the per cent conversion and yield of VA

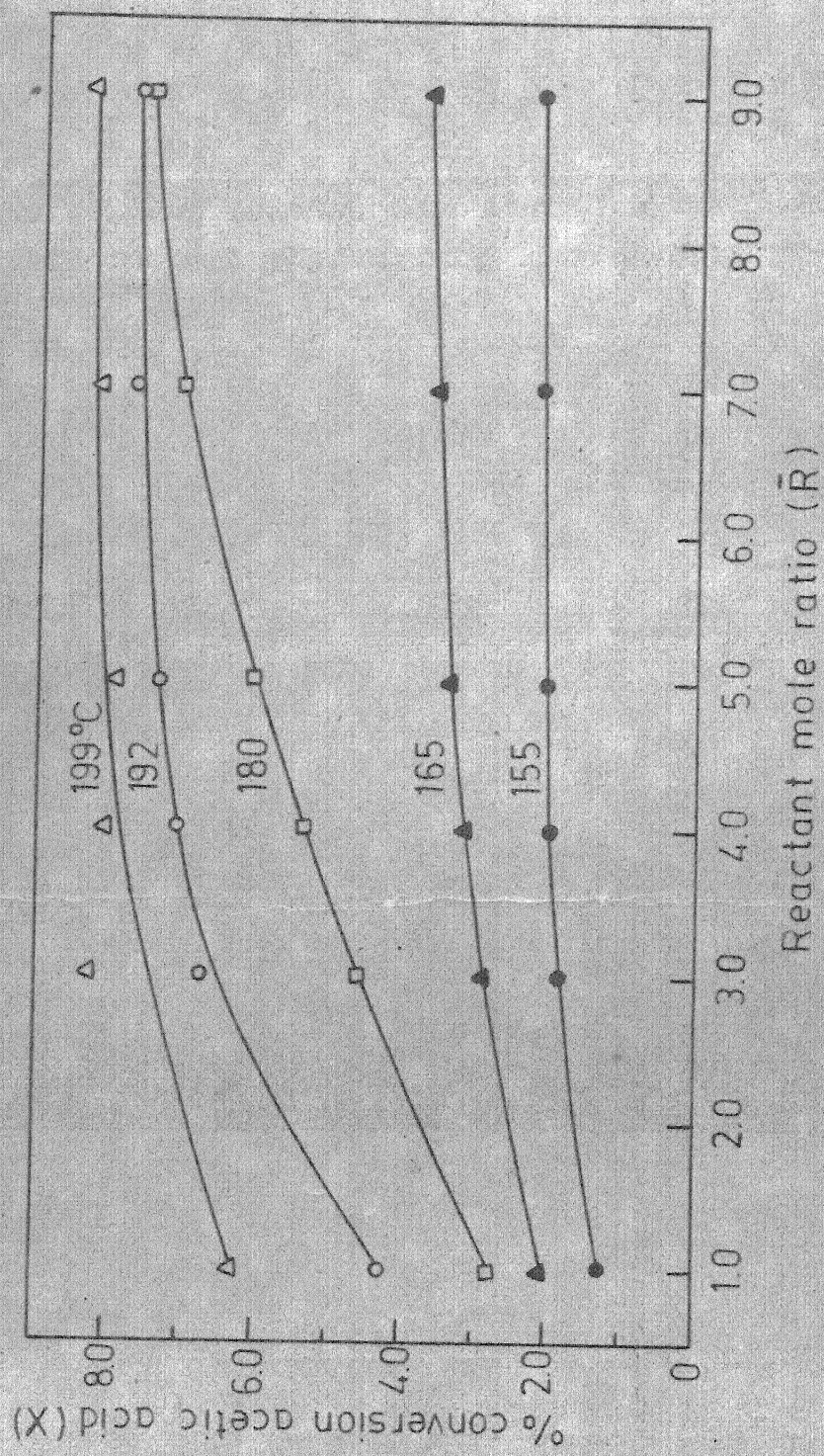


Fig. 9 - Effect of reactant mole ratio, acetylene to acetic acid, on percentage conversion of acetic acid at various temperatures, (W/F) = 30.

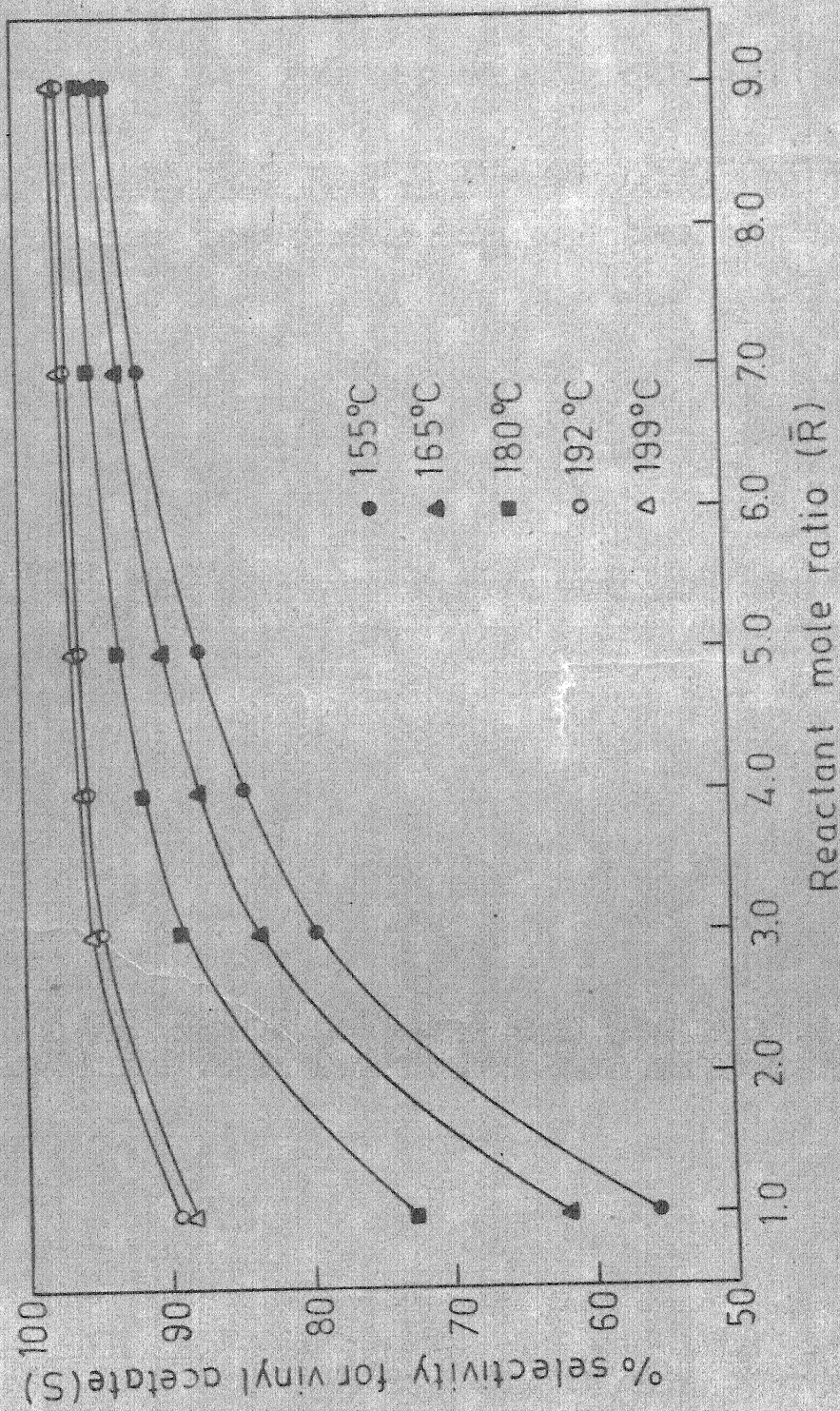


Fig. 10 - Effect of reactant mole ratio, acetylene to acetic acid on percentage selectivity for vinyl acetate at various temperatures, $(W/F) = 30$.

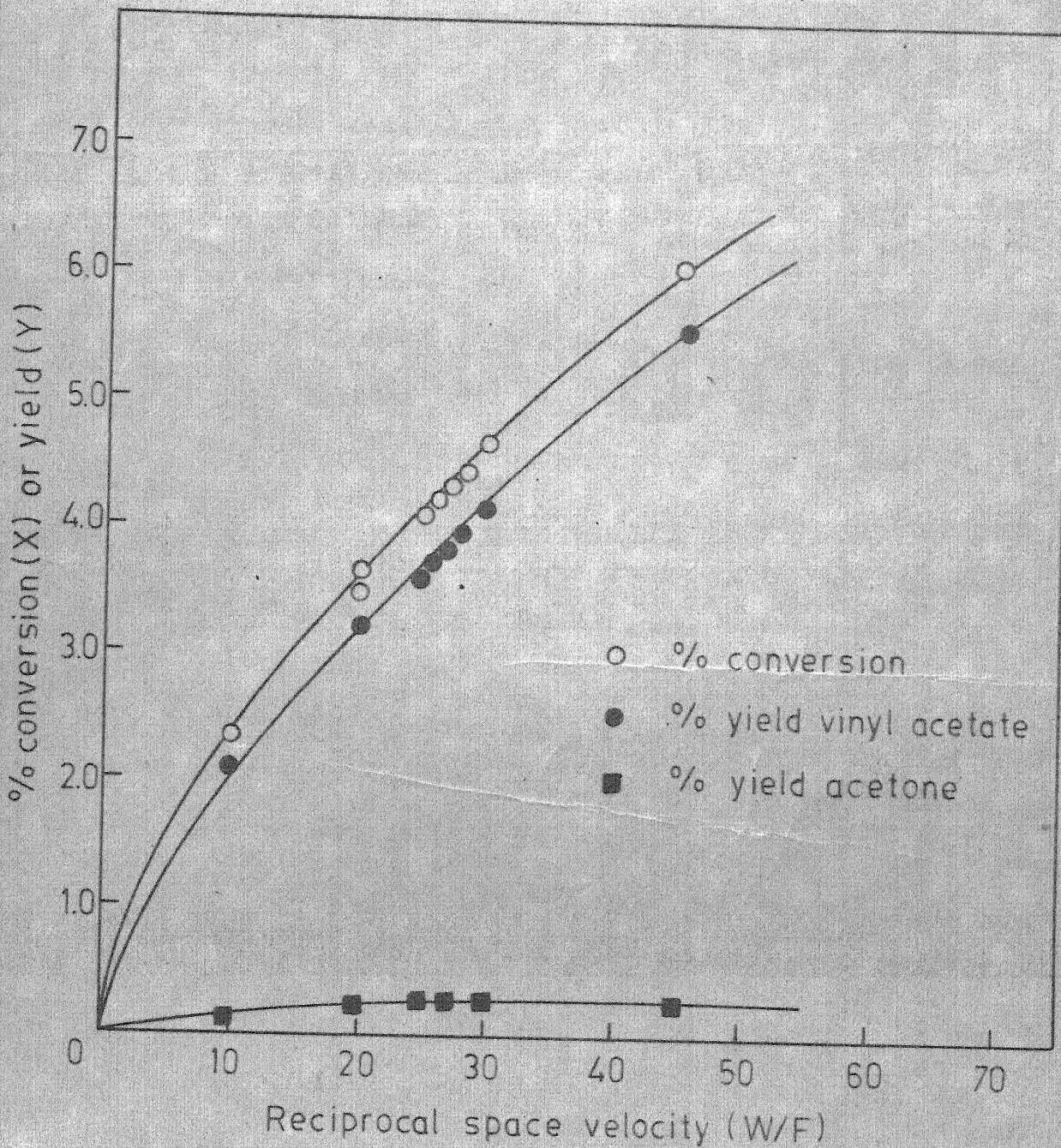


Fig. 11 - Effect of reciprocal space velocity on percentage conversion of acetic acid and yield of vinyl acetate at 180°C and $(\bar{R}) \approx 3.0$.

increased rapidly with the (W/F) ratios studied.

2.3.6 Effects of diffusion

The effects of diffusion were kept at a minimum by using high velocity of the gas through the catalyst. The reaction conditions were: $(\bar{R}) = 3.0$, reaction temperature, 180°C ; $(W/F) = 30$. The experimental data are shown in Table B11, Appendix B.

Figure 12 shows the effect of feed velocity on the conversion of acetic acid. The fair constancy of conversion obtained by changing the feed ratio while keeping (W/F) constant suggested that the diffusion of the gases was not controlling the rate.

The role of internal diffusion has been checked by varying the size of the catalyst particle while maintaining the catalyst weight, (\bar{R}) , and (W/F) constant. The internal diffusional resistance in the catalyst particles was practically negligible as shown by insignificant change in the reaction rate on varying the catalyst size between 2.8 to 1.4 mm (Table 6).

In order to study the effect of external diffusion it was necessary to increase the bed height while keeping (\bar{R}) and (W/F) constant. The results are presented in Table 7. The rate was unaffected by doubling the bed height. Thus, the external diffusion in the catalyst bed was negligible.

TABLE 6: ROLE OF INTERNAL DIFFUSION

Effect of particle size of catalyst on rate of formation of vinyl acetate per hour per gram of catalyst at 180°C.

$$\frac{W}{F} = 30.0 ; \bar{R} = 3.0 ; W = 15.0$$

Run No.	Average Particle Diameter, mm	(gm mol Vinyl Acetate formed hr ⁻¹ gm cat ⁻¹) x 10 ⁴
ID-1	2.8	3.48
ID-2	2.0	3.36
ID-3	1.4	3.42

TABLE 7: ROLE OF EXTERNAL DIFFUSION

Effect of doubling catalyst bed height on rate of formation of vinyl acetate per hour per gram of catalyst at 180°C.

$$\bar{R} = 3.0$$

Run No.	W, Weight of Catalyst, gm	F, Total Feed mol hr ⁻¹	$\frac{W}{F}$, gm cat hr mol ⁻¹	(gm mol Vinyl Acetate Formed hr ⁻¹ gm cat ⁻¹) $\times 10^4$
ED-1	6	0.6	10	5.20
ED-2		0.3	20	3.96
ED-3		0.2	30	3.70
ED-4	12	1.2	10	5.20
ED-5		0.6	20	3.96
ED-6		0.4	30	3.54

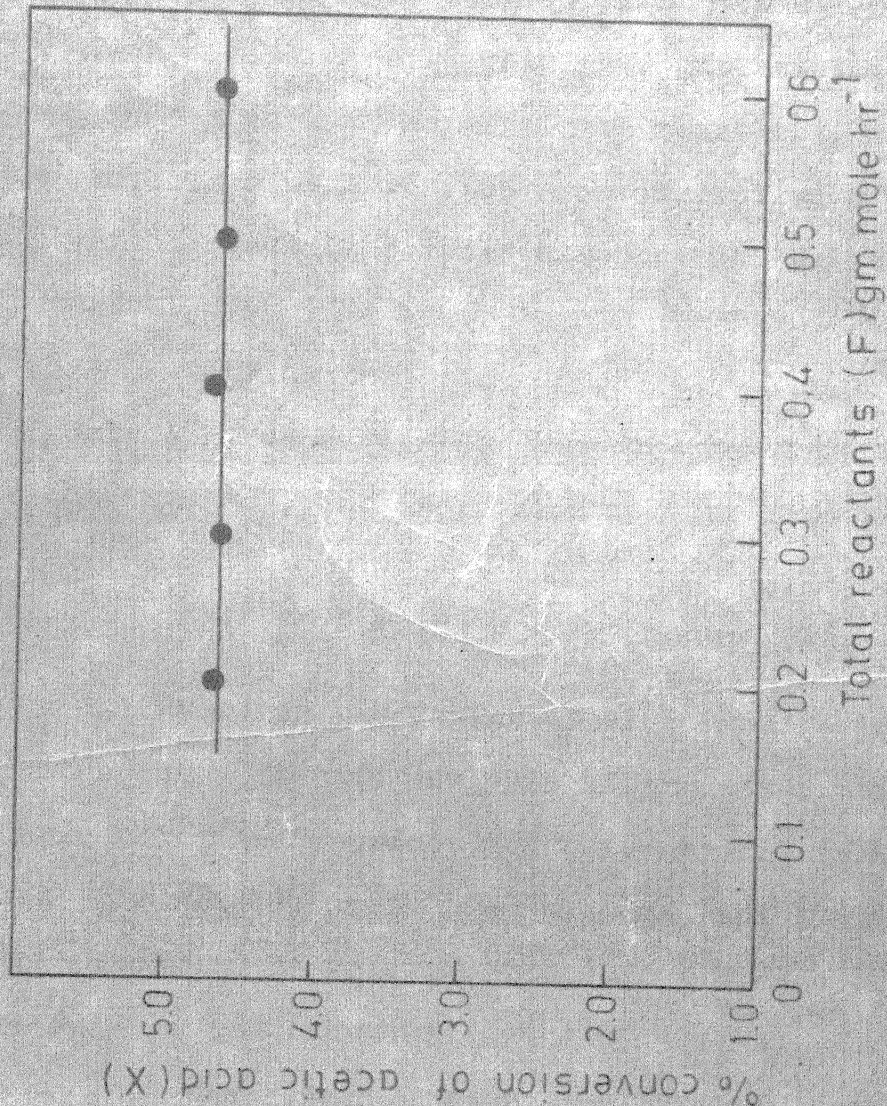


Fig. 12 - Effect of feed velocity on percentage conversion of acetic acid at 180 °C, $\bar{R} = 3.0$, $(W/F) = 30.0$

2.3.7 Kinetic models

Several kinetic models can be postulated based on the chemisorption behavior of zinc acetate-C system. The mechanism of the solid catalyzed gas reaction, in general, may be the mass transfer of the reactants, or products, or adsorption of the reactants or desorption of products, or chemical reaction between adsorbed molecules at the catalyst surface.

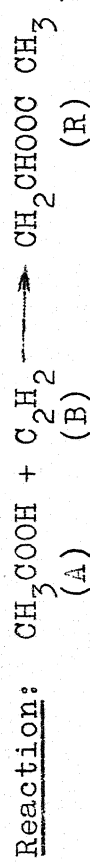
Assuming that the various acetylation processes involved have nearly the same functional dependence on $p_{C_2H_2}$, p_{CH_3COOH} , p_{VA} , the expression for the rate takes the form:

$$\text{Rate} = k \phi (p_{C_2H_2}, p_{CH_3COOH}, p_{VA}) \quad [10]$$

Based on the conventional Langmuir-Hinshelwood (35) mechanism a kinetic analysis of the experimental data was made using the approach suggested by Hougen and Watson (36). In this method, various mechanisms, which might control the reaction are postulated, based on a single site (Table 8a) and two types of active sites (Table 8b).

Neither zinc acetate nor activated carbon show any appreciable catalytic activity by themselves, nor do they chemisorb acetylene. The heat of adsorption of acetylene on active carbon is only $4.2 \text{ kcal mol}^{-1}$. It may be explained as follows: since activated carbon is mainly composed of graphite, a lattice spacing of 1.42 \AA could be chosen as the

TABLE 8: RATE EQUATIONS DERIVED USING HOUGEN-WATSON METHOD



S.No.	Rate Controlling Step	Mechanism	Rate Equation
(a) ONE TYPE OF ACTIVE SITES			
1	Adsorption of acetic acid	Surface reaction between adsorbed acetic acid and acetylene	$\frac{K_S p_A}{(1 + K_B p_B + K_R p_R)}$
2	Adsorption of acetic acid	Surface reaction between adsorbed acetic acid and acetylene in gas phase	$\frac{K_S p_A}{(1 + K_R p_R)}$
3	Adsorption of acetylene	Surface reaction between adsorbed acetylene and acetic acid	$\frac{K_S p_B}{(1 + K_A p_A + K_R p_R)}$
4	Adsorption of acetylene	Surface reaction between adsorbed acetylene and acetic acid in gas phase	$\frac{K_S p_B}{(1 + K_R p_R)}$
5	Desorption of vinyl acetate	Surface reaction between adsorbed acetic acid and acetylene	$\frac{K_S (K_A p_B - p_R)}{(1 + K_A p_A + K_B p_B + K_R p_A p_B)}$
6	Desorption of vinyl acetate	Surface reaction between adsorbed acetic acid and acetylene in gas phase	$\frac{K_S (K_A p_B - p_R)}{(1 + K_A p_A + K_R p_A p_B)}$

Table 8 (contd)

S.No.	Rate Controlling Step	Mechanism	Rate Equation
7	Desorption of vinyl acetate	Surface reaction between adsorbed acetylene and acetic acid in gas phase	$\frac{K_S (K_{A,PA} p_B - p_R)}{(1+K_{B,PB} + K_{R,PR} p_B)}$
8	Surface reaction	Surface reaction between adsorbed acetic acid and acetylene	$\frac{K_S K_{A,PA} (p_A p_B - p_R / K)}{(1+K_{A,PA} + K_{B,PB} + K_{R,PR})^2}$
9	Surface reaction	Surface reaction between adsorbed acetic acid and acetylene in gas phase	$\frac{K_S K_{A,PA} (p_A p_B - p_R / K)}{(1+K_{A,PA} + K_{R,PR})}$
10	Surface reaction	Surface reaction between adsorbed acetylene and acetic acid in gas phase	$\frac{K_S K_{B,PR} (p_A p_B - p_R / K)}{(1+K_{B,PB} + K_{R,PR})}$
11	Surface reaction	Equilibrium formation of an adsorbed acetylene layer and partial coverage of these sites by acetic acid and product	$\left(\frac{K_S K_{A,PA} p_A}{1+K_{A,PA} + K_{R,PR}} \right) \left(\frac{K_{B,PB}}{1+K_{B,PB}} \right)$
12	Surface reaction	Equilibrium formation of an adsorbed acetic acid layer and partial coverage of these sites by acetylene and product	$\left(\frac{K_S K_{B,PR} p_B}{1+K_{B,PB} + K_{R,PR}} \right) \left(\frac{K_{A,PA}}{1+K_{A,PA}} \right)$
13	Surface reaction	(b) <u>TWO TYPES OF ACTIVE SITES</u> Surface reaction between ionized adsorbed acetic acid and acetylene	$\left(\frac{K_S K_{A,PA}}{1+K_{A,PA} + K_{R,PR}} \right) \left(\frac{K_{B,PB}}{1+K_{B,PB}} \right) 53$

Table 8 (contd)

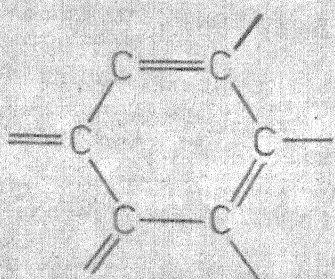
S.No.	Rate Controlling Step	Mechanism	Rate Equation
14	Irreversible ionized adsorption of acetylene and acetic acid	Surface reaction between ionized adsorbed acetic acid and acetylene	$\frac{K_A p_A}{1 + (\frac{K_A}{K_B}) (\frac{p_A}{p_B})}$
15	Irreversible ionized adsorption of acetylene and acetic acid	Surface reaction between ionized adsorbed acetic acid and acetylene, acetylene is dissociated	$\frac{K_A p_A}{1 + (\frac{K_A}{K_B}) (\frac{p_A}{p_B \cdot 2})}$

characteristic distance between carbon atoms in the graphite structure (37). If acetylene adsorbs by breaking a bond followed by bond formation with the carbon atoms of graphite (ethylene structure), then the optimum carbon carbon distance is 2.88 \AA for unstrained adsorption (38). Since the distance of 2.84 \AA exists in the graphite lattice, it may be possible that acetylene adsorbs on graphite by acquiring an ethylenic structure. However, the mode of adsorption and the energies involved would be expected to preclude easy mobility. A schematic model of acetylene adsorption on carbon is shown in Figure 13.

It is generally accepted that carbon acts as a Lewis acid, defined as an electron acceptor, and the zinc acetate as Lewis base, as the electron donor (1). The transfer of electrons from donor to acceptor would result in ionized species. It was assumed that this surface consists of two types of active sites. On these active sites acetylene and acetic acid are selectively adsorbed.

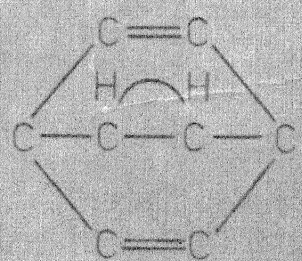
The heterogeneous catalytic reactions traditionally described as,

- (a) diffusion (external and internal) of reactants and products,
- (b) adsorption and desorption of reactants and products (physical adsorption and weak chemisorption),



Graphite structure

2.84 Å



Acetylene adsorption model

Fig. 13 - Acetylene adsorption model on carbon.

and (c) surface reaction

should be modified to take place as follows:

- (i) electron transfer from or to the reactants,
- (ii) homogeneous reaction (formation of activated complex and rearrangement of the ionized species on the surface),

and (iii) electron transfer from or to the products.

Writing the stoichiometric equation for the reaction as,



following the usual procedure of derivations (42), and neglecting the term P_{VA}/K , since K , equilibrium constant for the vapor phase acetylation of acetic acid was very large ($\ln K > 12$; temperature $150^{\circ}\text{--}200^{\circ}\text{C}$), equations for various postulated mechanisms, relating the rate of reaction were derived, (Table 8a and 8b) and tested for best fit of the data.

Linear regression analysis of Hougen and Watson models to obtain the least squares fit values of the kinetic constants (43) were performed on IBM 7044 system. The program prepared used centralization and correlation matrix for minimizing the round off errors. The linear regressions of the rate equations were made at each temperature. All possible combinations of the various adsorption terms were

examined in order to allow for various negligible adsorption terms. Rate expressions were eliminated from further considerations when any of the converged adsorption constants became negative.

The data were most satisfactorily correlated by mechanism 14 (Table 8). The square of the multiple correlation coefficient (R^2) was found to be above 95 per cent for this model at all temperatures. The mechanism is based on the surface reaction between ionized acetic acid and acetylene.

$$\text{rate} = \frac{K_A p_A}{1 + \left(\frac{K_A}{K_B} \right) \left(\frac{p_A}{p_B} \right)} \quad [12]$$

where K_A and K_B are temperature dependent and can be expressed by the following equations,

$$\log K_A = 6.305 - \frac{4.017 \times 10^3}{T} \quad [13]$$

$$\log K_B = 0.33 - \frac{1.434 \times 10^3}{T} \quad [14]$$

These constants also fit the rate data, Table B12 - B14, Appendix B. The plots of the experimental rate versus that predicted by the above expression are shown in Figures 14, 15 and 16 for the temperatures 155° , 180° and 192°C . The maximum deviation between the predicted values and the

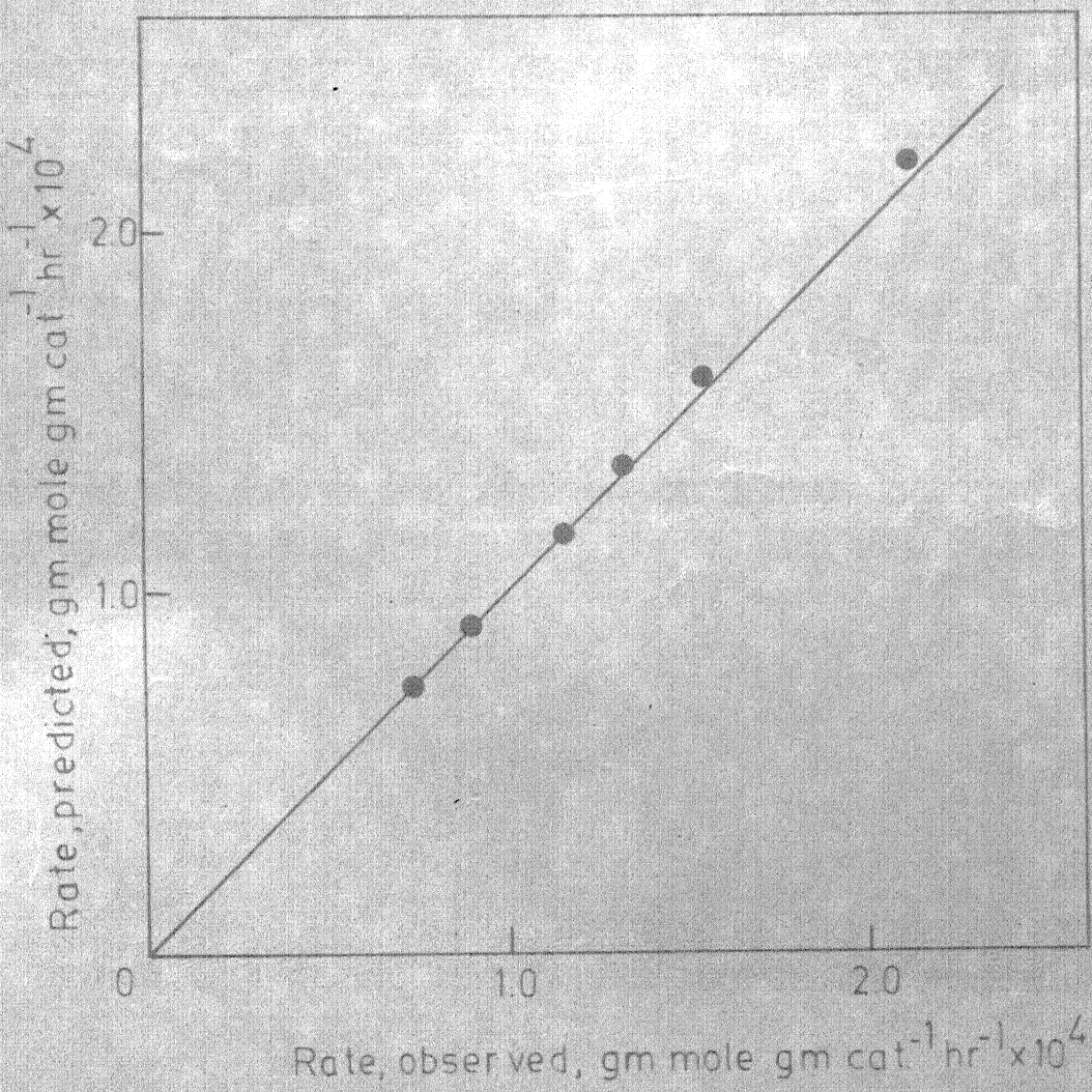


Fig. 14 - Comparison of observed and calculated rates
at 155°C and (W/F)=30.0.

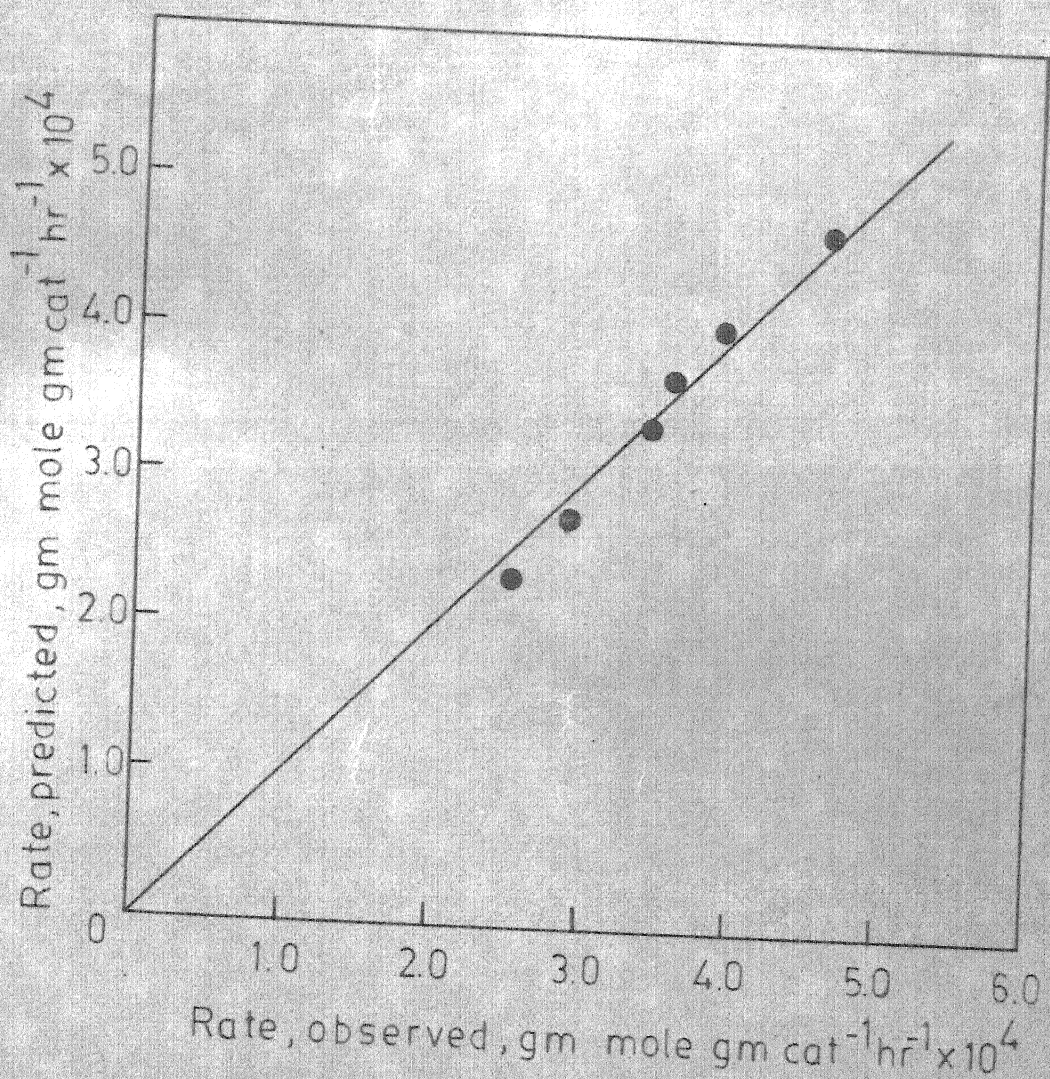


Fig. 15 - Comparison of observed and calculated rates
at 180°C and (W/F) = 30.0.

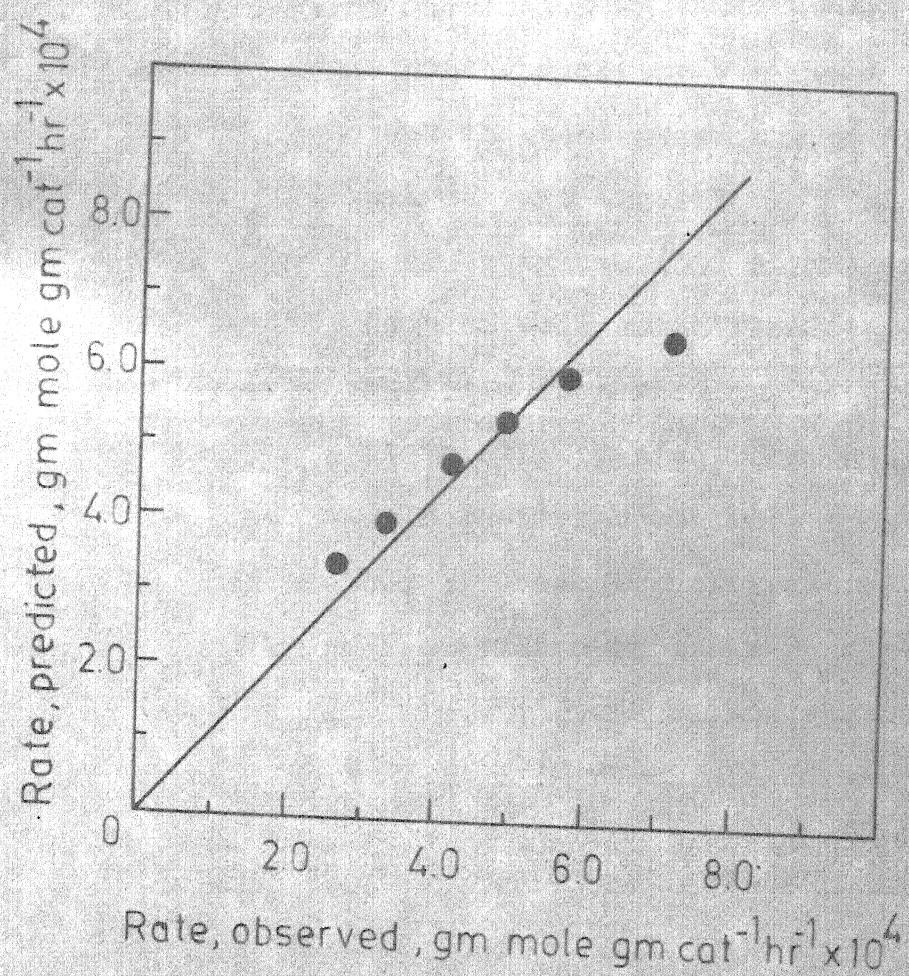


Fig. 16 - Comparison of observed and calculated rates at 192°C and (W/F) = 30.0.

experimental ones have been found to be \pm 7 per cent, except at temperatures above 190°C.

The model presented in this work differs from that given by Vasileva, et al. (34). In their study, the rate of reaction on zinc acetate on carbon was first order with respect to acetylene and independent of the partial pressures of acetic acid or vinyl acetate above 180°C. In analogy with the hydrochlorination of acetylene (39) a rate expression was presented. It has been well established that neither zinc acetate nor activated carbon show any catalytic activity by themselves, even at relatively high temperatures (180° - 218°C). This distinguishes it very clearly from the hydrochlorination of acetylene, which is catalyzed by one of the components. Careful examination of their results was not possible since most of the original data were not presented.

From the discussion of various mechanisms it is obvious that linear regression applied only to rate data will not be sufficient to determine a definite mechanism. The assumptions which are made in the development of the particular rate expression must be experimentally verified.

It is interesting to note that the form of rate expressions derived in Table 8 is similar to those derived by Mann and coworkers (40,41) for the oxidation of olefins

over bismuth molybdate where the surface was considered to consist of two types of active sites on which olefin and oxygen are selectively adsorbed.

+ + + + +

+ + +

SECTION III

THERMODYNAMIC PROPERTIES

3.1 INTRODUCTION

A detailed process engineering study of vinyl acetate manufacture requires the kinetic rate equation, vapor pressure-boiling point data, thermodynamic properties of the real gas at the process conditions, and the vapor-liquid equilibria of the multicomponent mixture comprising the reaction products. In Section II, the rate expression has been reported based upon the results of the present investigation.

The vapor pressure-boiling point data for vinyl acetate are reported by Capkova and Fried (44) and are given in Table C1, Appendix C along with the Antoine constants and the enthalpy of vaporization.

The real gas thermodynamic properties and the experimental pressure, volume, temperature data for vinyl acetate are not available in the literature. Hence we had to take recourse to some reliable predictive methods for obtaining an equation of state for vinyl acetate. The Martin-Hou equation of state (45) was selected for this purpose and the Martin-Hou constants were computed according to the procedures outlined by Martin and coworkers (45, 46, 47). The departure functions that is, the difference between the real gas property and the ideal gas property, were then derived using the following expressions involving the Martin-Hou constants.

Enthalpy content $(H-H^0)_T$

$$(H-H^0)_T = \int_0^P \left(\frac{\partial H}{\partial P} \right)_T dP = \int_0^P \left[V - T \left(\frac{\partial P}{\partial T} \right)_V \left(\frac{\partial P}{\partial V} \right)_T^{-1} \right] dP$$

[15]

Entropy content $(S-S^0)_T$

$$(S-S^0)_T = - \int_0^P \left[\left(\frac{\partial P}{\partial T} \right)_V \left(\frac{\partial P}{\partial V} \right)_T^{-1} \right]_P dP + R \ln P$$

[16]

Gibbs energy content $(G-G^0)_T$

$$(G-G^0)_T = - \int_0^P \left[\frac{RT}{P} - V \right] dP + RT \ln P$$

[17]

The thermodynamic properties of the real gas is the sum of the quantity for the ideal gas and the departure function calculated above. This section deals with the departure functions for vinyl acetate computed by the procedures outlined above. The ideal gas thermodynamic properties for vinyl acetate and crotonaldehyde are not available in the literature. Hence it was necessary to calculate these properties using the literature spectroscopic information and are reported in this section.

The other properties for vinyl acetate are reported in Table C2, Appendix C (1,3)

3.2 THE DEPARTURE FUNCTIONS FOR VINYL ACETATE

The departure functions were calculated using the Martin-Hou equation of state given below:

$$\log P = \frac{RT}{V-b} - \sum_{i=1}^5 \frac{A_i + B_i T + C_i e^{kT/T_c}}{(V-b)^i} \quad [18]$$

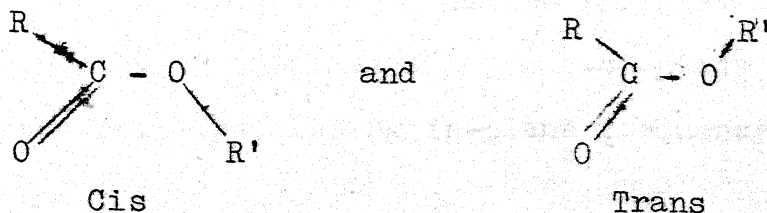
Here A_1 to A_5 , B_1 to B_5 , C_1 to C_5 , k , b are the Martin-Hou constants and could be determined from the critical constants T_c , P_c , V_c , and one point on the vapor pressure curve.

Using these properties for vinyl acetate as reported in Table C2, Appendix C, the Martin-Hou constants were computed. For this purpose a computer program was written according to the procedures given by Martin and coworkers (45,46,47). Equations [15 to 18] were used to compute the departure functions at selected temperatures and volumes in the vapor region and these along with the Martin-Hou constants are reported in Table C3, Appendix C. The computer program used for this purpose is reported in Appendix C.

3.3 IDEAL GAS THERMODYNAMIC PROPERTIES OF VINYL ACETATE

3.3.1 Molecular structure

Two planar conformations are possible for vinyl acetate:



where R and R' are methyl and vinyl groups, respectively. As no microwave studies have been carried out for vinyl acetate, the molecular conformation is not known. However, from infrared studies (48,49) it is found that no rotational isomers are present. Rao and Curl (50) have established cis conformation for vinyl formate from their microwave spectral studies. Crowder (51) interpreted the infrared and Raman data for vinyl trifluoroacetate in terms of one conformer of C_s symmetry. The review article by Jones and Owen (52) makes it very clear that vinyl acetate exists as cis conformer with C_s symmetry as shown in Figure 17. Here the carbon oxygen skeleton has a planar structure and one hydrogen of the methyl group is in plane while the other two are symmetrically arranged with respect to it. The values of the structural parameters adopted in this work are given in Figure 17. These are taken from the parameters of similar molecules, namely vinyl formate (48), divinylether (53), methyl acetate (53,54) and acetic acid (55).

3.3.2 Vibrational assignments

Kotorlenko et al. (49) reported assignments for this molecule only from infrared measurements. Feairheller and Katon (48) thoroughly studied the infrared and Raman spectra and reported 19 in-plane and 9 out-of-plane fundamental frequencies. The missing in-plane frequency is $\delta_{C=C-O}$ and

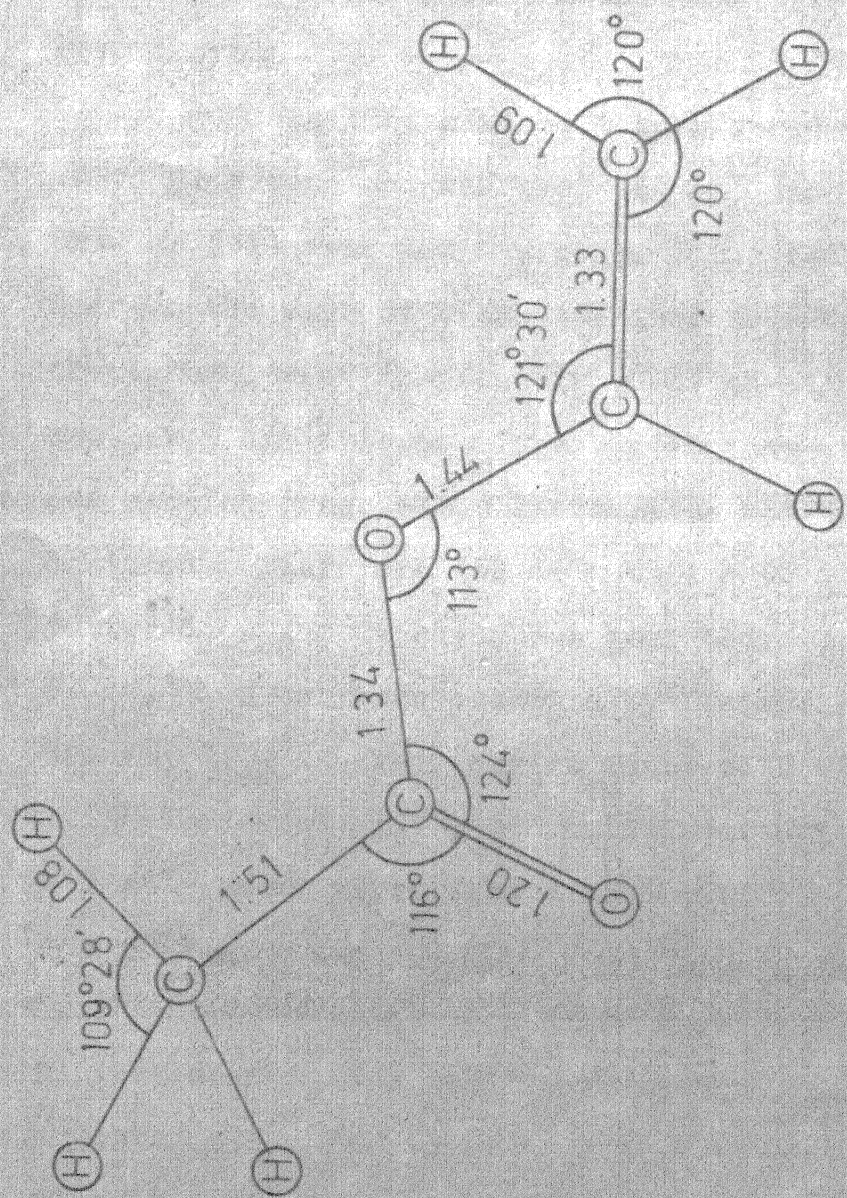


Fig. 17 - Molecular structure of vinyl acetate

the one out of plane is the torsional frequency due to methyl group.

McManis (56) studied the infrared spectra of series of vinyl esters and assigned 464 cm^{-1} to the $\delta_{\text{C}=\text{C}-\text{O}}$ mode. Crowder (51) reported a similar value (465 cm^{-1}) for this mode in the case of vinyl trifluoroacetate. Assignments of the three lowest in-plane frequencies of similar molecules are given in Table 9. It was felt that the two lowest in-plane frequencies reported by Feairheller and Katon (48) should be assigned. Therefore 462 cm^{-1} to the $\delta_{\text{C}=\text{C}-\text{O}}$ mode and 406 cm^{-1} to the $\delta_{\text{C}-\text{C}=\text{O}}$ mode have been assigned. This means that $\delta_{\text{C}-\text{O}-\text{C}}$ has not been observed by Feairheller and Katon. The missing $\delta_{\text{C}-\text{O}-\text{C}}$ frequency is found to be $306-323 \text{ cm}^{-1}$ in aliphatic esters (57), 303 cm^{-1} in methyl acetate (58) and 295 cm^{-1} in vinyl trifluoroacetate (51). The average value 299 cm^{-1} has been adopted in the calculations.

The out-of-plane missing torsional frequency adopted in this work is 100 cm^{-1} which is transferred from methyl acetate (59). In acetic acid this value is reported to be 93 cm^{-1} by Haurie and Novak (60) and 101 cm^{-1} by Fukushima and Zwolinski (61). The fundamental frequencies adopted in this work are given in Table 10.

TABLE 9: COMPARISON OF SOME IN-PLANE FREQUENCIES

Mode	Methyl Acetate (58)	Vinyl Trifluoro- acetate (51)	<u>Vinyl Acetate</u>	
			Ref.(48)	This Work
$\delta_{C=C-O}$	-	464	-	462
$\delta_{C-C=O}$	429	356 ^a	462	406
δ_{C-O-C}	303	295	406	299

^aLow value because of mass effect of CF_3 group.

TABLE 10: ADOPTED FUNDAMENTAL FREQUENCIES OF VINYL ACETATE(cm^{-1})

In-plane frequencies (a')						
1	3120	$\nu_a(\text{CH}_2)$	11	1353	$\delta(\text{CH})$	
2	3090	$\nu(\text{CH})$	12	1291	$\nu(\text{C-C})$	
3	3040	$\nu_s(\text{CH}_2)$	13	1217	$\nu_a(\text{COC})$	
4	2996	$\nu_a(\text{CH}_3)$	14	1018	$\delta(\text{CH}_2)$ rock	
5	2940	$\nu_s(\text{CH}_3)$	15	972	$\delta(\text{CH}_3)$ rock	
6	1760	$\nu(\text{C=O})$	16	847	$\nu_s(\text{COC})$	
7	1644	$\nu(\text{C=C})$	17	637	$\delta(\text{CO}_2)$	
8	1428	$\delta(\text{CH}_2)$	18	462	$\delta(\text{C=C-O})$	
9	1382	$\delta_a(\text{CH}_3)$	19	406	$\delta(\text{C-C=O})$	
10	1370	$\delta_s(\text{CH}_3)$	20	299	$\delta(\text{C-O-C})$	
Out-of-plane frequencies (a'')						
21	3020	$\nu_a(\text{CH}_3)$	26	712	$\gamma(\text{CH}_2)$ twist	
22	1428	$\delta_a(\text{CH}_3)$	27	583	$\gamma(\text{CH}_3\text{CO}_2)$	
23	1134	$\delta(\text{CH}_3)$ rock	28	238	Skeletal def.	
24	948	$\gamma(\text{CH}_2)$ wag	29	160	Skeletal def	
25	874	$\gamma(\text{CH})$	30	100	Torsion(C-CH_3)	

3.3.3 Thermodynamic functions

The ideal gas thermal functions C_p^0 , $(H^0 - H_0^0)$, S^0 , $-(G^0 - H_0^0)/T$ have been calculated using the moments of inertia obtained from the molecular parameters given in Figure 11 and the vibrational frequencies given in Table 10. The internal rotational contributions of the methyl group to the thermodynamic functions have been obtained using Pitzer and Gwinn's table (62). For this purpose the potential barrier height was obtained from equation [19]

$$V_0 = \frac{k^2}{n^2 F} \quad [19]$$

where n = Symmetry number of rotating group

$$F = h/8 \pi^2 c I_r$$

h = Planck's constant

c = Velocity of light

I_r = Reduced moment of inertia which is obtained by following formula

$$I_r = I_\alpha \left[1 - \sum_{i=1}^3 I_\alpha \lambda_i^2 / I_i \right] \quad [20]$$

where I_α = moment of inertia of the rotating group

λ_i = direction cosine

I_i = principal moment of inertia

These molecular parameters are given in Table 11.

As there is some uncertainty in the torsional frequency the internal rotational contributions were calculated by varying

TABLE 11: MOLECULAR PARAMETERS OF VINYL ACETATE

$$I_a = 47.230 \text{ amu } \text{\AA}^2$$

$$\lambda_a = 0.861$$

$$I_b = 235.820 \text{ amu } \text{\AA}^2$$

$$\lambda_b = 0.509$$

$$I_c = 279.921 \text{ amu } \text{\AA}^2$$

$$\lambda_c = 0.0$$

$$I_\alpha = 2.390 \text{ amu } \text{\AA}^2$$

$$\nu_\tau = 100 \text{ cm}^{-1}$$

$$I_r = 2.294 \text{ amu } \text{\AA}^2$$

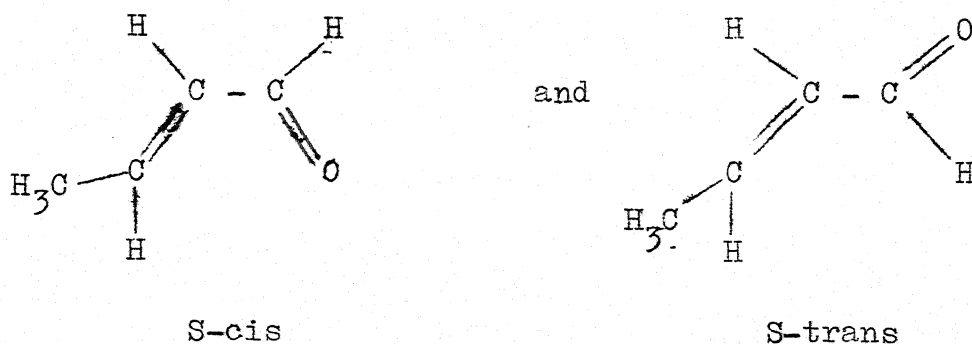
$$V_e = 622.8 \text{ cal mol}^{-1}$$

the torsional frequency by $\pm 10 \text{ cm}^{-1}$. The calculated potential barrier heights are 526, 623 and 728 cal mol $^{-1}$ corresponding to the torsional frequencies 90, 100 and 110 cm^{-1} , respectively. The maximum deviations due to the uncertainty in torsional frequency are at lower temperatures and they are ± 0.08 , ± 0.04 , ± 0.05 and $\pm 0.09 \text{ cal deg}^{-1} \text{ mol}^{-1}$ for $\text{C}_p^0, (\text{H}^0-\text{H}_0^0), \text{S}^0$ and $-(\text{G}^0-\text{H}_0^0)/T$, respectively. This shows that the errors in the thermal functions are very low owing to the uncertainty in the torsional frequency. The enthalpy of formation, Gibbs energy of formation and logarithm of equilibrium constant of formation as a function of temperature were calculated by the usual procedure. The enthalpy of formation (63) at 298.15°K was taken as $-75.46 \pm 0.18 \text{ kcal mol}^{-1}$. The values of thermal functions of C(64,65), H₂ (66), and O₂(67) in their reference states are used. The calculated thermodynamic properties are given in Table C4, Appendix C.

3.4 IDEAL GAS THERMODYNAMIC PROPERTIES OF CROTONALDEHYDE

3.4.1 Molecular structure

Crotonaldehyde can exist in the two forms, S-cis and S-trans as shown below. From the microwave (68,69) and infrared (70) spectral measurements it has been concluded that this molecule is planar and exists only in the S-trans conformation.



Suzuki and Kojima (68) and Hsu and Flygare (69) have independently carried out microwave spectral analysis. They reported the moments of inertia and the molecular parameters for crotonaldehyde. The agreement between the two sets of values is excellent. The molecular structure and structural parameters are given in Figure 18.

3.4.2 Vibrational assignments

Gredy and Piaux (71), Saunders et al. (72) and Behringer (73) have reported the spectral bands from their Raman spectral measurements. Bowles et al. (70) have reported almost complete assignments of fundamental frequencies from their infrared spectral work in the liquid state.

Crotonaldehyde belongs to C_S symmetry with nineteen in-plane frequencies [19a'] and eight out of plane frequencies [8a'']. Bowles et al. (70) have reported 25 frequencies. The missing ones are two torsional frequencies due to CH₃- and CHO- groups. Suzuki and Kojima, and Hsu and Flygare (68,69) have reported potential barrier height for CH₃- group. Using

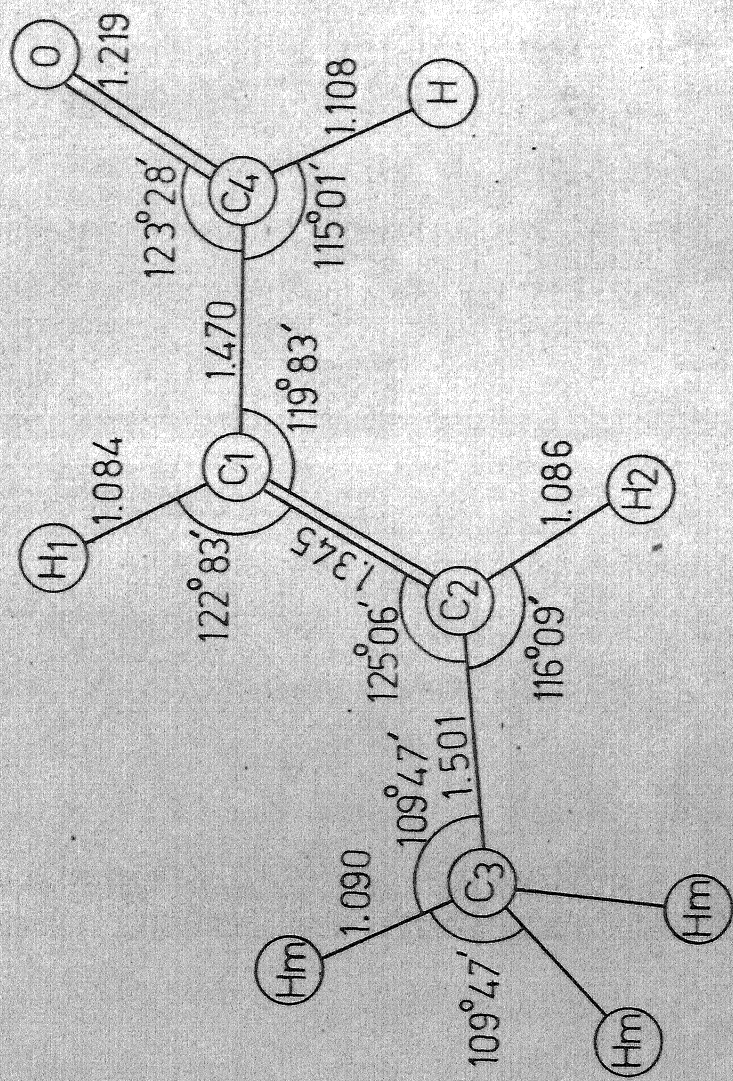


Fig. 18 - Molecular structure of crotonaldehyde-*S*-trans form.

the equation [19] given earlier in Section 3.3.3, the torsional frequency due to CH_3- group is calculated as 188 cm^{-1} . Acraldehyde has similar structure as crotonaldehyde. The torsional frequency due to CHO group is 157 cm^{-1} for acraldehyde. The band at 300 cm^{-1} observed in Raman spectrum by Saunders et al. (72) for crotonaldehyde could be an overtone $(2\nu_{\tau})$ of the torsional frequency which gives torsional frequency as 150 cm^{-1} . This value has been adopted here. The fundamental frequencies adopted in this work are given in Table 12.

3.4.3 Thermodynamic functions:

The ideal gas thermal functions C_p^0 , $H^0 - H_0^0$, S^0 and $-(G^0 - H_0^0)/T$ have been calculated using the moments of inertia (Table 13) of Suzuki and Kojima (68) and the vibrational frequencies given in Table 12. This molecule has two rotational groups, CH_3- and $\text{CHO}-$. To simplify the calculations the torsional frequency due to $\text{CHO}-$ group is used as a fundamental frequency as this would not change the thermodynamic values much. The internal rotational contributions due to CH_3- group to the thermodynamic properties were obtained using Pitzer and Gwinn's Tables (62). For this purpose, the potential barrier height reported by Suzuki and Kojima (68) was used. Reduced moment of inertia (I_r) was calculated using the parameters given by these authors (Table 13) using equation [20].

TABLE 12: ADOPTED FUNDAMENTAL FREQUENCIES OF CROTONALDEHYDE

In-plane frequencies (a')						
1	3042	$\nu_{(CH)}$	11	1305	$\delta_{(CH)}$	
2	3002	$\nu_{(CH)}$	12	1253	$\delta_{(CH)}$	
3	2944	$\nu_{(CH_3)}$	13	1158	$\nu_{(C-C)}$	
4	2862	$\nu_{(CH_3)}$	14	1109	$\delta_{(CH_3)}$ rock	
5	2778	$\nu_{(CH(O))}$	15	1075	$\nu_{(C-CH_3)}$	
6	1693	$\nu_{(C=O)}$	16	727	$\delta_{(C-CH_3)}$	
7	1641	$\nu_{(C=C)}$	17	542	$\delta_{(CHO)}$	
8	1444	$\delta_{(CH_3)}$	18	459	$\delta_{(C=C)}$	
9	1389	$\delta_{(CH(O))}$	19	150	Torsion(C-CHO)	
10	1375	$\delta_{(CH_3)}$				
Out-of-plane frequencies (a'')						
20	2944	$\nu_{(CH_3)}$	24	931	$\gamma_{(CH(O))}$	
21	1444	$\delta_{(CH_3)}$	25	984	$\gamma_{(C-CH_3)}$	
22	1023	$\delta_{(CH_3)}$ rock	26	542	$\gamma_{(C=C)}$	
23	966	$\gamma_{(CH=CH)}$	27	(188)	Torsion(CH_3)	

TABLE 13: MOLECULAR PARAMETERS OF CROTONALDEHYDE

I_a	$= 15.485 \text{ amu} \cdot \text{\AA}^2$	λ_a	$= 0.924$
I_b	$= 231.474 \text{ amu} \cdot \text{\AA}^2$	λ_b	$= 0.377$
I_c	$= 243.753 \text{ amu} \cdot \text{\AA}^2$	λ_c	$= 0.0$
I_α	$= 3.160 \text{ amu} \cdot \text{\AA}^2$	ν_τ	$= 188 \text{ cm}^{-1}$
I_r	$= 2.603 \text{ amu} \cdot \text{\AA}^2$	V_e	$= 1730 \text{ cal mol}^{-1}$

The enthalpy of formation, ΔH_f^0 ; the Gibbs energy of formation, ΔG_f^0 , and logarithm of equilibrium constant of formation as a function of temperature were calculated by the usual procedure. The enthalpy of formation at 298.15 was taken as $-24.03 \text{ kcal mole}^{-1}$ which is reported by Cox and Pilcher (62). The calculated thermodynamic properties are given in Table C5, Appendix C.

3.5 ACETONE, ACETIC ACID AND ACETALDEHYDE

The thermodynamic functions are available in the literature for these compounds (66, 74). The enthalpy of formation, ΔH_f^0 ; Gibbs energy of formation, ΔG_f^0 ; and logarithm of equilibrium constant of formation, $\log K_f$ as a function of temperature were calculated in this work using the values of ΔH_f^0 298 which are recommended by Cox and Pilcher (ΔH_f^0 298 = -51.9 , -103.26 , $-39.73 \text{ kcal mol}^{-1}$ for acetone, acetic acid and acetaldehyde respectively) (63). The thermodynamic properties are given in Tables C6 - C8, Appendix C.

3.6 ACETYLENE, CARBON DIOXIDE AND WATER

The thermodynamic properties of C_2H_2 , CO_2 and H_2O are available in the literature. The values have been reported by TRC (66) and are given in Tables C9 - C11, Appendix C.

3.7 THERMODYNAMIC PROPERTIES OF MIXTURES

The thermodynamic properties of the mixture comprising of vinyl acetate, crotonaldehyde, acetone, acetic acid, acetaldehyde, acetylene, carbon dioxide and water are required for design of reactor and the separation systems. These mixture properties could be calculated for a particular composition from the thermodynamic properties of the individual components in the mixture (Table C4-C11, appendix C) by the following formulae.

1. Heat capacity of the mixture

$$C_p^o (M) = \sum x_i C_{pi}^o$$

2. Enthalpy of the mixture

$$H^o - H_0^o = \sum x_i (H^o - H_0^o)_i$$

3. Entropy of the mixture

$$S^o = \sum x_i S_i^o - R \sum x_i \ln x_i$$

4. Gibbs energy of the mixture

$$\frac{G^o - H_0^o}{T} = \sum_{xi} x_i \left(\frac{G^o - H_0^o}{T} \right)_i + R \sum x_i \ln x_i$$

where x_i = molar fraction of the individual components.

3.8 ENTHALPY, GIBBS ENERGY AND EQUILIBRIUM CONSTANT OF REACTIONS

The following reactions are involved in the production of vinyl acetate from acetic acid and acetylene.

Reactions

1. $\text{CH}_3\text{COOH} + \text{C}_2\text{H}_2 \longrightarrow \text{CH}_2 = \text{CHOOCCH}_3$
2. $2\text{CH}_3\text{COOH} \longrightarrow (\text{CH}_3)_2\text{CO} + \text{H}_2\text{O} + \text{CO}_2$
3. $\text{C}_2\text{H}_2 + \text{H}_2\text{O} \longrightarrow \text{CH}_3\text{CHO}$
4. $2\text{C}_2\text{H}_2 + \text{H}_2\text{O} \longrightarrow \text{CH}_3\text{CH} = \text{CHCHO}$
5. $n \text{C}_2\text{H}_2 \longrightarrow (\text{C}_2\text{H}_2)_n$
6. $\text{CH}_3\text{COOH} + \text{CH}_2 = \text{CHOOCCH}_3 \longrightarrow (\text{CH}_3\text{COO})_2\text{CHCH}_3$

The relations for enthalpy, Gibbs energy and equilibrium constant, for first four reactions, in terms of temperature were derived as follows using the literature and the computed data (Table C4 - C11, Appendix C). These properties were calculated for various reaction temperatures and are reported in Table C12 - C15, Appendix C.

3.8.1 Reaction Number 1

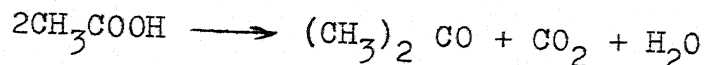


$$\Delta G_R^\circ = - 23.457 + 0.02714 T \text{ kcal mol}^{-1}$$

$$\Delta H_R^\circ = - 23.457 \text{ kcal mol}^{-1}$$

$$\ln K = \frac{1.1805 \times 10^4}{T} - 13.657$$

3.8.2 Reaction Number 2

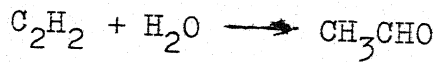


$$\Delta G_R^{\circ} = -96.848 + 8.2 \times 10^{-4} T + 6.17 \times 10^{-6} T^2 \text{ kcal mol}^{-1}$$

$$\Delta H_R^{\circ} = -96.848 - 6.17 \times 10^{-6} T^2 \text{ kcal mol}^{-1}$$

$$\ln K = \frac{48.741 \times 10^3}{T} - 4.127 \times 10^{-1} - 3.105 \times 10^3 T$$

3.8.3 Reaction Number 3



$$\Delta G_R^{\circ} = -35.951 + 2.382 \times 10^{-2} T + 3.750 \times 10^{-6} T^2 \text{ kcal mol}^{-1}$$

$$\Delta H_R^{\circ} = -35.951 - 3.750 \times 10^{-6} T^2 \text{ kcal mol}^{-1}$$

$$\ln K = \frac{18.093 \times 10^3}{T} - 14.254 - 1.887 \times 10^{-3} T$$

3.8.4 Reaction Number 4



$$\Delta G_R^{\circ} = -75.635 + 6.563 \times 10^{-2} T \text{ kcal mol}^{-1}$$

$$\Delta H_R^{\circ} = -75.635 \text{ kcal mol}^{-1}$$

$$\ln K = \frac{38.065 \times 10^3}{T} - 33.03$$

+++ +

+++

CONCLUSION AND RECOMMENDATIONS

CONCLUSION

This study has provided a comprehensive picture of the zinc acetate species on impregnated carbon samples both on the surface and in the bulk, as a function of the zinc acetate concentration. Evidence is presented for a monolayer deposition up to about 15 per cent zinc acetate. The zinc acetate species, present in the dried catalyst did not interact with carrier to form any stable carbon-zinc acetate complex at the surface.

The experimental data for the heterogeneous interaction of acetylene and acetic acid with activated carbon based catalysts containing up to 25 per cent zinc acetate have been obtained. It is considered that the greatest value of this part of the investigation was in setting up a mechanism and a rate equation which satisfy the behavior of the acetylene-acetic acid system with $Zn(OAc)_2-C$ as a catalyst.

The effect of several variables, molar feed ratio of acetylene to acetic acid, reaction temperature, and the reciprocal of space velocity on the conversion and product distribution were examined. Though fifteen different mechanisms were postulated, the rate equation, which satisfactorily correlated the experimental data, has been evaluated based on the mechanism of surface reaction between ionized acetic acid and acetylene. The mechanism assumed that the rate controlling

step was the irreversible ionic adsorption of acetylene and acetic acid. The rate was derived as

$$\text{rate}(r) = \frac{K_A p_A}{1 + \left(\frac{K_A}{K_B}\right)\left(\frac{p_A}{p_B}\right)} \quad [12]$$

where K_A and K_B are adsorption equilibrium constants for acetic acid and acetylene, respectively.

Complete vibrational assignments and calculations of the ideal gas thermodynamic properties of vinyl acetate and crotonaldehyde have been made for the first time from 298.15 to 1500°K using the literature information on the fundamental frequencies and molecular parameters. Internal rotational contributions due to CH_3 -group have been obtained for both the molecules using Pitzer and Gwinn's Tables.

For vinyl acetate the departure functions, that is, the difference between the real gas and the ideal gas property have been computed using the Martin-Hou equation of state. As the pressure-volume-temperature data are not available for this compound, the Martin-Hou constants have been predicted from the critical constants and the vapor pressure-boiling point data of vinyl acetate. These departure functions in combination with the ideal gas properties will give the values of the real gas thermodynamic properties of vinyl acetate. It is hoped that in the absence of the experimental values, these predicted values will be of use to the design engineer.

RECOMMENDATIONS

In the case of reaction studied in this work, additional experimental work is needed for further examination of the charge transfer (ionic) mechanism. Independent adsorption studies of the reaction products at reaction conditions along with simultaneous measurement of the electron concentration may help to determine the electron exchange between the adsorbed species and the catalyst.

Experimental pressure-volume-temperature studies of vinyl acetate and the vapor liquid equilibria of the system, vinyl acetate-acetic acid-acetene-acetaldehyde_crotonaldehyde should be carried out before detailed process engineering studies are made.

REFERENCES

- 1 Miller, S.A., 'ACETYLENE, Its Properties, Manufacture and Uses', Vol. II, Academic Press, New York, 1966.
- 2 Sittig, M., 'Vinyl Monomers and Polymers', Noyes Development Corp., U.S.A., 1966.
- 3 Leonard, E.C., 'Vinyl and Diene Monomers', Pt. 1, Wiley Interscience, New York, 1970.
- 4 Stobaugh, R.B., Allen, W.C. Jr., and Sternberg, Van R.H., 'Vinyl Acetate, How, Where, Who - Future', Hydrocarbon Processing, 51(5), 153 (1972).
- 5 Dabke, S.P., 'Vapor Liquid Equilibrium Studies of Vinyl Acetate-Crotonaldehyde, Crotonaldehyde - Acetic Acid and Vinyl Acetate - Acetic Acid Systems', M.Tech. Thesis, IIT-Kanpur, December, 1975.
- 6 Rostovskii, E.N., Zhur. Prikld. Khim. (Russian), 32, 2691 (1959), Chem. Abs., 54, 9479a (1960).
- 7 Rostovskii, E.N. and Arbuzova, I.A., Zhur. Prikld. Khim. (Russian), 32, 2258 (1959); Chem. Abs., 54, 10843e (1960).
- 8 Mitsutani, A., and Kominami, T., Nippon Kagaku Zasshi, (Japan), 80, 886 (1959); Chem. Abs., 55, 4384c (1961).
- 9 Yamada, N., Kogyo Kagaku Zasshi (Japan), 62, 1458 (1959); Chem. Abs., 57, 10563f (1962).
- 10 Cristea, I., Mihai, F., and Pop, Gr., Acad. Rep. Populare Romine Baza Cercetary Stiini Timisoara, Studii Cercetary, Stiint, Chim., 10(1), 101 (1963); Chem. Abs., 61, 9581e (1964).

- 11 Liverovskaya, N.V., Terushkin, V.R., Glushankova, Z.I., Gel'bshtein, A.I., Kravchenko, B.A., Golubev, V.N., Rozenberg, M.E., Satarova, R.A., Andruv, Yu. V., et al., U.S.S.R. Patent 276919, 22 July, (1970); Chem. Abs., 74 112633t (1971).
- 12 Akopyan, A.E., Boyadzhyan, V.K., Eritsyan, V.K., Eginyan, O.S. and Musaelyan, L.R., Arm. Khim. Zh. (Russian), 22(9), 848 (1969); Chem. Abs., 72, 21258s (1970).
- 13 Liverovskaya, N.V., Terushkin, V.R., Satarova, R.A., Glushankova, Z.I., Golubev, V.N., Kravchenko, B.A., and Gel'bshtein, A.I., Khim Prom. (Moscow), 48(2), 100 (1972); Chem. Abs., 76, 112626j (1972).
- 14 Bristol, J.E. and Call, R.N., U.S. Patent 2988517, June 13, 1961.
- 15 Hassler, J.N., 'Activated Carbon', Chemical Publishing Company, Inc., New York, 1963.
- 16 Mattson, J.S. and Mark, H.B Jr., 'Activated Carbon', Marcel Dekker, Inc., New York, 1971.
- 17 Strickland-Constable, R.F., Proc. Roy. Soc. (London), A189, 1 (1947).
- 18 Grigorev, A.I., Russ. J. Inor. Chem. (English), 8, 409 (1963).
- 19 Edward, D.A. and Hayward, R.N., Can. J. Chem., 46, 3443 (1968).
- 20 Ross, S.D., 'Inorganic Infrared and Raman Spectra', McGraw Hill, London, 1972.

21 Furukawa, J. Chem. High Polymers (Japan), 6, 116 (1949); Chem. Abs., 46, 1338ⁱ (1952).

22 Furukawa, J. and Ozawa, H., Bull. Inst. Chem. Res., Kyoto Univ., 26, 93 (1951); Chem. Abs., 48, 8018^d (1954).

23 Yamada, N. and Kobayashi, Y., J. Chem. Soc., Japan, Pure Chem. Sec., 76, 722 (1955); Chem. Abs. 50, 3051^b (1956).

24 Yamada, N., Nippon Kagaku Zasshi (Japan), 78, 252 (1957); Chem. Abs., 51, 14795b (1957).

25 Janda, J., Chem. Zvesti, 11, 478 (1957); Chem. Abs., 52, 8041h (1958).

26 Janda, J. and Vanko, A., Chem. Zvesti, 12, 657 (1958); Chem. Abs., 53, 11205f (1959).

27 Arbuzova, A., Ushakov, S.N., and Rostovskii, E.N., Zhur. Prikl. Khim. (Russian), 31, 1704 (1958); Chem. Abs., 53, 7002c (1959).

28 Mitsutani, A. and Matsumoto, M., Nippon Kagaku Zasshi (Japan), 79, 948 (1958); Chem. Abs., 54, 4366a (1960).

29 Flid, R.M. and Chirikova, A.V., Zhur. Prikl. Khim. (Russian), 32, 660 (1959); Chem. Abs., 53, 16944e (1959).

30 Rostovskii, E.N. and Ushakov, S.N., Zhur. Prikl. Khim. (Russian), 32, 2060 (1959); Chem. Abs. 54, 9744i (1960).

31 Mitsutani, A., Nippon Kagaku Zasshi (Japan), 81, 298, 508 (1960); Chem. Abs., 56, 313h (1962).

32 Nakamura, A., Kubota, S., Kobayashi, J., and Higuchi, I., Nippon Kagaku Zasshi (Japan), 87(10) 1042 (1966); Chem. Abs., 66, 64789j (1967).

33 Ho Sui Dao, Trofimova, I.V., and Flid, R.M., *Zhur. Prikld. Khim* (Russian), 45(3), 700 (1972); *Chem. Abs.*, 77, 163981z (1972).

34 Vasil'eva, I.B., Gel'bshteyn, A.I., Tolstikova, I.N., and Wangtjiong, T., *Kinetika i Kataliz* (English Translation), 5(1), 144 (1964).

35 Hinshelwood, C.N., 'The Kinetics of Chemical Change', The Clarendon Press, New York, 1940.

36 Hougen, O. and Watson, K.M., 'Chemical Process Principles', Pt III, John Wiley, New York, 1947.

37 Pauling, L., 'The Nature of Chemical Bond', Butterworths, London, 1963.

38 Bond, G.C., 'Catalysis by Metals', Academic Press, London, 1962.

39 Gel'bshteyn, A.I., Scheglova, G.G., and Khomenko, A.A., *Kinetika i Kataliz*, 4, 625 (1963); *Chem. Abs.*, 59, 13388h (1963).

40 Mann, R.S. and Ko, D.W., *J. Cat.*, 30, 276 (1973).

41 Mann, R.S. and Yao, K.C., *J. Appl. Chem. Biotech.*, 22, 1915 (1972).

42 Hougen, O.A., *Ind. Eng. Chem.*, 53, 509 (1961).

43 Draper, N.R. and Smith, H., 'Applied Regression Analysis', John Wiley, Inc., New York, 1966.

44 Capkova, I. and Fried, V., *Collection Czech Chem. Commun.*, 28, 2235 (1963).

45 Martin, J.J. and Hou, Y.C., *A.I.Ch.E.J.*, 1, 142 (1955).

46 Martin, J.J., Kapoor, R.M., and Nebers, N.D., *A.I.Ch.E.J.*, 5, 159 (1959).

47 Reid, R.C. and Sherwood, T.K., 'The Properties of Gases and Liquids', 2nd Ed., McGraw-Hill, New York, 1966.

48 Feairheller, W.R. and Katon, J.E., *J. Mol. Struct.*, 1, 239 (1968).

49 Kotarlenko, L.A., Gordenina, A.P., Rekasheva, A.F., and Kipriamova, L.A., *Zhur. Prikld. Spektrosk. (Russian)*, 5, 366 (1966).

50 Rao, V.M. and Curl, R.F., Jr., *J. Chem. Phys.*, 40, 3688 (1964).

51 Crowder, G.A., *Spectrochim. Acta*, 28A, 1625 (1972).

52 Jones, G.I.L. and Owen, N.L., *J. Mol. Struct.*, 18, 1 (1973).

53 Allen, P.W. and Sutton, L.E., *Acta Crystallogr.*, 3, 46 (1950).

54 O'Gorman, J.M., Shand, W., and Schomaker, V., *J. Amer. Chem. Soc.*, 72, 4222 (1950).

55 Tabor, W.J., *J. Chem. Phys.*, 27, 974 (1957).

56 McManis, G.E., *Appl. Spectrosc.*, 24, 495 (1970).

57 Lucier, J.J. and Bentley, F.F., *Spectrochim. Acta*, 20, 1 (1964).

58 Wilmshurst, J.K., *J. Mol. Spectrosc.*, 1, 201 (1957).

59 Miyazawa, T., *Bull. Chem. Soc. Japan*, 34, 691 (1961).

60 Haurie, M. and Novak, A., *J. Chem. Phys.*, 62, 137 (1965).

61 Fukushima, K. and Zwolinski, B.J., *J. Chem. Phys.*, 50, 737 (1969).

62 Pitzer, K.S. and Gwinn, W.D., *J.Chem. Phys.*, 10, 428 (1942).

63 Cox, J.D. and Pilcher, G., 'Thermochemistry of Organic and Organometallic Compounds', Academic Press, London and New York, 225 (1970).

64 William, E., Nat. Bur. Stand., Report No. 6928, Table B-39, (1960).

65 West, W.D. and Ishihara, S., *Amer. Soc. Test. Mater.* (1965).

66 'Selected Values of Properties of Chemical Compounds', Thermodynamic Research Center Data Project, Thermodynamic Research Center, Texas, A and M University, College Station, Texas (Loose leaf data sheets, extant, 1974).

67 'Selected Values of Properties of Hydrocarbons and Related Compounds', American Petroleum Institute Research Project 44, Thermodynamic Research Center, Texas A and M University, College Station, Texas (Loose leaf data sheets, extant, 1974).

68 Suzuki, M. and Kozima, K., *Bull. Chem. Soc. Japan*, 42, 2183 (1969).

69 Hsu, S.L. and Flygare, W.H., *Chem. Phys. Lett.*, 4(5), 317 (1964).

70 Bowles, A.I., George, W.O., and Maddams, W.F., *J.Chem. Soc. (B)*, 7, 810 (1961).

71 Gredy, B. and Piaux, L., *Bull. Soc. Chim. France*, 5, 1481 (1934).

72 Saunders, R.H., Murray, M.J., Cleveland, F.F., and Komarewsky, V.I., J.Amer. Chem. Soc., 65, 1309 (1943).

73 Behringer, J., Z. Elektrochem., 62, 544 (1958).

74 Stull, D.R., Westrum, E.F., Jr., and Sinke, G.C., 'The Chemical Thermodynamics of Organic Compounds', John Wiley and Sons, New York, 1969.

++ + + +
++ +

APPENDIX A

CHARACTERIZATION OF $\text{Zn}(\text{OAc})_2\text{-C}$ SYSTEM

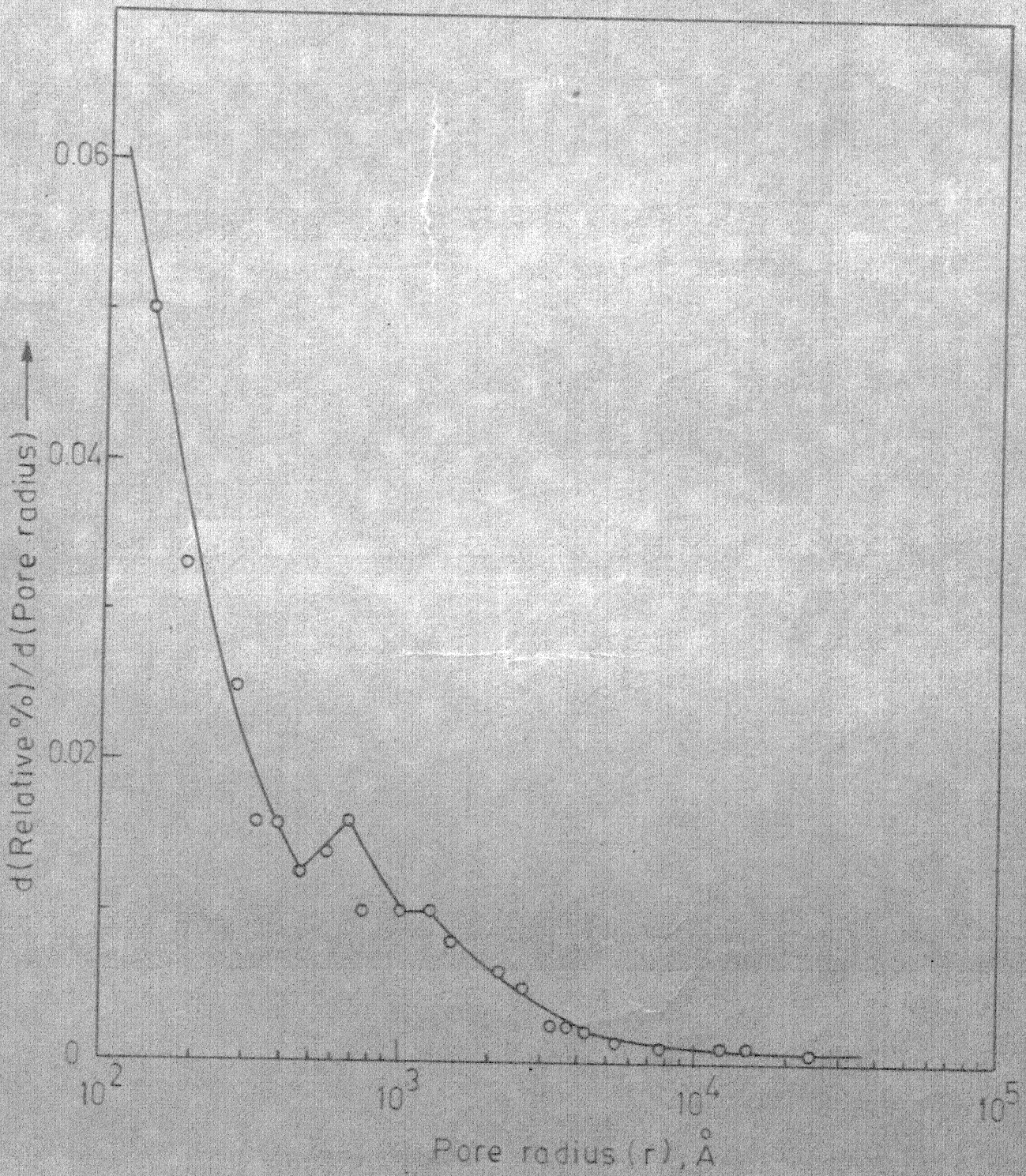


Fig.A1 - Pore size distribution of Zn^{2+} -000.

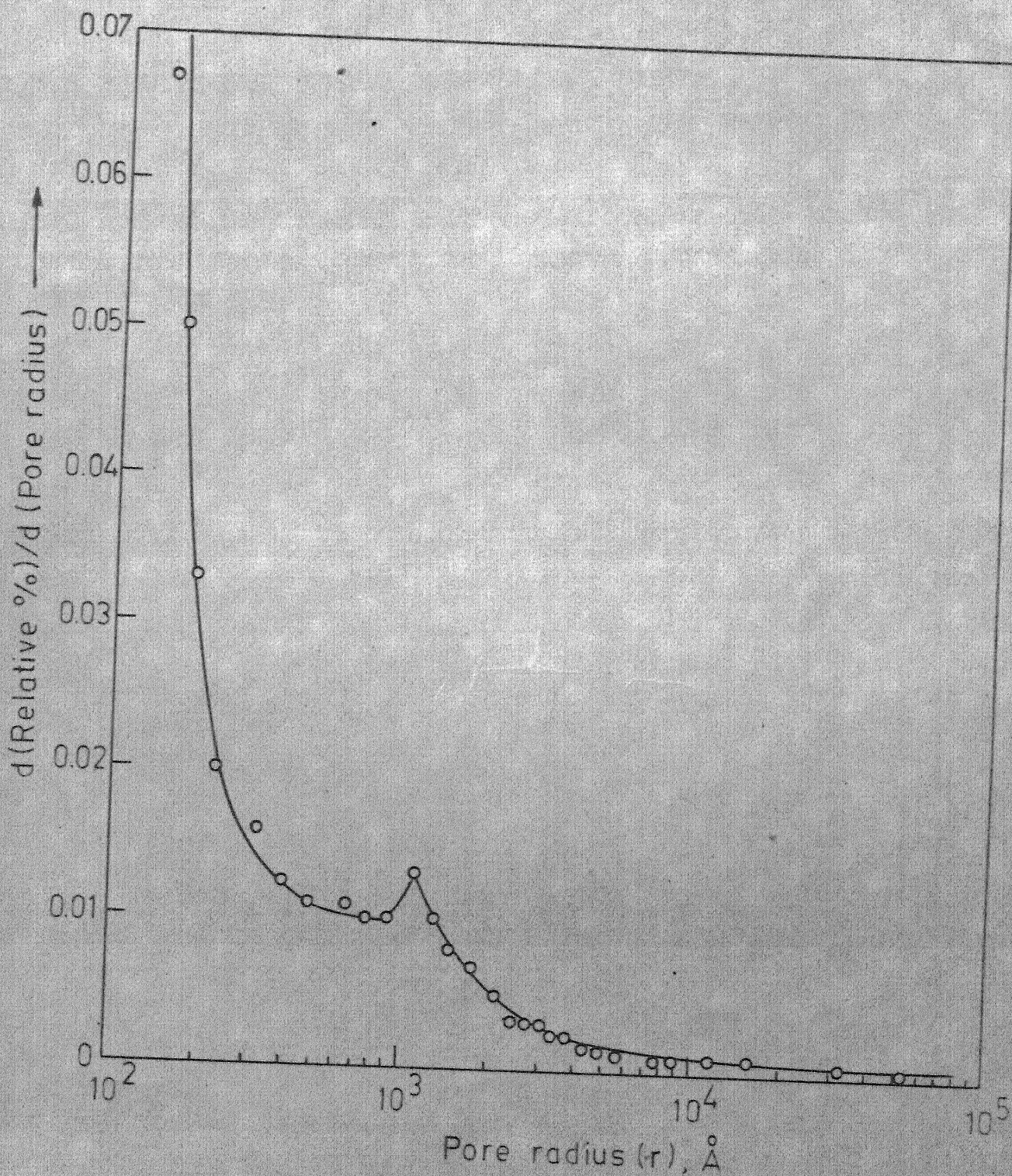


Fig.A2- Pore size distribution of Zn^{2+} -005.

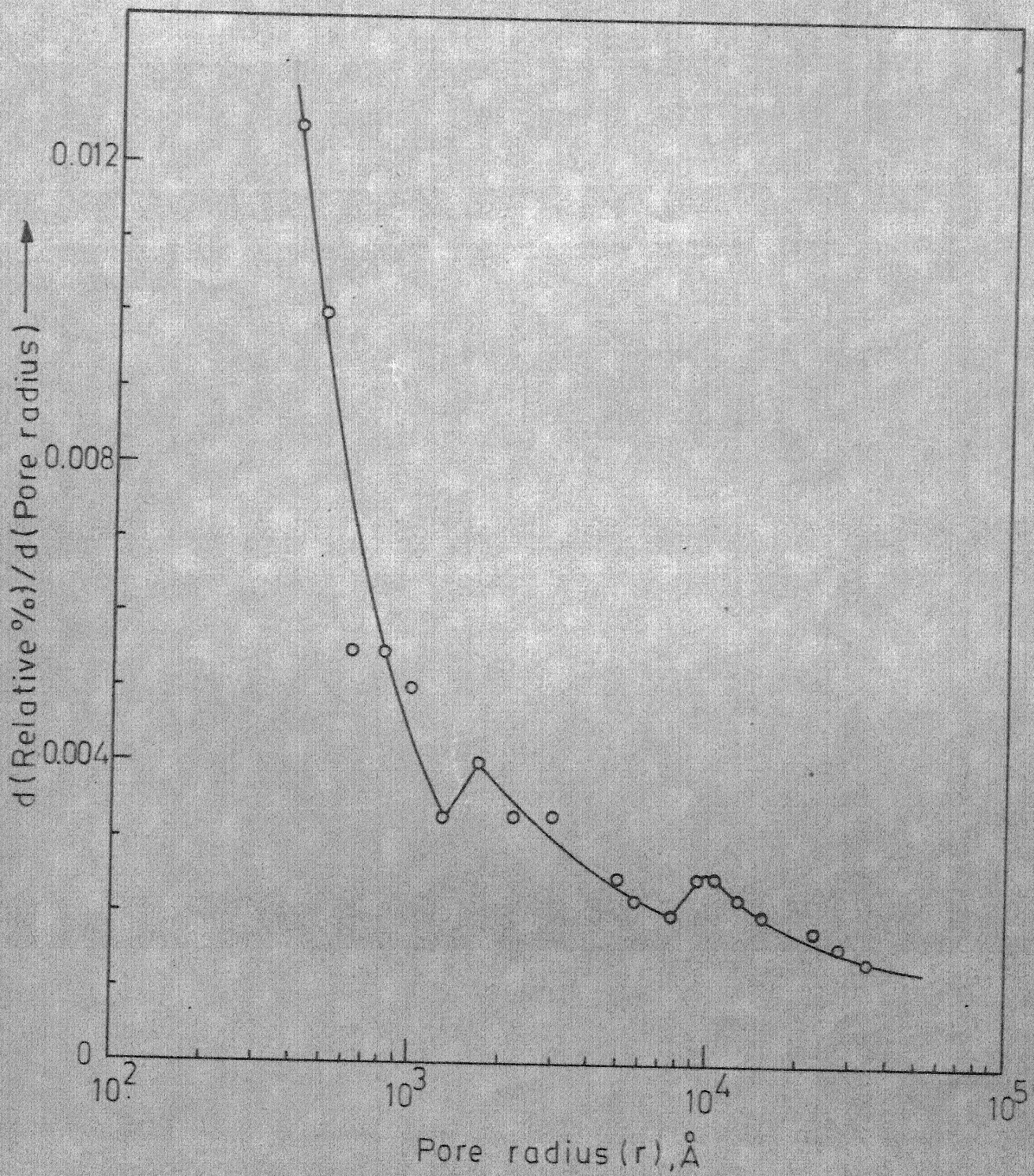


Fig. A 3- Pore size distribution of Zn²⁺-010.

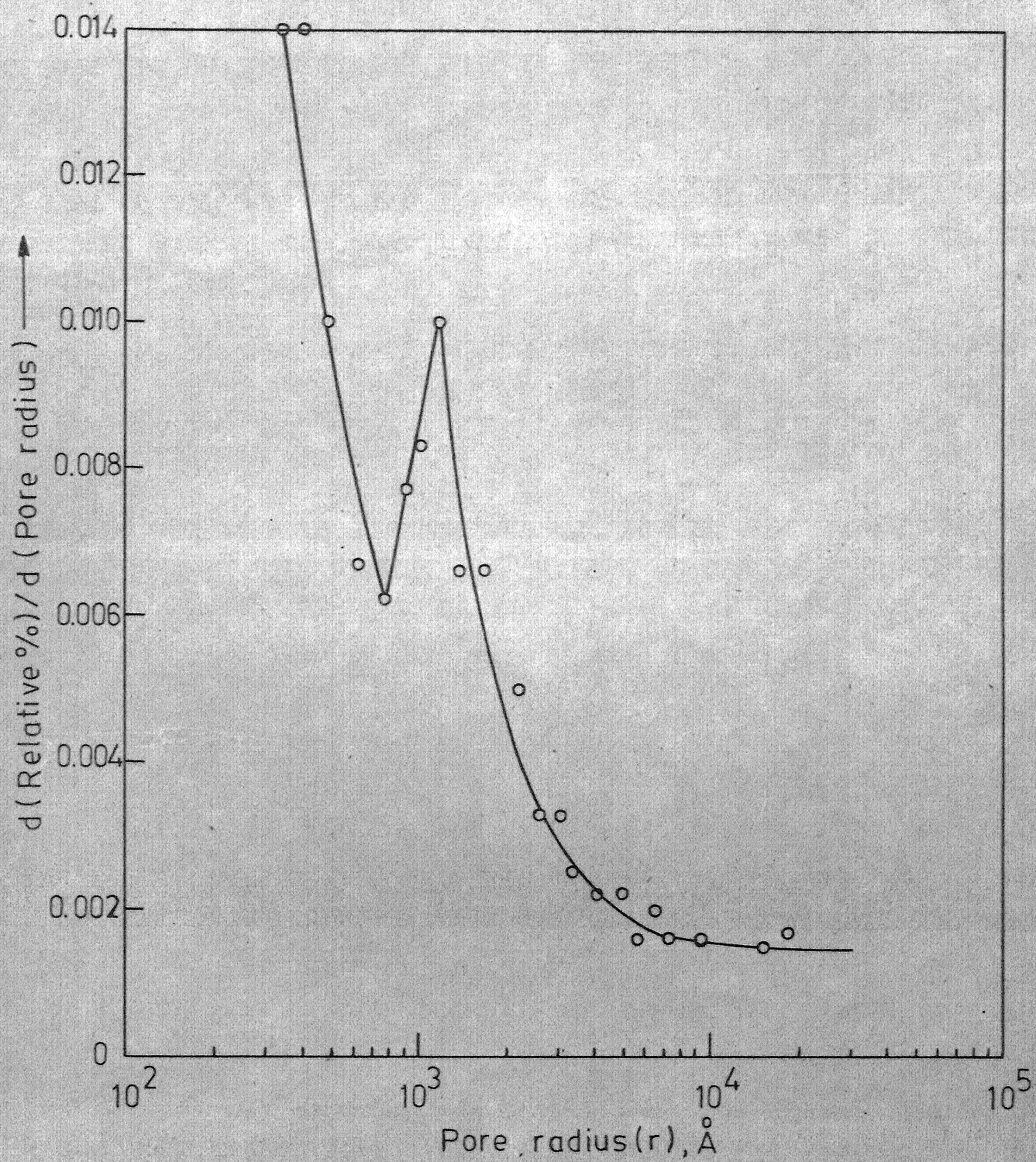


Fig.A 4 - Pore size distribution of Zn^{2+} -015.

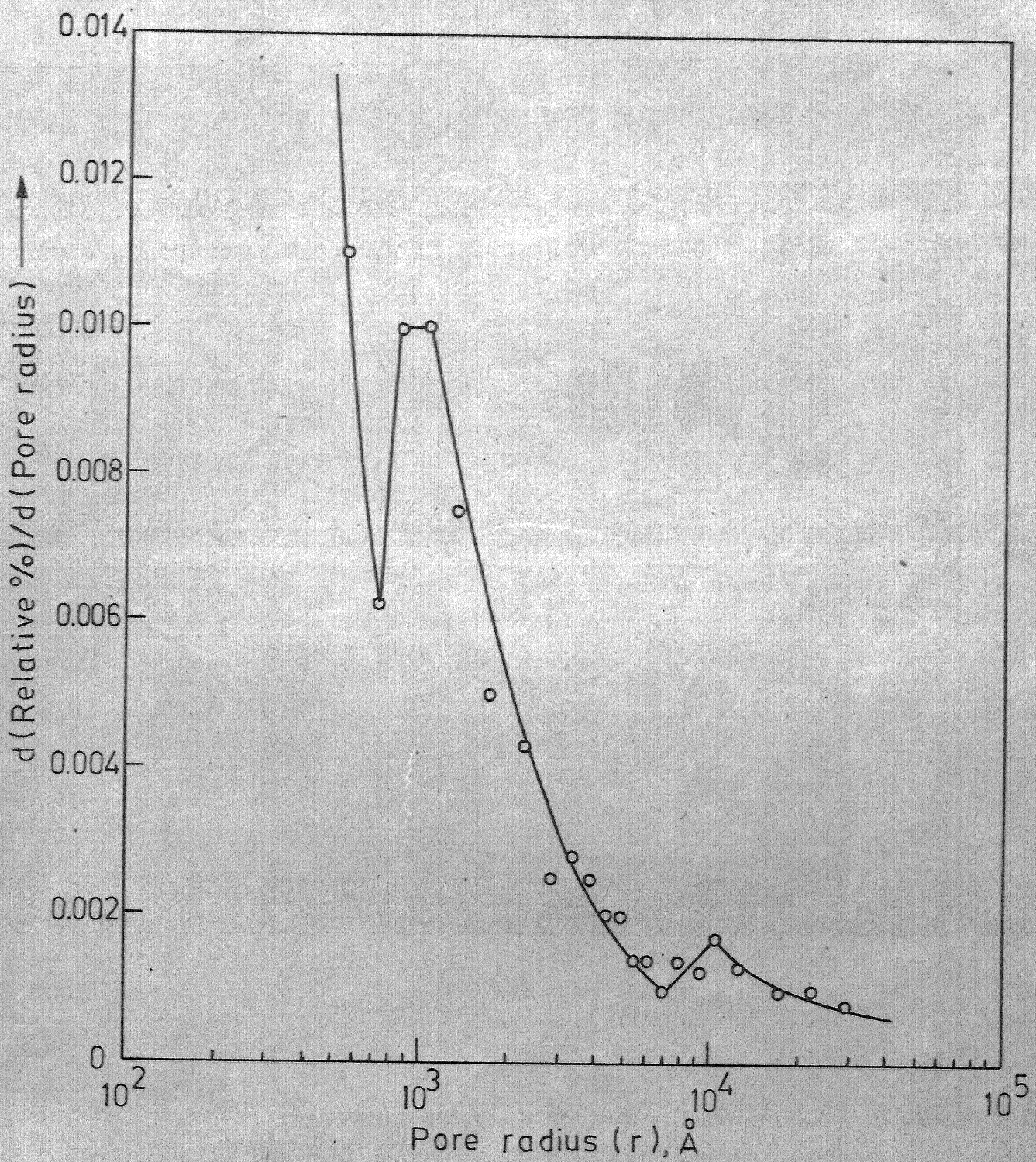


Fig.A5- Pore size distribution of $\text{Zn}^{2+}\text{-020}$.

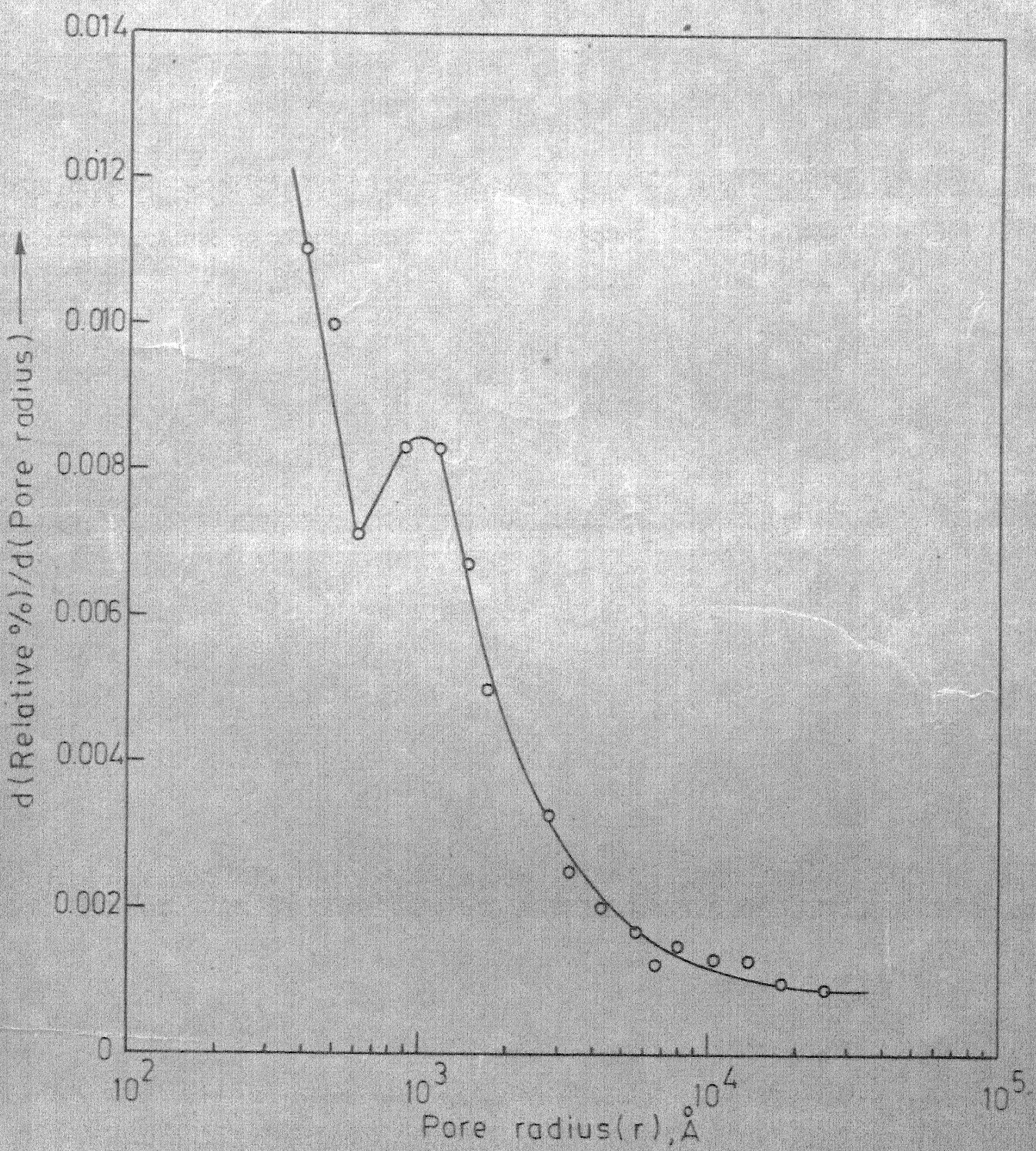


Fig. A 6- Pore size distribution of Zn^{2+} - 025.

APPENDIX B

KINETICS AND MECHANISM

TABLE B1: PERFORMANCE OF $Zn^{2+}O_2$ CATALYST

Reaction temperature 180°C ; (W) = 15.0

Run No.	Flow Rate, mol hr ⁻¹	Reactant Mole Ratio, (R)	Vinyl Acetate Formed, mol hr ⁻¹ $\times 10^3$	Per cent Yield Vinyl Acetate
M1	0.094	0.15	0.244	1.6
M2	0.053	0.15	0.203	2.8
M3	0.050	0.15	0.200	3.0
M4	0.030	0.15	0.180	5.0

100

TABLE B2: PERFORMANCE OF $Cd^{2+}025$ CATALYST

Reaction temperature $180^{\circ}C$; (W) = 15.0

Run No.	Acetic Acid	Flow Rate, mol hr ⁻¹	Reactant Acetylene	Total	Reactant Mole Ratio, (R)	Vinyl acetate Formed, mol hr ⁻¹ $\times 10^3$	Per cent Yield Vinyl acetate
M5	0.087	0.15		0.237	1.73	2.30	2.65
M6	0.071	0.15		0.221	2.10	2.13	3.00
M7	0.069	0.15		0.219	2.20	2.10	3.03
M8	0.067	0.15		0.217	2.25	2.08	3.11
M9	0.045	0.15		0.195	3.35	1.70	3.79

TABLE B2: PERFORMANCE OF $\text{Ni}^{2+}-025$ CATALYST

Reaction temperature 180°C ; $(W) = 15.0$

Run No.	Acetic Acid	Flow Rate, mol hr ⁻¹	Reactant Mole Ratio, (R)	Vinyl Acetate Formed, mol hr ⁻¹ $\times 10^4$	Per cent Yield Vinyl Acetate
M10	0.079	0.15	0.229	1.90	4.70
M11	0.055	0.15	0.205	2.73	4.59
M12	0.044	0.15	0.194	3.38	4.30
M13	0.029	0.15	0.179	5.25	4.00
				3.00	0.91
					1.03

TABLE B4: EFFECT OF ZINC ACETATE CONCENTRATION ON PER CENT
YIELD OF VINYL ACETATE

Reaction temperature 180°C ; (W/F) = 30.0 ;
 $(R) = 3.0$; (W) = 15.0

Run No.	Percentage Zinc Acetate (weight per cent)	Acetic Acid	Flow Rate, mol hr ⁻¹	Acetylene	Total	Vinyl Acetate Formed, mol hr ⁻¹ $\times 10^3$	Per cent Yield Vinyl Acetate
CC-1	5	0.125	0.375	0.5	2.19	1.75	
CC-2	10	0.125	0.375	0.5	3.96	3.17	
CC-3	12	0.125	0.375	0.5	4.63	3.70	
CC-4	15	0.125	0.375	0.5	5.13	4.10	
CC-5	18	0.125	0.375	0.5	4.13	3.30	
CC-6	20	0.125	0.375	0.5	3.50	2.80	
CC-7	25	0.125	0.375	0.5	2.38	1.90	

TABLE B5: EFFECT OF REACTANT MOLE RATIO ON PER CENT
CONVERSION OF ACETIC ACID AND PER CENT
SELECTIVITY FOR VINYL ACETATE AT 155°C

$$(W/F) = 30.0 ; \quad (W) = 15.0$$

Run No.	Flow Rate, mol hr ⁻¹	Acetic Acid	Acetylene Total	Reactant Mole Ratio, (R)	Acetic Acid Reacted, mol hr ⁻¹	Vinyl Acetate Formed, mol hr ⁻¹	Acetone Formed, mol hr ⁻¹	Per cent Acetic Acid for Vinyl Acetate Reacted	Per cent Selectivity for Vinyl Acetate	Rate of Acetone Formation, gm cat ⁻¹ hr ⁻¹ x 10 ⁴
TR-1	0.250	0.250	0.5	1	3.16	1.75	7.05	1.26	55.40	2.10
TR-2	0.125	0.375	0.5	3	2.29	1.82	2.34	1.83	79.60	1.53
TR-3	0.100	0.400	0.5	4	1.97	1.66	1.54	1.97	84.35	1.31
TR-4	0.084	0.416	0.5	5	1.71	1.50	1.05	2.03	87.55	1.14
TR-5	0.0625	0.4375	0.5	7	1.33	1.22	0.55	2.13	91.50	0.89
TR-6	0.050	0.450	0.5	9	1.10	1.03	0.35	2.20	93.50	0.73

TABLE B6: EFFECT OF REACTANT MOLE RATIO ON PER CENT CONVERSION
OF ACETIC ACID AND PER CENT SELECTIVITY FOR VINYL
ACETATE AT 165°C

$$(W/F) = 30 ; (W) = 15.0$$

Run No.	Flow Rate, mol hr ⁻¹	Acetic Acid	Total Acylene	Reactant Mole Ratio, (R)	Acetic Acid	Vinyl Acetate Formed, mol hr ⁻¹	Acetone Formed, mol hr ⁻¹	Acetic Acid converted x 10 ³	Per cent Selectivity for Vinyl Acetate	Per cent Acetic Acid Reacted, mol hr ⁻¹	Rate of Acetic Acid formation, gm cat ⁻¹ x 10 ⁴
TR-7	0.250	0.250	0.5	1	5.05	3.12	9.62	2.02	61.84	3.37	
TR-8	0.125	0.375	0.5	3	3.59	2.99	3.00	2.87	83.25	2.40	
TR-9	0.100	0.400	0.5	4	3.16	2.77	1.95	3.16	87.53	2.10	
TR-10	0.084	0.416	0.5	5	2.86	2.56	1.47	3.40	89.72	1.90	
TR-11	0.0625	0.4375	0.5	7	2.25	2.10	0.75	3.60	92.95	1.50	
TR-12	0.050	0.450	0.5	9	1.85	1.74	0.53	3.70	94.54	1.23	

TABLE B7: EFFECT OF REACTANT MOLE RATIO ON PER CENT CONVERSION OF
ACETIC ACID AND PER CENT SELECTIVITY FOR VINYL ACETATE
AT 180°C

(W/F) = 30.0 ; (W) = 15.0

Run No.	Flow Rate, mol hr ⁻¹	Reactant Ratio, (R)	Acetic Acid Reacted, mol hr ⁻¹	Vinyl Acetate Formed, mol hr ⁻¹	Acetone Formed, mol hr ⁻¹	Per cent Acetic Acid Converted	Per cent Selectivity for Vinyl Acetate	Rate of Acetic Acid Reacted, mol hr ⁻¹
TR-13	0.250	0.250	0.5	1	6.89	5.00	9.45	2.76
TR-14	0.125	0.375	0.5	3	5.77	5.12	3.23	4.62
TR-15	0.100	0.400	0.5	4	5.38	4.92	2.28	5.38
TR-16	0.084	0.416	0.5	5	5.08	4.73	1.73	6.04
TR-17	0.0625	0.4375	0.5	7	4.40	4.17	1.14	7.05
TR-18	0.050	0.450	0.5	9	3.75	3.57	0.88	7.50

TABLE B8: EFFECT OF REACTANT MOLE RATIO ON PER CENT CONVERSION OF
ACETIC ACID AND PER CENT SELECTIVITY FOR VINYL ACETATE

AT 192°C

$(W/F) = 30.0$; $(W) = 15.0$

Run No.	Flow Rate, mol hr ⁻¹	Acetic Acid	Acetyl Lene	Total	Reactant Ratio, (R)	Vinyl Acetate Reacted, mol hr ⁻¹	Acetone Formed, mol hr ⁻¹	Acetic Acid Formed, mol hr ⁻¹	Conversion, %	Per cent Selectivity for Vinyl Acetate	Rate of Acetic Acid Reacted, mol hr ⁻¹	gm cat ⁻¹ x 10 ⁴
TR-19	0.250	0.250	0.5	1	10.68	9.55	5.67	4.27	89.38	7.12		
TR-20	0.125	0.375	0.5	3	8.43	8.00	2.15	6.74	94.90	5.62		
TR-21	0.100	0.400	0.5	4	7.10	6.78	1.58	7.10	95.55	4.73		
TR-22	0.084	0.416	0.5	5	6.15	5.90	1.24	7.32	95.96	4.10		
TR-23	0.0625	0.4375	0.5	7	4.82	4.65	0.84	7.71	96.51	3.21		
TR-24	0.050	0.450	0.5	9	3.85	3.72	0.63	7.70	96.71	2.57		

TABLE B2: EFFECT OF REACTANT MOLE RATIO ON PER CENT CONVERSION OF ACETIC ACID AND PER CENT SELECTIVITY FOR VINYL ACETATE AT 199°C

$$(W/F) = 30.0 ; (W) = 15.0$$

Run No.	Flow Rate, mol hr ⁻¹	Reactant Ratio, (R)	Acetic Acid Reacted, mol hr ⁻¹	Vinyl Acetate Formed, mol hr ⁻¹	Acetone Formed, mol hr ⁻¹	Acetic acid converted, mol hr ⁻¹ x 10 ⁴	Selectivity for Vinyl Acetate, mol hr ⁻¹	Per cent Acetic acid Reacted, gm cat ⁻¹ x 10 ⁴
TR-25	0.250	0.250	0.5	1	15.71	13.87	9.17	6.28
TR-26	0.125	0.375	0.5	3	10.32	9.82	2.46	8.25
TR-27	0.100	0.400	0.5	4	8.08	7.75	1.65	8.08
TR-28	0.084	0.416	0.5	5	6.65	6.41	1.20	7.92
TR-29	0.0625	0.4375	0.5	7	5.12	4.97	0.74	8.19
TR-30	0.050	0.450	0.5	9	4.17	4.06	0.55	8.34

TABLE B10: EFFECT OF RECIPROCAL OF SPACE VELOCITY ON PER CENT
CONVERSION OF ACETIC ACID AND PER CENT YIELD OF
VINYL ACETATE AT 180°C

Run No.	Weight of Catalyst, gms	Feed Rate, mol hr ⁻¹			Space Velocity, hr ⁻¹	Acetato Acid Mol L ⁻¹	VinyL Acetate Mol L ⁻¹	Formed Acetone Mol L ⁻¹	Acetone Mol L ⁻¹ x 10 ⁴	ConverSion Per cent	Acetate VinyL Mol L ⁻¹ x 10 ⁴	Acetate VinyL Per cent	Acetone VinyL Mol L ⁻¹ x 10 ⁴
		Acetic Acid	Acetyl Lene	Total									
WF-1	12	0.300	0.900	1.200	10.00	6.88	6.24	3.20	2.29	2.08	0.10		
WF-2	12	0.150	0.450	0.600	20.00	5.45	4.76	3.45	3.63	3.17	0.23		
WF-3	12	0.100	0.300	0.400	30.00	4.68	4.15	2.66	4.68	4.15	0.26		
WF-4	15	0.150	0.450	0.600	25.00	6.12	5.34	3.87	4.08	3.56	0.26		
WF-5	15	0.146	0.437	0.583	25.73	6.11	5.35	3.77	4.19	3.67	0.26		
WF-6	15	0.139	0.416	0.555	27.03	5.96	5.24	3.59	4.29	3.77	0.26		
WF-7	15	0.133	0.400	0.533	28.14	5.87	5.18	3.43	4.42	3.90	0.26		
WF-8	15	0.125	0.375	0.500	30.00	5.77	5.12	3.23	4.62	4.10	0.26		
WF-9	15	0.083	0.250	0.333	45.05	5.02	4.59	2.16	6.05	5.53	0.26		

TABLE BII: HEAT AND MASS TRANSFER EFFECTS

Reaction temperature = 180°C ; $(\bar{R}) = 3.0$;
 $(W/F) = 30.0$

Run No.	Flow Rate, mol hr ⁻¹			Catalyst Weight, gm.	Acetic Acid Reacted, mol hr ⁻¹	Per cent Conversion acetic Acid x 10 ³
	Acetic Acid	Acetylene	Total			
HM-1	0.050	0.150	0.2	6	2.33	4.67
HM-2	0.075	0.225	0.3	9	3.45	4.60
HM-3	0.100	0.300	0.4	12	4.68	4.68
HM-4	0.125	0.375	0.5	15	5.77	4.62
HM-5	0.150	0.450	0.6	18	6.96	4.64

TABLE B12: COMPARISON OF OBSERVED AND PREDICTED
RATES AT 155°C

(W/F) = 30.0

Sl. No.	Experimental			Predicted	
	$p_{\text{CH}_3\text{COOH}}$, atm	$p_{\text{C}_2\text{H}_2}$, atm	Rate, mol gm cat^{-1} $\text{hr}^{-1} \times 10^4$	Rate, $\text{mol gm cat}^{-1} \text{hr}^{-1}$	$\times 10^4$
1	0.498	0.499	2.10	2.22	
2	0.248	0.749	1.53	1.60	
3	0.198	0.799	1.31	1.35	
4	0.166	0.832	1.15	1.18	
5	0.123	0.874	0.90	0.92	
6	0.099	0.899	0.73	0.75	

TABLE B13: COMPARISON OF OBSERVED AND PREDICTED
RATES AT 180°C

(W/F) = 30.0

Sl. No.	Experimental			Predicted	
	$p_{\text{CH}_3\text{COOH}}$, atm	$p_{\text{C}_2\text{H}_2}$, atm	Rate mol hr ⁻¹ $\times 10^4$	Rate, gm cat ⁻¹ hr ⁻¹ $\times 10^4$	mol hr ⁻¹
1	0.496	0.498	4.60	4.70	
2	0.245	0.749	3.90	4.18	
3	0.195	0.799	3.60	3.69	
4	0.163	0.833	3.40	3.30	
5	0.121	0.874	2.93	2.70	
6	0.966	0.899	2.50	2.25	

TABLE B14: COMPARISON OF OBSERVED AND PREDICTED
RATES AT 192°C

(W/F) = 30.0

Sl. No.	Experimental		Rate, mol gmcat ⁻¹ hr ⁻¹ x 10 ⁴	Predicted
	pCH ₃ COOH, atm	pC ₂ H ₂ , atm		Rate, mol gm cat ⁻¹ hr ⁻¹ x 10 ⁴
1	0.494	0.495	7.12	6.4
2	0.243	0.748	5.62	6.1
3	0.194	0.798	4.73	5.5
4	0.162	0.831	4.10	4.9
5	0.120	0.874	3.21	4.1
6	0.096	0.899	2.57	3.5

APPENDIX C

THERMODYNAMIC PROPERTIES

TABLE C1: VAPOR PRESSURE-BOILING POINT DATA FOR VINYL ACETATE

$$\text{Antoine equation: } \log P \text{ mm} = 7.2550 - \frac{1320.2716}{t(\text{°C})+229.19}$$

$$\text{Enthalpy of vaporization (H}_v\text{)} = 8.32 \pm 0.3 \text{ kcal mol}^{-1}$$

Temperature (t) °C	Pressure (P) cm Hg
3.65	3.84
7.80	4.83
13.15	6.41
19.15	8.68
23.05	10.49
27.30	12.80
31.62	15.59
36.94	19.68
42.17	24.52
48.42	31.56
55.62	41.63
61.32	51.33
66.62	61.91
68.90	66.97
72.10	74.64
72.50	75.63

TABLE C2: PHYSICAL PROPERTIES OF VINYL ACETATE

Boiling point, $^{\circ}\text{C}$, 760 mm	72.7
Freezing point, $^{\circ}\text{C}$, 760 mm	-92.8
Critical temperature, $^{\circ}\text{C}$	228.9
Critical pressure, psia	609
Critical volume, litre mol $^{-1}$	0.265
Flash point, tag open cup, $^{\circ}\text{C}$	-5
Autoignition temperature, $^{\circ}\text{C}$	427
Explosive limit, lower volume per cent in air	2.6
Explosive limit, upper volume per cent in air	13.4
Specific gravity, 20/20 $^{\circ}\text{C}$	0.9338
Coefficient of cubical expansion per degree C (20-40 $^{\circ}\text{C}$)	1.52×10^{-3}
Specific heat of liquid, 20 $^{\circ}\text{C}$, cal gm $^{-1}$ deg $^{-1}$	0.47
Refractive index, n_D^{25}	1.3940
Surface tension, 25 $^{\circ}\text{C}$, dyne cm $^{-1}$	23.8
Viscosity, 20 $^{\circ}\text{C}$, cp	0.41
Dielectric constant 25 $^{\circ}\text{C}$	5.8
Dipole moment, Debye units	1.75
Thermal conductivity at $t^{\circ}\text{C}$ cal sec $^{-1}$ cm $^{-1}$ deg $^{-1}$	370-1.035 (t-20)

Table C2 (contd)

Second Virial Coefficient

Temperature, °K	B
298.16	-795.6
428.16	-438.9
438.16	-425.3
453.16	-406.2
465.16	-392.0
472.16	-384.0
493.16	-361.6

TABLE C3: MARTIN-HOU CONSTANTS AND THE DEPARTURE FUNCTIONS
FOR VINYL ACETATE

$$\begin{array}{lll}
 A_1 = 0.0 & B_1 = 0.082056 & C_1 = 0.0 \\
 A_2 = -45.20401 & B_2 = 0.040952 & C_2 = 0.12129 \\
 A_3 = 82.80420 & B_3 = -0.15889 & C_3 = -3851.47 \\
 A_4 = 2.45173 & B_4 = 0.0 & C_4 = 0.0 \\
 A_5 = -6.03472 & B_5 = -0.011323 & C_5 = 44.77613 \\
 b = 0.03937 & & k = -5.0
 \end{array}$$

T, $^{\circ}\text{K}$	P, atm	V, lit. mol^{-1}	$(\text{H}-\text{H}^{\circ})$, cal mol^{-1}	$(\text{S}-\text{S}^{\circ})$, cal $\text{mol}^{-1}\text{deg}^{-1}$
400		Saturation pressure = 4.634 atm		
	1.60	28.67	43.20	-0.237
	2.31	21.50	56.91	-0.230
	3.09	17.20	70.27	-0.222
	3.94	14.33	83.30	-0.213
450		Saturation pressure = 13.262 atm		
	1.55	28.67	27.78	-0.256
	2.16	21.50	36.57	-0.255
	2.80	17.20	45.11	-0.252
	3.46	14.33	53.43	-0.248
	4.14	12.29	61.50	-0.244
	4.83	10.75	69.35	-0.239
	5.51	9.56	77.00	-0.234
	6.19	8.60	84.36	-0.228
	6.85	7.82	91.53	-0.223
	7.50	7.17	98.47	-0.217

Table C3 (contd)

T, °K	P, atm	V, lit. mol ⁻¹	(H-H ⁰) _{cal} , mol ⁻¹	(S-S ⁰) _{cal} , mol ⁻¹ deg ⁻¹
500	Saturation pressure = 30.138 atm			
	1.57	28.67	17.53	-0.268
	2.14	21.50	23.02	-0.270
	2.71	17.20	28.34	-0.270
	3.28	14.33	33.48	-0.270
	3.84	12.29	38.45	-0.268
	4.38	10.75	43.26	-0.267
	4.90	9.56	47.90	-0.264
	5.39	8.60	52.37	-0.262
	5.84	7.82	56.69	-0.259
	6.24	7.17	60.85	-0.256

TABLE C4: IDEAL GAS THERMODYNAMIC PROPERTIES OF VINYL ACETATE

Temp., °K	C_p^o	S^o	$-(G^o - H_0^o)/T$		$H^o - H_0^o$	ΔH_f^o	G_f^o	$\log K_f$
			Cal	$deg^{-1} mol^{-1}$				
298.15	23.662	78.386	63.146	4.544	-75.460	-54.672	40.07530	
300.00	23.773	78.533	63.241	4.588	-75.482	-54.540	39.73194	
400.00	29.567	86.181	68.034	7.258	-76.503	-47.383	25.88859	
500.00	34.648	93.340	72.388	10.476	-77.479	-39.980	17.47523	
600.00	38.900	100.044	76.441	14.161	-78.157	-32.411	11.80567	
700.00	42.441	106.314	80.264	18.235	-78.663	-24.740	7.72403	
800.00	45.418	112.182	83.889	22.633	-79.018	-17.007	4.64606	
900.00	47.946	117.681	87.340	27.306	-79.241	-9.241	2.24396	
1000.00	50.104	122.847	90.634	32.211	-79.337	-1.436	0.31374	
1100.00	51.955	127.711	93.786	37.316	-79.334	6.303	-1.25223	
1200.00	53.547	132.302	96.807	42.592	-79.261	14.123	-2.57219	
1300.00	54.919	136.643	99.707	48.016	-79.131	21.891	-3.68020	
1400.00	56.107	140.758	102.495	53.567	-78.952	29.701	-4.63647	
1500.00	57.138	144.665	105.178	59.230	-78.733	37.434	-5.45408	

TABLE C5: IDEAL GAS THERMODYNAMIC PROPERTIES OF CROTONALDEHYDE

Temp., °K	C_p^o	S^o	$-(G^o - H_0^o)/T$	$H^o - H_0^o$	ΔH_f^o	ΔG_f^o	$\log K_f$
Cal deg ⁻¹ mol ⁻¹	kcal mol ⁻¹						
298.15	19.760	78.398	65.384	3.880	-24.030	-10.550	7.73366
300.00	19.857	78.520	65.464	3.917	-24.053	-10.464	7.62289
400.00	25.049	84.948	69.539	6.164	-25.188	-5.748	3.14041
500.00	29.778	91.058	73.237	8.910	-26.223	-0.764	0.33389
600.00	33.827	96.855	76.695	12.096	-27.023	4.406	-1.60492
700.00	37.250	102.334	79.970	15.655	-27.655	9.700	-3.02841
800.00	40.153	107.503	83.091	19.529	-28.137	15.073	-4.11776
900.00	42.625	112.379	86.077	23.571	-28.483	20.495	-4.97681
1000.00	44.738	116.982	88.940	28.042	-28.700	25.970	-5.57577
1100.00	46.548	121.333	91.689	32.509	-28.816	31.392	-6.23697
1200.00	48.101	125.451	94.332	37.343	-28.860	36.907	-6.72165
1300.00	49.439	129.356	96.877	42.222	-28.847	42.379	-7.12462
1400.00	50.593	133.063	99.331	47.225	-28.784	47.903	-7.47798
1500.00	51.592	136.588	101.698	52.335	-28.682	53.358	-7.77421

TABLE G6: IDEAL GAS THERMODYNAMIC PROPERTIES OF ACETONE

Temp. °K	C_p^o	S^o	$-(g^o - H_f^o)/T$	$H^o - H_f^o$	ΔH_f^o	ΔG_f^o	Log K_f
		cal deg ⁻¹ mol ⁻¹	cal deg ⁻¹ mol ⁻¹	cal mol ⁻¹	cal mol ⁻¹	cal mol ⁻¹	
298.15	17.733	70.636	57.652	3.371	-51.900	-56.515	26.76640
300.00	17.806	70.746	57.737	3.904	-51.923	-56.419	26.53082
400.00	21.877	76.423	61.710	5.887	-53.075	-31.063	16.97199
500.00	25.750	81.728	65.190	8.272	-54.153	-25.431	11.11585
600.00	29.150	86.730	68.360	11.020	-55.014	-19.598	7.13855
700.00	32.090	91.450	71.330	14.086	-55.714	-13.639	4.25831
800.00	34.620	95.900	74.120	17.424	-56.272	-7.582	2.07125
900.00	36.820	100.110	76.780	20.993	-56.698	-1.474	0.35803
1000.00	38.730	104.090	79.310	24.779	-57.001	4.698	-1.02674

TABLE C7: IDEAL GAS THERMODYNAMIC PROPERTIES OF ACETIC ACID

Temp., °K	C_p^o	S^o		$-(G^o - H_0^o)/T$		$H_0^o - H_f^o$ kcal mol ⁻¹	ΔG_f^o kcal mol ⁻¹	$\log K_f$
		Cal	deg ⁻¹ mol ⁻¹					
298.15	15.900	67.520	56.500	3.286	-103.260	-89.355	65.49870	
300.00	15.970	67.620	56.510	3.316	-103.276	-89.249	65.01774	
400.00	19.520	72.720	57.180	5.096	-103.999	-83.348	45.53910	
500.00	22.600	77.410	58.560	7.206	-104.745	-77.266	33.77268	
600.00	25.150	81.760	60.230	9.596	-105.265	-71.059	25.88322	
700.00	27.350	85.810	62.020	12.226	-105.664	-64.772	20.22261	
800.00	29.080	89.580	63.860	15.056	-105.963	-58.442	15.96546	
900.00	30.600	93.090	65.690	18.036	-106.193	-52.076	12.64570	
1000.00	31.990	96.390	67.490	21.166	-106.337	-45.674	9.98193	

TABLE 08: IDEAL GAS THERMODYNAMIC PROPERTIES OF ACETALDEHYDE

Temp., (°K)	C_p^o	S^o	$-(G^o - H_0^o)/T$	$H^o - H_0^o$	ΔH_f^o	ΔG_f^o	$\log K_f$
		Cal deg ⁻¹ mol ⁻¹	Cal deg ⁻¹ mol ⁻¹	kcalmol ⁻¹	kcalmol ⁻¹	kcalmol ⁻¹	kcalmol ⁻¹
298.15	13.060	63.150	52.850	3.070	-39.780	-31.826	23.32886
300.00	13.110	63.240	52.860	3.100	-39.739	-31.759	23.13617
400.00	15.730	67.370	56.030	4.535	-40.498	-28.999	15.84400
500.00	18.270	71.140	58.670	6.240	-41.238	-26.027	11.37654
600.00	20.520	74.680	61.050	8.180	-41.830	-22.929	8.35197
700.00	22.500	78.000	63.240	10.340	-42.311	-19.740	6.16293
800.00	24.200	81.120	65.280	12.580	-42.701	-16.483	4.50302
900.00	25.680	84.060	67.200	15.170	-43.014	-13.183	3.20124
1000.00	26.960	86.840	69.030	17.810	-43.234	-9.850	2.15269

TABLE C9: IDEAL GAS THERMODYNAMIC PROPERTIES OF ACETYLENE

Temp. °K	C_p^o	S^o Cal deg $^{-1}$ mol $^{-1}$	$-(G^o - H_O^o)/T$	$H^o - H_O^o$		ΔG_f^o kcal mol $^{-1}$	Log K _f
					ΔH_f^o kcal mol $^{-1}$		
298.15	10.499	47.997	39.976	2.392	54.194	50.000	-36.649
300.00	10.532	48.061	40.025	2.411	54.193	49.975	-36.406
400.00	11.973	51.304	42.451	3.541	54.134	48.577	-26.541
500.00	12.967	54.090	44.508	4.791	54.049	47.196	-20.629
600.00	13.728	56.525	46.313	6.127	53.931	45.835	-16.695
700.00	14.366	58.692	47.930	7.533	53.787	44.498	-13.893
800.00	14.933	60.649	49.400	8.999	53.627	43.178	-11.798
900.00	15.449	62.441	50.752	10.520	53.462	41.882	-10.170
1000.00	15.922	64.095	52.005	12.090	53.304	40.604	-8.874

TABLE C10: IDEAL GAS THERMODYNAMIC PROPERTIES OF CARBON DIOXIDE

Temp., °K	C_p^o Cal deg ⁻¹ mol ⁻¹	S^o		$-(G^o - H_0^o)/T$	$H^o - H_0^o$ kcal mol ⁻¹	$- \Delta H_f^o$ kcal mol ⁻¹	$-\Delta G_f^o$ kcal mol ⁻¹	$\log K_f$
		C_p^o	$-(G^o - H_0^o)/T$	$H^o - H_0^o$	$- \Delta H_f^o$	$-\Delta G_f^o$		
298.15	8.874	51.070	46.563	2.238	94.051	94.258	69.092	
300.00	8.894	51.125	43.610	2.254	94.050	94.260	68.667	
400.00	9.876	53.823	45.836	3.195	94.060	94.320	51.536	
500.00	10.665	56.115	47.668	4.223	94.090	94.390	41.256	
600.00	11.310	58.118	49.246	5.323	94.120	94.440	34.400	
700.00	11.846	59.903	50.644	6.481	94.160	94.490	29.502	
800.00	12.293	61.515	51.903	7.689	94.220	94.530	25.826	
900.00	12.667	62.985	53.054	8.938	94.270	94.570	22.965	
1000.00	12.980	64.337	54.116	10.221	94.310	94.600	20.674	

TABLE C11: IDEAL GAS THERMODYNAMIC PROPERTIES OF WATER

Temp., ($^{\circ}$ K)	C_p^o	S^o	$-(G^o - H^o)/T$	$H^o - H^o$	$-\Delta H_f^o$	$-\Delta G_f^o$	Log K_f
Cal deg $^{-1}$ mol $^{-1}$	kcal mol $^{-1}$						
298.15	8.025	45.106	37.167	2.367	-57.798	54.636	40.048
300.00	8.027	45.155	37.216	2.382	-57.803	54.617	39.786
400.00	8.186	47.484	39.505	3.192	-58.042	53.519	29.240
500.00	8.415	49.334	41.292	4.021	-58.277	52.361	22.886
600.00	8.676	50.891	42.765	4.876	-58.500	51.156	18.633
700.00	8.954	52.249	44.025	5.757	-58.710	49.915	15.583
800.00	9.246	53.464	45.130	6.667	-58.905	48.646	13.289
900.00	9.547	54.570	46.119	7.607	-59.084	47.352	11.498
1000.00	9.851	55.592	47.015	8.576	-59.246	46.040	10.062

TABLE C12: ENTHALPY, GIBBS ENERGY, AND EQUILIBRIUM
CONSTANT AT VARIOUS TEMPERATURES

Reaction No. 1			
T, °K	- ΔG_R° kcal mol ⁻¹	- ΔH_R° kcal mol ⁻¹	K
298.15	15.365	23.457	1.831×10^{11}
428.15	11.837	23.457	1.103×10^6
438.15	11.567	23.457	5.878×10^5
453.15	11.159	23.457	2.409×10^5
465.15	10.833	23.457	1.230×10^5
472.15	10.643	23.457	8.447×10^4
493.15	10.073	23.457	2.914×10^4

TABLE C13: ENTHALPY, GIBBS ENERGY, AND EQUILIBRIUM
CONSTANT AT VARIOUS TEMPERATURES

Reaction No. 2

T, $^{\circ}\text{K}$	$-\Delta G_{\text{R}}^{\circ}$ kcal mol^{-1}	$-\Delta H_{\text{R}}^{\circ}$ kcal mol^{-1}	K
298.15	96.055	97.396	2.529×10^{70}
428.15	95.366	97.980	4.732×10^{48}
438.15	95.304	98.032	3.412×10^{47}
453.15	95.209	98.115	8.204×10^{45}
465.15	95.132	98.183	4.932×10^{44}
472.15	95.085	98.223	1.021×10^{44}
493.15	94.943	98.348	1.180×10^{42}

TABLE C14: ENTHALPY, GIBBS ENERGY, AND EQUILIBRIUM
CONSTANT AT VARIOUS TEMPERATURES

Reaction No. 3

T, $^{\circ}\text{K}$	$-\Delta G_{\text{R}}^{\circ}$ kcal mol $^{-1}$	$-\Delta H_{\text{R}}^{\circ}$ kcal mol $^{-1}$	K
298.15	27.174	36.280	8.260×10^{19}
428.15	23.137	36.640	6.457×10^{11}
438.15	22.822	36.670	2.399×10^{11}
453.15	22.347	36.720	5.984×10^{10}
465.15	21.965	36.760	2.089×10^{10}
472.15	21.743	36.790	1.148×10^{10}
493.15	21.072	36.860	2.178×10^9

TABLE C15: ENTHALPY, GIBBS ENERGY, AND EQUILIBRIUM
CONSTANT AT VARIOUS TEMPERATURES

Reaction No.4

T, $^{\circ}$ K	$-\Delta G_R^{\circ}$ kcal mol $^{-1}$	$-\Delta H_R^{\circ}$ kcal mol $^{-1}$	K
298.15	56.067	75.635	1.230×10^{41}
428.15	47.535	75.635	1.820×10^{24}
438.15	46.879	75.635	2.399×10^{23}
453.15	45.895	75.635	1.349×10^{22}
465.15	45.107	75.635	1.549×10^{21}
472.15	44.648	75.635	4.571×10^{20}
493.15	43.270	75.635	1.479×10^{19}

COMPUTER PROGRAM C1

```

C THIS PROGRAM CALCULATES MARTIN-HOU CONSTANTS
DIMENSION TITLE(30)
1,XX(10)
COMMON/MARTIN/A1,A2,A3,A4,A5,B1,B2,B3,B4,B5,C1,C2,C3,C4,C5,B
COMMON/LANCY/T(200),V(200),P(200)
COMMON/POINT/N
COMMON/NANCY/AK,AN,YS
COMMON/CRITI/TC,PC,VC,R,BP
COMMON/FORMAT/NINT,MOUT
C COMMON/FORMAT/NINT(FOR READ INPUT LOCATION),NOUT(FOR WRITE
OUTPUT LOCATION)
DATA NINT,NOUT/5,6/
DATA E0,E1,E2/0.2973223E 01,-0.19272384E-01,0.35306520E-04/
N=1
DATA AK,AN/5,475, 1.7995/
READ (NINT,1)NCOMP
FORMAT (12)
C NTIME FOR CONTROLLED CARD
NTIME=1
200 WRITE(NOUT,11)
11 FORMAT (1H1)
READ(NINT,2) NK,(TITLE(I),I=1,NK)
2 FORMAT (I2,I5A5)
READ(NINT,3)TC,PC,VC,BP,R
3 FORMAT (4F10.4,F12.6)
TB=BP
GO TO 123
122 READ (NINT,32)N
32 FORMAT(13)
READ(NINT,4)(P(I),I=1,N)
READ(NINT,4)(V(I),I=1,N)
READ(NINT,4)(T(I),I=1,N)
4 FORMAT (BF10.3)
C VOLUME CONVERSION FROM CC TO LITER
DO 300 I=1,N
300 V(I)=V(I)/1000.
123 CONTINUE
R=R/1000.
VC=VC/1000.
YSL=E0+E1*TC+E2* TC**2
YS=EXP(2.3026*YSL)
C WRITING OUTPUT FOR INPUT DATA
WRITE (NOUT,6)(TITLE(I),I=1,NK)
6 FORMAT (4X,1545/)
WRITE (NOUT,7)
7 FORMAT(3X,* CALCULATING MARTIN-HOU CONSTANT BY PREDICTION*)

```

```

8  WRITE(NOUT,8) TC,PC,VC,R,BP,AK
8  FORMAT(3X,13H INPUT DATA--/3X,60H T(K) PC(ATM) VC(CC/GMOLE
1  R BP(K) K-CONSTANT/3X,3F10.2,3F10.4/)
1  CALL GOYAL (TC,PC,VC,R,BP)
1  IF(NTIME-NCOMP) 100,150,150
100 NTIME-NTIME+1
100 GO TO 200
150 STOP
150 END

$IBFTC GOYAL
SUBROUTINE GOYAL(TC,PC,VC,R,BP)
COMMON/MARTIN/A1,A2,A3,A4,A5,B1,B2,B3,B4,B5,C1,C2,C3,C4,C5,B
COMMON/NANCY/AKM,AN,YS
COMMON/LANCY/T(200),P(200),V(200)
COMMON/POINT/N
COMMON/FORMAT/NINT,NOUT
REAL KFI
WRITE (NOUT, 106) TC,PC,VC,BP,R
106 FORMAT(3X,* TC,K PC VC TB R*/F10.2,3F8.3,F9.4)
KFI=-AKM
TB=BP
TBR=BP/TC
W=3./7.* (TBR/(1.-TBR))* ALOG10(PC)-1.
C CALCULATION OF ZC
ZC=0.291-0.080*W
C CALCULATING AC
AC=0.9076*(1.+(TBR*ALOG(PC))/(1.-TBR))
WRITE (NOUT, 121) AC,ZC,W
12  FORMAT(2X,20H CALCULATED VALUE--/1X,26H AC ZC
1/3F10.4/)
C CALCULATION OF THE BOYLES TEMPERATURE, DEG.K---
TBO=30.+2.42*TC-5.67*(10.**(-4))* TC *2
BTA=20.533*ZC-31.883*ZC *2
TF1=TC*(0.9869-0.6751*ZC)
C CALCULATION OF M,AMS AND B
AM=-AC-0.25
C DEFINE VALUE -- AN,YS
AMS=-AM*PC/TC
B=R*TC*(ZC-BTA/15.)/PC
AN=1.70
C YS=3.0
C CALCULATION OF MARTIN-HOU PARAMETERS---
A1=0.
B1=R
C1=0
Y2=9.*PC*(VC-B)**2-3.8*R*TC*(VC-B)
Y3=5.4*R*TC*(VC-B)**2-17.*PC*(VC-B)**3
Y4=12.*PC*(VC-B)**4-3.4*R*TC*(VC-B)**3

```

```

Y5=0.8*R*(VC-B)**4-3.*PC*(VC-B)**5
C2=((Y2+B*R*TFI+(R*TFI)**2/PC)*(1.-ZC))*(TBO-TC) +
1((Y2+B*R*TBO)*(TC-TFI)))/((TB-TC)*(EXP(KFI)-EXP(KFI*TFI)-
2TC))-(TC-TFI)*(EXP(KFI*TBO/TC)*EXP(KFI)))
B2=(-Y2-B*R*TBO-C2*(EXP(KFI*TBO/TC)-EXP(KFI)))/(TBO-TC)
A2=Y2-B2*TC-C2*EXP(KFI)
C3=C2*((VC-B)**3-(VC/AN)-B)*3)/((VC/AN-B)**2-(VC-B)**2)
B4=(AMS*(VC-B)**5-AMS*YS*(VC/AN)-B)*5)/((VC-B)**2-(VC/AN-
1B)**2)
BAA=B2*((VC-B)**3+(VC/AN-B)*3)/((VC-B)**2-(VC/AN-B)**2)
BAA=R*((VC-B)**2+(VC/AN-B)**2)
B3=B1-BAA-BAA
A3=Y3-B3*TC-C3*EXP(KFI)
A4=Y4
B4=0.
C4=0.
C5=C2*(VC-B)**3-C3*(VC-B)**2
A5=AMS*(VC-B)**5-R*(VC-B)**4-B2*(VC-B)**3-B3*(VC-B)**2
A5=Y5-B5*TC-C5*EXP(KFI)
C
      WRITE OUTPUT
      WRITE (NOUT,100)A1,B1,C1,A2,B2,C2,A3,B3,C3,A4,B4,C4,A5,B5,C5
100  FORMAT (10X,2H A1, 18X,2HB1,18X,2HC1/3E20.8/10X,2H12,18X,
12HB2,18X,2HC2/3E20.8/10X,2HA3,18X,2HB3,18X,2HC2/3E20.8/
210X,2HA4,18X,2HB4,18X,2 HC4/3E20.8/10X,2HA5,18X,2HB5,18X,
32HC5/3E20.8)
      WRITE (NOUT, 105)B,KFI
105  FORMAT (10X,1HB,18X,2HK/3E20.8/)
      RETURN
      END

```

\$ENTRY

COMPUTER PROGRAM C2

C THIS PROGRAM USES MARTIN-HOU EQUATION AND MARTIN
 C EQUATION (V.P.) TO CALCULATE THERMAL FUNCTION AND PVT
 C DATA
 C MARTIN-HOU EQUATION IS $P=RT/(V-B)+\Sigma(A(I)+B(I)*T+C(I))$
 C $1*EXP(AK*T/TC))/(V-B)$
 C P(PSI), T(DEG.R), V AND B(FT³/LB).
 C A2..A5, B2..B5, C2..C5 ARE CONSTANT IN MARTIN-HOU EQUATION
 C R=10.7351, (GAS CONSTANT), TC(DEG.R).
 C TEMPI, TMIN, TMAX, TLIMIT, TRISE ALL IN DEG R
 C MARTIN EQUATION IS ..LOGP(ATM)=X1+X2/T+X3*T+X4*T²+X5*T³+LOG10(TC-T+8.0) T IN DEG.K.
 C DEN IS DENSITY, TEMP IS TEMPERATURE IN DEG K
 C THIS PROGRAM CALCULATES THERMAL FUNCTIONS IF DENSITY
 C IS KNOWN AT ANY TEMPERATURE
 C TMAX=UPPER LIMIT FOR TEMP..., TMIN=LOWER LIMIT FOR TEMP.
 C TRISE=INCREMENT AT WHICH PVT VALUES ARE WANTED
 C TEMPI=INITIAL TEMP., WM=MOL.WT.
 C SEQUENCE OF DATA CARDS..TEMPI, TMIN, TMAX, TLIMIT, TRISE
 C (6F10.5), A2, B2, C2,..A5, B5, C5, TC, WM, R, B, AK(6F10.5),
 C X1,..X6(6F10.6), TEMP (F10.5).
 C DIMENSION DEN(60), PCALC(60)
 PRINT 50
 PRINT 20
 READ 9, TEMPI, TMIN, TMAX, TLIMIT, TRISE
 READ 8, A2, B2, C2
 READ 8, A3, B3, C3
 READ 8, A4, B4, C4
 READ 8, A5, B5, C5
 8 FORMAT (E15.8,4X,E15.8,5X,E15.8)
 READ 7, TC, WM, R, PC
 7 FORMAT (F8.3,F8.3,F12.6,F8.2)
 TC=TC * 1.8
 C TC MUST BE FED IN DEGREES KELVIN
 R=R/WM
 TEMP=TEMPI
 9 FORMAT (6F10.5)
 10 FORMAT (F10.5)
 DEN(1)=0.003
 N=10
 DO 11 I=1,N
 II=I+1
 DEN(II)=DEN(I)+0.001
 11 CONTINUE
 AK=5.0/TC
 100 PI=0.0001
 PRINT 40

```

IF(TEMP.GE.TMIN.AND.TEMP.LT.TMAX)READ 10,TEMP
T=TEMP
IF(T*1.8.GT.TC) GO TO 101
C THE VALUE OF PMM SHOULD BE IN ATMOSPHERES
PMM=7.255-1320.2716/(T-43.96)
PP=(10.0 *PMM)/760.0
PRINT 1,PP
FORMAT(/55X,*      SATURATION PRESSURE=*, E15.6)
101 EX=EXP(-AK*T*I.8)
PCALC(1)=0.0

```

FORTRAN SOURCE LIST MAIN

ISN	SOURCE STATEMENT
	PC=PC*14.696
	B=R *TC/(8.0*PC)
	T=TEMP*1.8
	DO 60 I=1,N
	V=1.0/(DEN(I)*62.482)
	VB=V-B
	F1T=R*T/VB
	F2T=(A2+B2*T+C2*EX)/VB**2
	F3T=(A3+B3*T+C3*EX)/VB**3
	F4T=(A4+B4*T+C4*EX)/VB**4
	F5T=(A5+B5*T+C5*EX)/VB**5
	PCALC(I+1)=F1T+F2T+F3T+F4T+F5T
	IF(T.GE.TC) GO TO 14
	IF(PCALC(I+1).GT.PP*14.7) GO TO 60
	IF (ABS (PCALC(I+1)),LT.ABS(PCALC(I))) GO TO 88
14	P=PCALC(I+1)
	TERM1=P*V-R*T
	TERM2 = (A2+(1.0+AK*T)*C2*EX)/VB
	TERM3 = (A3+(1.0+AK*T)*C3*EX)/(2.0 VB**2)
	TERM4 = (A4+(1.0+AK*T)*C4*EX)/(3.0 VB**3)
	TERM5 = (A5+(1.0+AK*T)*C5*EX)/(4.0 VB**4)
	DELH=TERM1+TERM2+TERM3+TERM4+TERM5
	VBB=R*T/P(I)-B
	TERM1=R* ALOG (VB/VBB)
	TERM2=-(B2-AK*C2*EX)*(1.0/VB-1.0/VBB)
	TERM3=-0.5*(B3-AK*C3*EX)*(1.0/VB**2-1.0/VBB**2)
	TERM4=-1.0/3.0*(B4-AK*C4*EX)*(1.0/VB**3-1.0/VBB**3)
	TERM5=-0.25*(B5-AK*C5*EX)*(1.0/VB**4-1.0/VBB **4)
	DELS=TERM1+TERM2+TERM3+TERM4+TERM5
	DELH=DELH*1.98589/10.7315
	DELS=DELS*1.98589/10.7315
	TEMPK=T/1.8
	PATM=P/14.696
	VCGS=WM/DEN(I)
	PRINT 30,TEMPK,PATM,VCGS,DELH,DELS

```
60 CONTINUE
88 CONTINUE
  IF(TEMP.GE.TMIN.AND.TEMP.LT.TMAX) GOTO 100
  TEMP=TEMP+TRISE
  IF (TEMP.EQ.TLIMIT) STOP
  GO TO 100
20 FORMAT (30X,87(1H*))//30X,87H * TEMPERATURE * PRESSURE
1 * VOLUME * DELTA*H * DELTA S * /30X,87H * DEGREES * ATMOS.
2 *CC2GM MOLE*CAL/GM.MOLE * CAL/(GM.MOLE,DEGREES)* )
30 FORMAT(5X,1H*, 4X, F9.3, 4X,1H*, 4X,E15.6,3X,1H*, 1X,
        1E15.6, 1X,1H*, 2X, E15.6,2X,1H*,4X, E15.6,4X, 1H*)
40 FORMAT(30X, 87(1H-))
50 FORMAT (1H1)
70 CONTINUE
END
```

\$ENTRY